Aus dem Institut für Integrative Neuroanatomie
Abteilung für Elektronenmikroskopie und molekulare Neuroanatomie
Medizinische Fakultät
Charité – Universitätsmedizin Berlin

Dissertation

The Lateral Habenula – Crossroad between Homeostatic Systems and Reward Circuitries

Zur Erlangung des akademischen Grades
Doctor medicinae (Dr. med.)

vorgelegt der Medizinischen Fakultät
Charité – Universitätsmedizin Berlin

von
Wolfram Christian Poller
aus Bochum

Gutachter:

1. Prof. Dr. R. W. Veh
2. Prof. Dr. P. Falkai
3. MD, PhD O. Hikosaka

Datum der Promotion: 03.06.2012

1. Introduction 9

1.1 The habenula is an important diencephalic relay station 9

1.1.1 The habenula is a bilateral epithalamic structure 9

1.1.2 The habenula is part of the dorsal diencephalic conduction system 11

1.1.3 The lateral habenula is involved in various physiological processes and the pathophysiology of major psychiatric diseases 13

1.1.4 The lateral habenula is an important signal integrator in reward circuitries 16

1.1.4.1 Reward is necessary for learning and economic decision making 16

1.1.4.2 The lateral habenula receives reward-encoding information and transmits them to the monoaminergic systems 17

1.2. The ventral tegmental area is the origin of the mesocorticolimbic dopamine system 18

1.2.1 The ventral tegmental area is located at the floor of the midbrain 18

1.2.2 The ventral tegmental area is reciprocally connected to a wide range of structures throughout the brain 19

1.2.3 The ventral tegmental area is implicated in reward circuitries, cognition and motivation 20

1.3 The mesencephalic serotonin system originates from the dorsal and median raphe nuclei 20

1.3.1 Dorsal and median raphe nuclei provide serotonergic innervations to various forebrain regions 21

1.3.2 The mesencephalic serotonergic system modulates various physiological, behavioral, and cognitive functions 21

1.4 Hyperpolarization-activated cyclic nucleotide-gated cation channels generate pacemaker activity in neuronal networks 22

1.4.1 HCN channels are tetrameric transmembrane proteins 22

1.4.2 HCN channels generate Ih currents 23

1.4.3 HCN channels are widely expressed throughout the brain 23

1.4.4 HCN channels are involved in various physiological functions of heart and brain cells 24

1.5 The hypothalamus is the superior regulator of the homeostatic system 25

1.5.1 The hypothalamus forms the ventral part of the diencephalon 25

1.5.2 The lateral hypothalamic area mainly projects to the lateral habenula.....25

1.5.3 The hypothalamus coordinates various homeostatic mechanisms .....

1.6 Objectives of the study.....26

1.6.1 Molecular mechanism underlying the lateral habenular inhibition on monoamine release 26

1.6.2 Characterization of a projection from the lateral hypothalamic area to the lateral habenula 27

2. Materials and Methods 29

2.1 Animals.....29

2.2 Materials.....29

2.2.1 Chemicals and Substances 29

2.2.2 Kits, Enzymes and Buffers.....31

2.2.3 Installations, Equipments and Devices 31

2.2.4 Antibodies and Dilutions 32

2.3 Quantitative PCR.....33

2.4 Riboprobe generation.....33

2.4.1 Selection of cDNA sequences for the HCN riboprobes.....33

2.4.2 PCR amplification of cDNA 34

2.4.3 Gel electrophoresis of the PCR products 35

2.4.4 Gel-extraction of DNA fragments 35

2.4.5 Cloning of DNA fragments into a pGEM-T vector system 35

2.4.6 Transformation of pGEM-T vectors into *E.coli* XL1 blue 36

2.4.7 Small scale - preparation of plasmid – DNA (Mini Prep) 36

2.4.8 Restriction analysis and sequencing 37

2.4.9 Intermediate scale - preparation of plasmid DNA (Midi Prep)....37

2.4.10 Linearization of MidiPrep Plasmid DNA....38

2.4.11 Digoxigenin labeling of the linearized plasmid....38

2.5 Tracing Experiments....38

2.5.1 Anesthesia....38

2.5.2 Stereotactic surgery....38

2.5.3 Tracer application....39

2.5.3.1 Anterograde tracing....39

2.5.3.2 Retrograde tracing....40

2.5.4 Perfusion fixation....41

2.5.5 Obtaining series of sections....42

2.5.5.1 Cryomicrotome....42

2.5.5.2 Vibratome....42

2.6 Immunocytochemistry....42

2.6.1 Pre - treatment of brain sections....42

2.6.2 Primary antibodies....42

2.6.3 Secondary antibodies....43

2.6.4 Visualization of secondary antibodies....43

2.6.5 Mounting and coverslipping of brain sections....43

2.7 *In Situ* Hybridization....43

2.7.1 *In situ* hybridization with digoxigenin-labeled riboprobes....43

2.7.2 Visualization of Digoxigenin....44

2.8 Silver intensification and gold toning....44

2.9 Kluever - Barrera staining....45

2.10 Methyl green staining....45

2.11 Coating of slides....45

2.12 Confocal laser scanning microscopy 46

2.12.1 Processing of slices for confocal laser scanning microscopy 46

2.12.2 Acquiring images with the CLSM 46

2.13 Electron microscopy 46

2.13.1 Pre - treatment of the brain sections 46

2.13.2 Pre - embedding immunocytochemistry 46

2.13.3 Araldite embedding 47

2.13.4 Preparation of Semi- and Ultrathin sections 47

2.13.5 Post - embedding immunocytochemistry 47

2.13.5.1 Semithin sections 47

2.13.5.2 Ultrathin sections 48

2.13.6 Staining of ultrathin sections 48

2.13.7 Toluidine blue staining 49

2.14 Documentation and images 49

3. Results 50

3.1 Lateral habenular neurons projecting to the monoaminergic systems express HCN channels 50

3.1.1 Quantitative PCR analyses confirm high levels of HCN2-4 and low levels of HCN1 mRNA expression 50

3.1.2 Digoxigenin labeled riboprobes, against HCN1-4 mRNAs are highly Specific 51

3.1.2.1 Selection of HCN1-4 cDNA sequences 51

3.1.2.2 Gel electrophoresis of PCR products 52

3.1.2.3 Restriction analysis and sequencing 53

3.1.2.4 Specificity of HCN riboprobes 54

3.1.3 *In situ* hybridization reveals significant subnuclear differences in the percentages of HCN-positive cells 56

3.1.4 HCN channels are mainly expressed in the habenular neuropil....60

3.1.5 The lateral habenula strongly projects to VTA, DR, and MnR....63

3.1.5.1 Injection sites of the retrograde tracer WGA-apo HRP gold are located in VTA, DR, and MnR....64

3.1.5.2 Distribution of retrogradely-traced neurons in the lateral Habenula....67

3.1.6 Lateral habenular neurons projecting to VTA, DR or MnR strongly express HCN subunits....69

3.2 A glutamatergic projection from the lateral hypothalamus directly targets VTA-projecting neurons in the lateral habenula....72

3.2.1 The lateral hypothalamus strongly projects to the lateral habenula....72

3.2.1.1 Neurons projecting to the lateral habenula are distributed throughout many hypothalamic subnuclei....72

3.2.1.2 Lateral hypothalamic axons mainly target the medial division of the lateral habenula....73

3.2.1.3 Projections from the lateral hypothalamus to the lateral habenula are glutamatergic....75

3.2.1.4 GAD is not expressed in lateral hypothalamic terminals....82

3.2.2.5 Lateral hypothalamic axons in the lateral habenula do not contain the neuropeptides orexin and galanin....83

3.2.2 Lateral hypothalamic terminals directly target VTA-projecting neurons in the lateral habenula....87

3.2.2.1 VTA-projecting neurons and axons from the lateral hypothalamus are similarly distributed within most of the lateral habenular subnuclei....87

3.2.2.2 Lateral hypothalamic terminals directly contact VTA-projecting neurons in the lateral habenula....90

4. Discussion....93

4.1 Methodical considerations....93

4.2 HCN channels might be the molecular mechanism underlying lateral habenular baseline inhibition of monoamine release....95

4.2.1 All HCN subunits are expressed within the lateral habenula....95

4.2.2 HCN channels explain electrophysiological characteristics of lateral habenular neurons 98

4.2.3 The lateral habenula is in a perfect position to control monoaminergic circuitry 99

4.2.4 Lateral habenular projections to VTA, MnR and DR have a lot in common 100

4.2.5 Conclusions and future prospects 100

4.3 The lateral hypothalamus seems to be an important source of modulatory input to lateral habenular projection neurons 101

4.3.1 A strong lateral hypothalamic projection preferentially innervates the medial division of the lateral habenula 101

4.3.2 Lateral hypothalamic terminals in the lateral habenula mainly use glutamate as neurotransmitter 102

4.3.3 VTA-projecting lateral habenular neurons are directly targeted by the lateral hypothalamic projection 104

4.3.4 The lateral hypothalamus might be a major provider of reward-encoding information 106

4.3.5 Conclusions and future prospects 107

5. Summary 108

6. Zusammenfassung 110

7. Abbreviations 113

8. References 115

9. Publications 125

10. Danksagung 126

11. Eidesstattliche Erklärung 127

12. Curriculum vitae 128

1. Introduction

“La fixité du milieu intérieur est la condition de la vie libre et indépendante."

This sentence published in 1865 by the French physiologist Claude Bernard was the first description of the pivotal biological principle of homeostasis. Homeostasis describes the ability of a biological system to maintain stable internal states for all environmental conditions. This requires complex regulatory mechanisms to appropriately react to internal and external changes. These reactions include internal adjustments as well as behavioral responses. In vertebrates, the coordination of these mechanisms is primarily managed by phylogenetically well preserved structures in the diencephalon and the brainstem. These structures include the hypothalamus, the habenula as a part of the epithalamus, and several brainstem nuclei. While the hypothalamus is responsible for the measurement of homeostatic parameters and induces appropriate internal responses, the habenula and the monoaminergic brainstem nuclei, both important parts of the reward system, seem to be involved in the regulation of behavior. The precise relation between the homeostatic system and the reward system remains mostly unknown at present.

1.1 The habenula is an important diencephalic relay station

1.1.1 The habenula is a bilateral epithalamic structure

The habenula (Hb) is a bilateral complex of small nuclei, located close to the midline on top of the posterior thalamus. It forms the epithalamus together with the pineal gland, situated directly behind the Hb. In analogy to the “stalk of the pituitary gland”, a protrusion of the ventral hypothalamus, it was originally denoted as the “stalk of the pineal gland”. The term habenula was finally introduced by anatomists, who were reminded of small reins (habenula is the diminutive of the Latin word for rein “habena”) by the bilateral longish shape of the Hb. It is a phylogenetically well conserved structure found in ancient fish as well as primates and humans (Yanez and Anadon, 1994; Concha and Wilson, 2001). While in mammals the two habenulae may exhibit a bilateral symmetry, there is a considerable asymmetry of size in many non-mammalian vertebrates (Yanez and Anadon, 1996; Concha and Wilson, 2001). In coronal sections of the rat brain, the Hb appears as a triangular structure with its basis seated on the thalamus, one side facing the third ventricle and the other side facing the lateral ventricle. Further rostral the Hb becomes flat and wider until it finally gives way to the stria medullaris (sm), the main input fiber bundle of the Hb. Towards the posterior end the shape of the Hb becomes higher and narrower and releases a massive fiber bundle of efferent Hb and

Hb-passing axons, the fasciculus retroflexus (fr), which is also known as the habenula-interpeduncular tract. The dorsal end of the Hb is the habenular commissure directly in front of the pineal gland. Based on Nissl-stained sections, the Hb of birds and mammals is traditionally divided into a very cell dense medial (MHb) and a less cell dense lateral complex (LHb) (Nissl, 1913). Further examination of the LHb resulted in an additional differentiation of the LHb into a medial (LHbM) and lateral (LHbL) division (Herkenham and Nauta, 1977). Finally, detailed investigations of the subnuclear organization, based on criteria including ultrastructure, cell morphology and immunocytochemical characteristics, resulted in the delineation of five subnuclei of the LHbM and five subnuclei of the LHbL (Andres et al., 1999; Geisler et al., 2003).

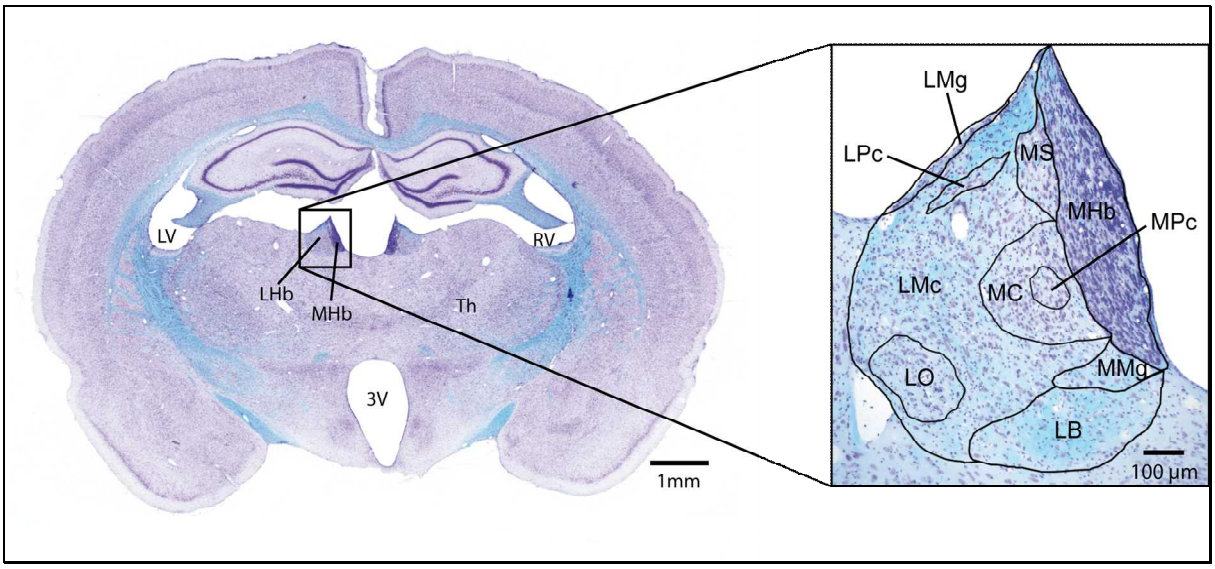

Figure 1: The coronal section of the rat brain at a level of Bregma -2.7 mm in Kluever Barrera stain displays fibers in blue and cells in violet. The Hb appears as a triangular structure located on top of the posterior thalamus. The inset shows the subnuclear organization of the habenular complex. MHb - medial habenula; LHb - lateral habenula; LV/RV - left/right ventricle; 3V - third ventricle; Th - thalamus; Hb subnuclei: MS - superior subnucleus; MPc - parvocellular subnucleus; MC - central subnucleus; MMg - marginal subnucleus; LPc - parvocellular subnucleus; LMc - magnocellular subnucleus; LO - oval subnucleus; LMg - marginal subnucleus; LB - basal subnucleus

1.1.2 The habenula is part of the dorsal diencephalic conduction system

There are two pathways for information flow from forebrain regions through the diencephalon to the regulatory midbrain nuclei (Herkenham and Nauta, 1977; Herkenham and Nauta, 1979; Sutherland, 1982). The first one is the medial forebrain bundle (mfb) that directly guides efferences from the septal nuclei, the amygdala, the lateral preoptic area (LPOA) and the lateral hypothalamic area (LHA) towards the mesencephalic tegmentum. However, the Hb is part of the second pathway, the dorsal diencephalic conduction system, which conveys information from the basal ganglia and the limbic forebrain (Herkenham and Nauta, 1977) through the epithalamus towards the regulatory midbrain nuclei (Herkenham and Nauta, 1979; Phillipson, 1979; Sutherland, 1982; Oades and Halliday, 1987). This conduction system is composed of two major fiber bundles, the stria medullaris (sm) and the fasciculus retroflexus (fr), with the Hb located in-between (Herkenham and Nauta, 1977; Sutherland, 1982).

Nearly all afferences reach the Hb via the sm. At least three areas with diverse input can be distinguished within the Hb. The more obvious one is a separation of MHb and LHb afferences. While the MHb receives its major input from the septum, the main LHb input originates in the basal ganglia, limbic areas, the LPOA and the LHA (Conrad and Pfaff, 1976; Herkenham and Nauta, 1977; Rajakumar et al., 1993; Kowski et al., 2008). Another distinction exists within the LHb itself. The LHbM primarily receives information from areas of the limbic system including the LHA, the medial prefrontal cortex, the accumbens nucleus, parts of the amygdala, the ventral pallidum and the diagonal band of Broca. In contrast, the LHbL is mainly targeted by the basal ganglia, particularly by the “entopeduncular nucleus”, the rodent equivalent of the globus pallidus internus (Herkenham and Nauta, 1977).

In addition to these major inputs via the sm, there are minor afferences reaching the Hb via the fr. These afferences originate in the mesencephal tegmentum and the pons and are known as the mesohabenular pathway (Herkenham and Nauta, 1977; Skagerberg et al., 1984; Gruber et al., 2007). Projections from the caudal areas of the LHA reach the LHb on a loop way via the mfb and the fr (Herkenham and Nauta, 1977).

The major pathway for efferences leaving the Hb is the fr. In contrast to the input, there is only a bisection of the Hb regarding the output, as LHbM and LHbL target similar areas (Herkenham and Nauta, 1979; Phillipson, 1979; Sutherland, 1982; Oades and Halliday, 1987). The MHb on the one hand mainly projects to the interpeduncular nucleus (IP). The LHb on the other hand shows a more complex pattern of target regions. Major LHb efferences target monoaminergic brainstem nuclei, including the dopaminergic ventral tegmental area (VTA)

and its GABAergic "tail", the rostro-medial tegmental nucleus (RMTg) (Omelchenko and Sesack, 2009; Brinschwitz et al., 2010) and the substantia nigra pars compacta (SNc), the serotonergic dorsal (DR) and median raphe (MnR) and the cholinergic laterodorsal tegmentum (LDTg) (Phillipson, 1979; Herkenham and Nauta, 1979; Oades and Halliday, 1987). Recently a reverse projection of dopaminergic neurons in the VTA to the LHb was described, which is thought to function as a feedback loop (Gruber et al., 2007).

Other and less pronounced projections of the LHb target rostral structures, including some of the main Hb input areas, particularly the LHA, the bed nucleus of the stria terminalis, and the septum. These efferences either take the sm as the direct way or the loop way of fr and mfb to reach their targets (Herkenham and Nauta, 1979). Given that most of the Hb connections are bidirectional, it seems likely that the information flow towards the Hb and from the Hb towards other structures is under feedback control.

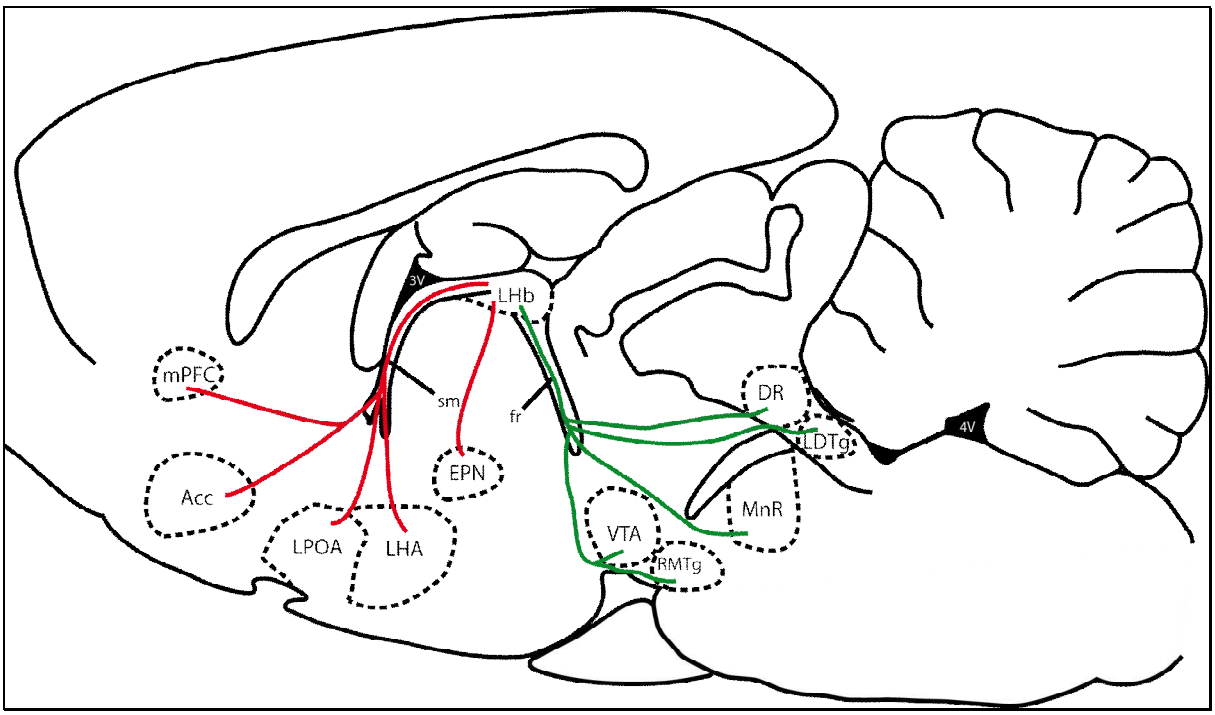

Figure 2: The connections of the LHb are shown with afferences in red and efferences in green. Most afferences from limbic forebrain areas and the basal ganglia reach the LHb via the stria medullaris (sm). Efferences to the monoaminergic nuclei leave the LHb via the fasciculus retroflexus (fr). Abbreviations: mPFC: medial prefrontal cortex; Acc: accumbens nucleus; LPOA: lateral preoptic area; LHA: lateral hypothalamic area; EPN: entopeduncular nucleus; VTA: ventral tegmental area; RMTg: rostromedial tegmental nucleus; MnR: median raphe nucleus; LDTg: laterodorsal tegmental nucleus; DR: dorsal raphe nucleus. Image modified from Paxinos and Watson 1998.

1.1.3 The lateral habenula is involved in various physiological processes and the pathophysiology of major psychiatric diseases

Despite its small size, the LHb has a highly complex structure and various connections to other brain areas (see paragraph 1.1.2). This is reflected by the broad spectrum of functions and diseases associated with the LHb (Table 1). Currently less is known about the function of the MHb. This cell dense area mainly receives input from limbic parts of the septum (Herkenham and Nauta, 1977) and projects to the IP (Herkenham and Nauta, 1979). The IP in turn innervates the VTA and the DR, two major target areas of the LHb. Thus the MHb might have similar functions as the LHb but in an indirect way (via the IP). Another finding indicates a potential role of the MHb in endocrine and immunological stress responses (Silver et al., 1996; Carboni et al., 1998; Sugama et al., 2002).

Topic and Title	**Authors and Journal**
Physiological functions of the LHb	
Nutrition:	
- Localization of quinine aversion within the septum, habenula, and interpeduncular nucleus of the rat.	Donovick et al., 1970 J Comp Physiology
- Functional mapping of the rat brain during drinking behavior: a fluorodeoxyglucose study.	Gonzalez-Lima et al., 1993 Physiol. Behavior
- Fos expression in feeding-related brain areas following intracerebroventricular administration of orphanin FQ in rats	Olszewski et al., 2000 Brain Research
Circadian rhythms and sleep	
- A GABAergic habenulo-raphe pathway mediation of the hypnogenic effects of vasotocin in cat.	Goldstein, 1983 Neuroscience
- c-Fos expression in the brains of behaviorally "split" hamsters in constant light: calling attention to a dorsolateral region of the suprachiasmatic nucleus and the medial division of the lateral habenula.	Tavakoli-Nezhad, 2005 J Biol. Rhythms
- Hamsters running on time: is the lateral habenula a part of the clock?	Tavakoli-Nezhad, 2006 Chronobiol Int.
Blood pressure	
- Peripheral pathway of the blood pressure raised by exciting habenular nuclei.	Zhao and Wang, 1989 Zhongguo Yao Li Xue Bao

Maternal behavior	
- Neurons in the lateral subdivision of the habenular complex mediate the hormonal onset of maternal behavior in rats.	Corodimas et al., 1993 Behavioral Neuroscience
- First and second order maternal behavior related afferents of the lateral habenula.	Felton et al., 1999 Neuroreport
- Evidence for estrogen receptor in cell nuclei and axon terminals within the lateral habenula of the rat: regulation during pregnancy.	Kalinichev et al., 2000 J Comp Neurology
Learning	
- Mapping of olfactory memory circuits: region-specific c-fos activation after odor-reward associative learning or after its retrieval.	Tronel and Sara, 2002 Learn Memory
- Water maze training in aged rats: effects on brain metabolic capacity and behavior.	Villarreal et al., 2002 Brain Research
Cognitive performance	
- Habenula lesions cause impaired cognitive performance in rats: implications for schizophrenia.	Lecourtier et al., 2004 Eur J Neuroscience
- Habenula lesions alter synaptic plasticity within the fimbria-accumbens pathway in the rat.	Lecourtier et al., 2006 Neuroscience
Pain processing	
- Habenular stimulation produces analgesia in the formalin test.	Cohen and Melzack, 1986 Neuroscience Letters
- The habenula and pain: repeated electrical stimulation produces prolonged analgesia but lesions have no effect on formalin pain or morphine analgesia.	Cohen and Melzack, 1993 Behav. Brain Res.
- Simultaneous recording of spontaneous activities and nociceptive responses from neurons in the pars compacta of substantia nigra and in the lateral habenula.	Gao et al., 1996 Eur J Neuroscience
Stress response	
- The role of the habenular complex in the elevation of dorsal raphe nucleus serotonin and the changes in the behavioral responses produced by uncontrollable stress.	Amat et al., 2001 Brain Research
- Opposite metabolic changes in the habenula and ventral tegmental area of a genetic model of helpless behavior.	Shumake et al., 2003 Brain Research

Reward	
- Error monitoring using external feedback: specific roles of the habenular complex, the reward system, and the cingulate motor area revealed by functional magnetic resonance imaging.	Ullsperger, 2003 J Neuroscience
- Lateral habenula as a source of negative reward signals in dopamine neurons.	Matsumoto, 2007 Nature
- Representation of negative motivational value in the primate lateral habenula.	Matsumoto, 2009 Nature Neuroscience
- Distinct tonic and phasic anticipatory activity in lateral Habenula and dopamine neurons.	Bromberg-Martin, 2010 Neuron

<u>Psychiatric Diseases associated with LHb dysfunction</u>

Drug addiction	
- Microiontophoresis of cocaine, desipramine, sulpiride, methysergide, and naloxone in habenula and parafasciculus.	Dougherty et al., 1990 Exp. Neurology
- The neurotoxic effects of continuous cocaine and amphetamine in Habenula: implications for the substrates of psychosis.	Ellison et al., 1996 NIDA Res. Monogr.
- Prenatal cocaine produces signs of neurodegeneration in the lateral habenula.	Murphy et al., 1999 Brain Research
Mood disorders	
- Lateral habenula lesions improve the behavioral response in depressed rats via increasing the serotonin level in dorsal raphe nucleus.	Yang et al., 2008 Behav Brain Research
- Deep brain stimulation of the lateral habenula in treatment resistant major depression.	Sartorius and Henn, 2007 Med. Hypotheses
- Remission of major depression under deep brain stimulation of the lateral habenula in a therapy-refractory patient.	Sartorius et al., 2010 Biol. Psychiatry
Schizophrenia	
- Stimulant-induced psychosis, the dopamine theory of schizophrenia, and the habenula.	Ellison, 1994 Brain Research
- Pineal and habenula calcification in schizophrenia.	Sandyk, 1992 Int J Neuroscience

- Schizophrenia in translation: the presence of absence: habenular regulation of dopamine neurons and the encoding of negative outcomes.	Shepard et al., 2006 Schizophr. Bulletin

Table 1: The habenula is associated with various physiological functions, but it is also implicated in the etiology of psychiatric diseases. Table 1 gives an overview of the corresponding literature.

1.1.4 The lateral habenula is an important signal integrator in reward circuitries

Among the various functions of the LHb, particularly its role in reward processing has recently come into focus. The LHb strongly inhibits dopamine and serotonin release in situations when individuals recognize mistakes or receive punishments, thereby causing the unpleasant feelings associated with those events (Wang and Aghajanian, 1977; Christoph et al., 1986; Matsumoto and Hikosaka, 2007; Ji and Shepard, 2007; Matsumoto and Hikosaka, 2009a).

1.1.4.1 Reward is necessary for learning and economic decision making

The neurobiological basis of reward is an increased release of the neurotransmitter dopamine in forebrain regions, particularly the accumbens nucleus (Wise, 1989; Ikemoto and Panksepp, 1999; Lecourtier et al., 2008). Through reward, individuals ascribe a positive value to environmental stimuli or internal physical states and adapt their behavior accordingly. So-called “primary rewards” reinforce behaviors directly and are responsible for the survival of an individual or a species. Examples for primary rewards include food intake, fighting, escaping and sexual activities. “Secondary rewards” reinforce behaviors, which increase the probability of receiving primary rewards or that predict primary rewards. Thus, secondary rewards are closely related to primary rewards. The different rewards can be directly transmitted to the brain’s reward areas by various external sensory systems including the visual, olfactory, somatosensory and auditory system. On the other hand, primary and many of the secondary rewards directly change internal states, which can be sensed by the organism, for example an increased blood sugar after eating, which is measured in the hypothalamus. However, identification and reaction to more abstract rewards, like money or social acceptance, requires higher cognitive evaluation. Thus, rewards are not defined by their sensory properties but by the reinforcement of behaviors they induce.

In analogy to the term “positive reward” for something that increases the repetition-frequency of a behavioral act, something that decreases the frequency of a behavioral act constitutes a “negative reward”. Negative rewards cause a decreased dopamine release and thereby unpleasant feelings. These negative rewards include punishments as well as the absence of an expected positive reward (Lecourtier et al., 2006; Matsumoto and Hikosaka, 2007; Ji and Shepard, 2007; Matsumoto and Hikosaka, 2009a).

Taken together, the reward system is responsible for the pivotal process of learning and economic decision making based on otherwise neutral environmental stimuli and thereby contributes to the maintenance of constant internal states.

1.1.4.2 The lateral habenula receives reward-encoding information and transmits them to the monoaminergic systems

The major efferent pathway of the reward system is the mesocortical and mesolimbic dopamine system, which originates in the VTA and releases dopamine in various forebrain areas. Changes in the activity of dopaminergic neurons in the VTA directly elicit the pleasurable effects that are triggered by rewards (chapter 1.2). However, reward-related properties are obviously not directly sensed by the VTA, but relayed via multiple sensory systems. Therefore the various sensory information needs to be filtered, reviewed and integrated before it is transmitted to the VTA.

One promising candidate for a central role in the transmission of reward-related signals to the VTA is the LHb. The LHb receives information from the entopeduncular nucleus (Hong and Hikosaka, 2008) the hypothalamus (Blander and Wise, 1989), and other limbic forebrain structures (Herkenham and Nauta, 1977; Sutherland, 1982), and relays those signals to systems, which mainly influence emotion and motivation (Herkenham and Nauta, 1979; Hikosaka et al., 2008; Matsumoto, 2009). These systems include the dopaminergic ventral tegmental area (VTA), but also the serotonergic median (MnR) and dorsal raphe (DR) nuclei, which strongly interact with the VTA (chapter 1.3). The LHb is the only structure known so far that is activated by negative reward and inhibited by positive reward (Gallistel et al., 1985; Matsumoto and Hikosaka, 2007). Negative rewards activate the LHb (Ullsperger and von Cramon, 2003; Matsumoto and Hikosaka, 2009a), which in turn suppresses dopaminergic neurons in the VTA (Christoph et al., 1986; Shepard et al., 2006; Matsumoto and Hikosaka, 2007) and raphe (Wang and Aghajanian, 1977) via a GABAergic mechanism. Thus, LHb activation causes decreased dopamine and serotonin release in various forebrain regions (Lecourtier et al., 2006; Matsumoto and Hikosaka, 2007; Matsumoto and Hikosaka, 2008).

Conversely, positive rewards suppress LHb activity, resulting in an increased monoamine release via disinhibition of VTA and raphe nuclei (Matsumoto and Hikosaka, 2007; Lecourtier et al., 2008; Nakamura et al., 2008).

Thus, changes of the activity of LHb neurons lead to an opposite reaction of VTA and raphe cell activity (Matsumoto and Hikosaka, 2007). As shown recently for the LHb-VTA pathway, inhibition on dopamine-release is mediated by glutamatergic LHb neurons, which inhibit dopaminergic VTA neurons via GABAergic interneurons (Omelchenko and Sesack, 2009) (Brinschwitz et al., 2010). A similar mechanism was described for the LHb-DR pathway leading to LHb-mediated inhibition of serotonergic DR neurons (Wang and Aghajanian, 1977; Ferraro et al., 1996; Yang et al., 2008). Besides the activity changes triggered by rewards recent electrophysiological studies suggest that the LHb exerts a strong continuous inhibition on monoamine release (Kim and Chang, 2005; Lecourtier et al., 2008; Weiss and Veh, 2010).

Consistent with this view, the LHb has often been implicated in the processing of negative experiences, such as anxiety, stress or pain (references: see Table 1.).

Thus, the LHb is a pivotal structure for reward-related decision-making and learning processes. By blocking reward, the LHb is able to inhibit behaviors in situations when individuals expect negative outcomes, while the transmission of positive rewards could increase the motivation to engage in certain behavior (Lecourtier et al., 2006; Matsumoto and Hikosaka, 2007). The LHb thereby contributes to the appropriate behavioral response to various internal and external stimuli and conditions (Matsumoto, 2009).

1.2. The ventral tegmental area is the origin of the mesocorticolimbic dopamine system

1.2.1 The ventral tegmental area is located at the floor of the midbrain

Like the Hb, the ventral tegmental area **(**VTA) is a phylogenetically well-preserved structure showing only slight differences between rodents and humans. The VTA is a group of neurons bilaterally located close to the midline in the mesencephalic tegmentum, the most anterior part of the midbrain (Tsai, 1925; Papez, 1932). In contrast to other cell groups of the brain, which are usually called “nuclei”, the VTA was designated as an “area”, because it is not clearly discriminable from surrounding structures and presents a very heterogeneous cytoarchitecture (Nauta, 1958). The major criterion to differentiate the VTA from surrounding areas is the selective limbic input of VTA neurons (Nauta, 1958; Nauta, 1960). The VTA is surrounded by several other important areas, including the red nucleus (RN) situated dorsolaterally, the

substantia nigra (SN) on the lateral side, the interpeduncular nucleus (IP) located medially, the mammillary bodies as the rostral extension, and the pons as the caudal neighbor.
The VTA is divided into four subareas, the paranigral nucleus (PN), the parabrachial pigmented area (PBP), the parafasciculus retroflexus area (PFR) and the ventral tegmental tail (VTT). The dopaminergic cells are primarily located within the PN and PBP (Oades and Halliday, 1987). Recently, a discrete GABAergic region extending caudally from the VTA has been described. According to the anatomy it has been called the "tail of the VTA" or the "mesopontine rostromedial tegmental nucleus" (RMTg) (Omelchenko and Sesack, 2009; Kaufling et al., 2009; Brinschwitz et al., 2010).

1.2.2 The ventral tegmental area is reciprocally connected to a wide range of structures throughout the brain

The two major efferences of the dopaminergic VTA are the mesolimbic and the mesocortical pathway (Ungerstedt, 1971; Swanson, 1982). The mesolimbic pathway innervates phylogenetically old limbic structures, including the accumbens nucleus, the olfactory tubercle, the septum, the amygdala and the hippocampus. In contrast, the mesocortical pathway primarily projects to phylogenetically younger cortical regions, including the prefrontal, orbitofrontal, insular and cingulate cortices (Ungerstedt, 1971; Swanson, 1982).
Afferent projections to the VTA arise from various structures throughout the brain extending from the prefrontal cortex to the caudal brainstem. Most of these areas send excitatory glutamatergic projections to the VTA, which increase the firing rate of dopaminergic cells in the VTA when they are activated (Grace and Bunney, 1984; Murase et al., 1993; Geisler et al., 2007). Only a few direct inhibitory GABAergic afferences to the VTA have been described, mainly arising from the ventral pallidum (Wu et al., 1996). Recently a third type of afferences to the VTA came into focus, which is also glutamatergic, but terminates on GABAergic interneurons (Omelchenko and Sesack, 2009; Brinschwitz et al., 2010). In contrast to the glutamatergic afferences that directly target dopaminergic neurons, activation of this third type of afferences results in an inhibition of dopamine-cell firing. These afferences mainly originate in the LHb and inhibit dopaminergic cells in the VTA via two different pathways. LHb neurons either target GABAergic cells within the VTA itself or within its "tail", the recently defined RMTg. GABAergic cells from the RMTg then in turn inhibit dopaminergic cells within the VTA, so that the inhibitory effect of both pathways is similar (Omelchenko and Sesack, 2009; Kaufling et al., 2009; Brinschwitz et al., 2010).

1.2.3 The ventral tegmental area is implicated in reward circuitries, cognition and motivation

Within the VTA, three cell types have been described, including dopaminergic-, GABAergic- and glutamatergic cells (Geisler et al., 2007; Olson and Nestler, 2007; Yamaguchi et al., 2007). The dopaminergic neurons represent more than 50% of all VTA cells and are the functionally most important group, responsible for the regulation of reward circuitries, cognition and motivation (Schultz, 1998; Morris et al., 2004; Matsumoto and Hikosaka, 2009b) (paragraph 1.1.4.2). Besides the various physiological effects of dopaminergic neurons, they also play a key role in drug addiction, as most of the common drugs increase dopamine release (Wise, 1989; McBride et al., 1999; Rodd-Henricks et al., 2002; Ikemoto et al., 2003). The dopaminergic system is also involved in the etiology of psychiatric disorders, such as psychosis in general (Curran et al., 2004; Seeman et al., 2005), schizophrenia (Seeman et al., 1976; Howes et al., 2009; Murray et al., 2008), and attention deficit hyperactivity disorder (ADHD) (Sagvolden et al., 2005). The GABAergic population seems to have regulatory effects on the dopaminergic neurons and projects to various other parts of the brain (Olson and Nestler, 2007). Less is known about the role of glutamatergic cells in the VTA.

1.3 The mesencephalic serotonin system originates from the dorsal and median raphe nuclei

The raphe is a group of small nuclei, located around the midline of the brainstem along its entire rostro-caudal extent (Nissl, 1913). The name raphe (Latin for “fissure”) refers to the location of the raphe nuclei along the midline, the “fissure” of the two halves of the brainstem. The raphe nuclei use serotonin as their neurotransmitter and project to various areas from the spinal cord to the neocortex (see paragraph 1.3.2). The raphe nuclei can be divided into a medullar-, pontine- and midbrain group. This study focuses on the upward projecting midbrain group, consisting of the median raphe nucleus (MnR), also denoted as superior central nucleus, and the dorsal raphe nucleus (DR).

The DR is located below the aqueduct and above the decussation of the superior cerebellar peduncle. It is divided into an interfascicular, ventral, ventrolateral, dorsal and caudal subnucleus.

The MnR is situated exactly in the midline below the superior cerebellar peduncle. It is surrounded by the paramedian raphe (PMnR) and not further divided into subnuclei.

1.3.1 Dorsal and median raphe nuclei provide serotonergic innervations to various forebrain regions

Both midbrain raphe nuclei (MnR and DR) are part of the ascending serotonergic system, which projects to multiple forebrain areas, subcortical regions and brainstem nuclei. Their fibers mainly ascend within the medial forebrain bundle. A comparison of MnR and DR projections reveals that they basically target separate areas within the forebrain (Vertes, 1991; Vertes et al., 1999). While the MnR mainly projects to median structures and the limbic system, the DR has strong projections to cortical and striatal areas. This clear separation of DR and MnR projections suggests important functional differences between the two ascending serotonin systems (Vertes, 1991; Vertes et al., 1999).

Various structures provide input to DR and MnR, including cortical-, striatal- and limbic areas (Behzadi et al., 1990; Peyron et al., 1998; Vazquez-Borsetti et al., 2009). However, the strongest input comes from the LHb (Aghajanian and Wang, 1977; Herkenham and Nauta, 1979; Behzadi et al., 1990). The LHb projections to the raphe nuclei are thought to exert inhibitory effects on serotonergic cells (see paragraph 1.1.4.2) via a GABAergic mechanism (Wang and Aghajanian, 1977; Stern et al., 1979; Varga et al., 2003).

1.3.2 The mesencephalic serotonergic system modulates various physiological-, behavioral-, and cognitive functions

The mesencephalic serotonergic system originating in DR and MnR is implicated in a broad spectrum of functions. This is represented by widespread projections to almost every brain structure between the brainstem and the neocortex. Important functions of serotonergic neurons include the regulation of appetite (Curzon, 1990), locomotion (Jacobs and Fornal, 1993), stress response (Graeff et al., 1996), emotional and social behavior (Graeff, 2004), cognition and associative learning (Meneses and Hong, 1999), and the sleep-wake cycle (Dugovic, 2001).

Additionally, serotonin seems to be directly involved in reward-related behaviors (Schweighofer et al., 2007; Nakamura et al., 2008). Recent studies revealed that the activity of DR neurons encodes the reward value associated with the current behavior and the expected outcome and reward during behavioral tasks (Nakamura et al., 2008) (Bromberg-Martin et al., 2010). Moreover, the serotonergic system plays a key role in the etiology of psychiatric disorders, such as major depression and schizophrenia (Sandyk, 1992; Ellison, 1994; Lecourtier et al., 2004; Shepard et al., 2006).

1.4 Hyperpolarization-activated cyclic nucleotide-gated cation channels generate pacemaker activity in neuronal networks

Hyperpolarization-activated cyclic nucleotide-gated cation (HCN) channels are proteins that form ion-permeable pores across plasma membranes of nerve and muscle cells. Due to their ability to generate rhythmic cell activity, they are also known as "pacemaker channels". HCN channel proteins are encoded by four genes. They are widely expressed throughout the heart, the mesenteric plexus of the bowl, and the central nervous system (Biel and Michalakis, 2009).

1.4.1 HCN channels are tetrameric transmembrane proteins

HCN channels are a member of the superfamily of voltage gated potassium channels (Kv) (Gauss et al., 1998; Ludwig et al., 1998). They have a tetrameric structure that is either composed of four identical (homotetrameric) (Ludwig et al., 1998; Santoro and Tibbs, 1999) or non-identical (heterotetrameric) subunits (Chen et al., 2001; Much et al., 2003). Four of these subunits assemble in the plasma membrane to form a central ion pore. Each HCN subunit contains six transmembrane domains (S1-S6) with the pore-forming region between S5 and S6 and a cyclic-nucleotide (cAMP) binding-domain in the cytoplasmic C-terminal region (Craven and Zagotta, 2006).

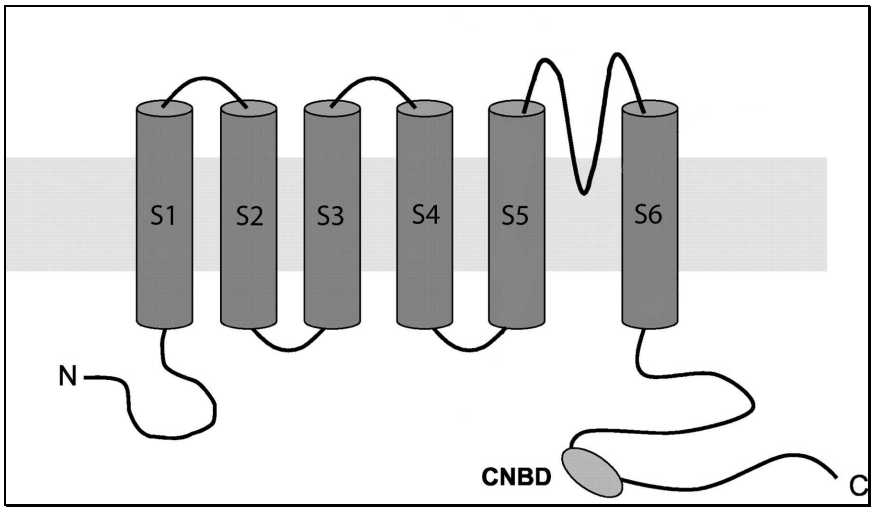

Figure 3: Each HCN subunit contains 6 transmembrane domains (S1-S6). The pore forming region is located between S5 and S6 and the cyclic nucleotide binding domain (CNBD) is located at the cytoplasmic C-terminal region.

1.4.2 HCN channels generate Ih currents

HCN channels are characterized by their outstanding ion selectivity and gating properties (Biel et al., 2002). In contrast to most other ion channels that are activated by membrane depolarization, HCN channels open in response to membrane hyperpolarization (Biel et al., 2002). Activated HCN channels conduct a slow non-selective inward cation current, which is known as Ih or If current (McCormick and Bal, 1997; Bal and McCormick, 1997; Luthi and McCormick, 1998). Electrophysiologically the Ih is characterized by its small magnitude and overlapping ion currents, including inward Na^+- and Ca^{2+}-currents (Pape, 1996; Robinson and Siegelbaum, 2003). Since Ih currents are inwardly rectified, the activation of HCN channels depolarizes the cell membrane (DiFrancesco, 1993).

A short hyperpolarization of the cell membrane occurs after every action potential (AP), but is also caused by accumulation of incoming inhibitory postsynaptic potentials (IPSPs). These short hyperpolarizations open the HCN channel and lead to a cation influx into the cell. The resulting currents slowly depolarize the cell toward the AP-threshold (DiFrancesco, 1993). Once the membrane potential reaches this threshold, other channels (mainly voltage - gated sodium channels) open and trigger the next AP. Thus, HCN channels generate spontaneous ongoing series of APs, in a pacemaker fashion (McCormick and Bal, 1997; Bal and McCormick, 1997; Luthi and McCormick, 1998). HCN channels are regulated by the concentration of intracellular cAMP, an important second messenger in various signaling cascades. Elevated cAMP levels induce a faster membrane depolarization resulting in an increased firing rate (DiFrancesco, 1993).

1.4.3 HCN channels are widely expressed throughout the brain

Spontaneously active cells exist throughout the entire brain. In most cases the spontaneous activity relies on the existence of HCN channels and their characteristic Ih currents (Luthi and McCormick, 1998). However, spontaneous activity can also be generated by other channels, including TTX sensitive-sodium channels or Cav1.3 calcium channels (Raman and Bean, 1999; Vandael et al., 2010). Consistent with this observation, previous studies demonstrate that all four HCN subunits are expressed throughout the adult mouse and rat brain at mRNA (Ludwig et al., 1998; Santoro et al., 1998; Moosmang et al., 2001; Santoro et al., 2000) and protein level (Notomi and Shigemoto, 2004). HCN1-immunoreactivity (ir) is predominantly located in neurons of the cerebral cortex, while HCN3 and HCN4 are mainly expressed in neurons of subcortical regions. HCN2-ir exists on neurons widespread throughout the brain but also on oligodendrocytes (Notomi and Shigemoto, 2004).

1.4.4 HCN channels are involved in various physiological functions of heart and brain cells

In addition to their role in the generation of pacemaker activity in heart and nerve cells (McCormick and Bal, 1997; Bal and McCormick, 1997; Luthi and McCormick, 1998; Ludwig et al., 1999), HCN channels are also involved in other physiological processes, such as dendritic integration (Magee, 2000), synaptic transmission (Beaumont and Zucker, 2000) and setting of the resting membrane potential in non-pacing cells (Nolan et al., 2007).

1.5 The hypothalamus is the superior regulator of the homeostatic system

1.5.1 The hypothalamus forms the ventral part of the diencephalon

The hypothalamus is formed by a group of small nuclei, located just below the thalamus on both sides of the third ventricle. It is anatomically divided into several subregions and areas. Along the rostro-caudal axis, the hypothalamus is separated into an anterior (preoptic), intermediate (infundibular) and posterior (mammillary) region. In the medio-lateral axis, each of these three regions can again be divided into a periventricular, a medial (MHA) and a lateral (LHA) area (Nissl, 1913). Within the medial area, several distinct nuclei produce releasing- and inhibiting- factors that exert control over the hormone release from the adenohypophysis. Two hormones with important vegetative functions, oxytocin and vasopressin (ADH) are produced in nuclei of the medial zone and released from the neurohypophysis. Thus, particularly the MHA links the central nervous system to the endocrine and vegetative nervous system.

In contrast to the well defined nuclei and functions of the MHA, less is known about the composition and functions of the lateral areas. These are located along the medial forebrain bundle and are divided into the rostral lateral preoptic area (LPOA) and the caudal lateral hypothalamic area (LHA) (Nissl, 1913). Based on morphological and immunocytochemical criteria, the LHA was further divided into various subareas (Nieuwenhuys et al., 1982; Geeraedts et al., 1990; Dissertation by Kowski, 2007). This division is still controversially discussed, particularly because no functional differences have been described so far.

1.5.2 The lateral hypothalamic area mainly projects to the lateral habenula

The hypothalamus integrates a large number of internal and external information. Major neuronal inputs originate in the reticular formation and other autonomic zones of the brainstem (Mikkelsen, 1990; Qi et al., 2008), where information from the vegetative periphery is relayed, as well as in many structures of the limbic forebrain (Herkenham and

Nauta, 1979; Elmquist, 2001). Information about internal states, like body temperature, hormone concentrations, osmolarity and glucose levels, is directly measured in the hypothalamus.

The hypothalamic output can be divided into an endocrine and a neural pathway. Endocrine control is primarily exerted by the MHA via the pituitary gland and the hypophyseal portal system. The neuronal output of the MHA targets most of the areas where input to the hypothalamus originates (Herkenham and Nauta, 1977; Palkovits, 1999).

Detailed tracing studies of the LHA found multiple efferent projections to some MHA nuclei, the rostral ventromedial medulla, the mammillary complex, the periventricular hypothalamic gray, the amygdala, the substantia nigra, the dorsal raphe nucleus, the VTA, the locus coeruleus and some thalamic nuclei. However the strongest of these projections targets the LHb (Swanson, 1976; Berk and Finkelstein, 1982; Kowski et al., 2008).

1.5.3 The hypothalamus coordinates various homeostatic mechanisms

Constituting the vegetative center of the brain, the hypothalamus is responsible for the regulation of pivotal homeostatic systems, including respiration, blood pressure, temperature, hormonal and behavioral circadian rhythms, food intake, and reproductive behavior. It therefore collects information from all these systems, integrates it and induces appropriate reactions (see paragraph 1.5.2). These reactions are either triggered via hormone release, via the vegetative nervous system, or via activation of the limbic system and reward circuitries. While the endocrine and the vegetative nervous system are mainly regulated by the MHA, the output to the limbic system mainly comes from the LHA (Swanson, 1976; Berk and Finkelstein, 1982; Kowski et al., 2008). The LHA is a very heterogeneous brain area with neurons producing various types of neurotransmitters, including GABA and glutamate as well as various neuropeptides. Neuropeptides produced by LHA cells are galanin, orexin-A and orexin-B, arginin-vasopressin (AVP), Neuropeptide Y (NPY) and melanocyte-stimulating hormone (MCH) (Melander et al., 1986; Miller et al., 1993; Nambu et al., 1999). However, less is known about how the influence on the limbic system is mediated and which structures are involved. One promising candidate to transmit important homeostatic information from the LHA to the reward circuitries is the LHb, which is connected to both systems (Phillipson, 1979; Herkenham and Nauta, 1979; Oades and Halliday, 1987).

1.6 Objectives of the study

1.6.1 Molecular mechanism underlying the lateral habenular inhibition on monoamine release

Based on the anatomy, the LHb is in an excellent position to integrate reward-encoding information from the hypothalamus and other forebrain areas and to transmit this information to reward-mediating brainstem nuclei. Recent studies suggest that the LHb tonically suppresses the activity of monoaminergic brainstem cells and that this inhibition may be modified when required by the ongoing situation (Kim and Chang, 2005; Lecourtier et al., 2008; Matsumoto and Hikosaka, 2009a). This inhibition seems to be near-maximal, as stimulation of the LHb produces only minimal further decreases of extracellular dopamine levels (Lecourtier et al., 2008). Currently it is unknown how and where this tonic inhibition is generated. Two possible models may underlie this phenomenon. LHb neurons may be more or less continuously activated by other brain areas. Alternatively, spontaneous activity may be directly generated within the LHb and only modulated by other areas. Here we hypothesize that the tonic activity responsible for the inhibition of monoaminergic cells is intrinsically generated within the LHb projection neurons.

In the LHb spontaneously active cells are known (Kim and Chang, 2005; Weiss and Veh, 2010). It is not clear, however, whether these cells are responsible for the tonic inhibition of monoaminergic neurons. In heart- and nerve cells, spontaneous activity is generated by a family of ion channels (Ludwig et al., 1998), the so-called hyperpolarization-activated cyclic nucleotide-gated cation (HCN) channels (paragraph 1.4) (Luthi and McCormick, 1998). In the first part of the present investigation, therefore, we have analyzed the regional and cellular localization of HCN1 to HCN4 mRNAs and their respective proteins in the habenular complex of the rat. Our interest was focused on those LHb neurons, which project to the VTA, the DR and the MnR. In particular, we aimed to answer the following questions:

1) How are the four HCN subunit mRNAs and proteins distributed within the lateral habenular subnuclei?

Initially, HCN mRNA expression levels were evaluated in tissue samples of the rat Hb by quantitative PCR analysis. Thereafter, HCN riboprobes against the four subunits were generated and the distribution of HCN mRNAs and proteins within the LHb subnuclei was analyzed.

2) Do LHb neurons projecting to VTA, MnR or DR express HCN mRNAs?

To answer this question, retrograde tracing into VTA, MnR and DR was combined with subsequent HCN *insitu* hybridization. Double-labeled lateral habenular sections were then analyzed for HCN-positive retrogradely traced neurons.

3) What is the subunit pattern of HCN expression, and does it differ between VTA-, MnR- and DR-projecting neurons?

For each of the three target areas, the percentages of HCN mRNA expressing projection neurons were evaluated by quantifying retrogradely traced- and HCN-positive cells in LHb sections.

1.6.2 Characterization of a projection from the lateral hypothalamic area to the lateral habenula

Negative and positive rewards induce significant changes in the activity of LHb neurons (Matsumoto, 2009). Thus, the second part of this study focuses on the modulation of the LHb baseline inhibition. The LHA is a promising candidate to provide reward-related information, especially about internal states and the effects of behaviors, to the LHb. While there is a massive projection from the LHA to the LHb (Herkenham and Nauta, 1977), the effects of this projection on LHb activity and the structures specifically targeted within the LHb are currently unknown.

To learn about potential effects of this connection the following questions were posed:

1) Which neurotransmitters are used by LHA axons projecting to the LHb?

Therefore, anterograde tracing into the LHA was combined with subsequent double-labeling of neurotransmitters and tracer. Double-labeled LHb sections were then analyzed at the confocal laser scanning microscope (CLSM) and electron microscope (EM).

2) Do LHA terminals directly target LHb neurons projecting to the VTA?

To answer this question, double tracing studies injecting an anterograde tracer into the LHA and a retrograde tracer into the VTA were performed. LHb sections of double-raced rats were subsequently checked for direct synaptic contacts between anterogradely traced terminals and retrogradely traced neurons using the CLSM.

The biological role of the reward system is to induce or omit behaviors necessary to keep the body homeostatically balanced. The present investigation will help to understand how these two systems interact. The LHb appears to be involved in the pathomechanisms of important neuropsychiatric disorders. Thus, the present work may also be helpful in identifying novel potential targets for pharmacotherapeutical intervention.

2. Materials and Methods

2.1 Animals

For this study, adult male Wistar rats, weighing 250–300 g, were used. They were obtained from the department for experimental medicine (FEM) at Charité Berlin, where they were kept in group housing under standard conditions (22 °C; 12/12 hours light/dark cycle; water and food ad libitum). All animal experiments were carried out in compliance with institutional guidelines and were approved by the Regional Berlin Animals Ethics Committee (G0371/08). Fourteen animals were used for tracing and twelve for PCR experiments.

2.2 Materials

2.2.1 Chemicals and Substances

Acetate	Roth, Germany
Acetic acid	Merck, Germany
Acetone	Roth, Germany
Agarose	Roth, Germany
Aminosilane	Merck, Germany
Ammonium nickel sulfate (ANS)	Fluka, Germany
Ampicillin	Roth, Germany
Araldite	Serva, Germany
Bovine serum albumin (BSA)	Sigma-Aldrich, Germany
Bromophenolblue	Roth, Germany
Casein	Sigma-Aldrich, Germany
Cresyl violet	Sigma-Aldrich, Germany
Deltadex 60 plasma substitute	Delta Select, Germany
Dextrane sulfate	Fluka, Germany
Diaminobenzidine (DAB)	Sigma-Aldrich, Germany
Dimethylformamide (DMF)	Sigma-Aldrich, Germany
Disodium hydrogen phosphate	Merck, Germany
DL-dithiothreitol (DTT)	Sigma-Aldrich, Germany
DMP 30	Sigma-Aldrich, Germany
Dodecenylsuccinicanhydride (DDSA)	Serva, Germany
E. coli t-RNA	Roche, Germany
Ethanol	Herbeta, Germany
Ethidium bromide	Roth, Germany
Ethylenediaminetetraacetic acid (EDTA)	Roth, Germany
Entellan	Merck, Germany
Ethanol	Merck, Germany
Ethylene glycol	Merck, Germany
Ficoll	Sigma, Germany
FluoroGold (FG)	Fluorochrome, USA
Gelatine	Merck, Germany
Glutaraldehyde	Merck, Germany
Glycerol	Merck, Germany
Gold chloride	Sigma-Aldrich, Germany

Gum Arabic	Sigma-Aldrich, Germany
Hexane	Merck, Germany
Hydrogen peroxide	Merck, Germany
Imidazole	Sigma-Aldrich, Germany
Isoflurane	Abbott, Germany
Isopropanol	Braun, Germany
Isopropyl-β-D-thiogalactopyranosid (IPTG)	Sigma-Aldrich, Germany
Ketamine hydrochloride	Delta Select, Germany
Lead nitrate	Fluka, Germany
Lithium carbonate	Ferak Laborat, Germany
Longasteril	Fresenius, Germany
Luxol fast blue	Sigma-Aldrich, Germany
Mercaptoethanol	Sigma-Aldrich, Germany
Methanol	Merck, Germany
Methyl green	Sigma-Aldrich, Germany
Mount Fluor	BioCyc, Germany
Normal goat serum (NGS)	Interchem., Germany
Normal horse serum (NHS)	Interchem., Germany
Osmium tetroxide	Sigma-Aldrich, Germany
Paraformaldehyde	EM Sciences, USA
Periodic acid	Merck, Germany
Phaseolus-Leucoagglutinin (PhaL)	Vector, USA
Phenylhydrazine	Merck, Germany
Picric acid	Sigma-Aldrich, Germany
Pioloform	Sigma-Aldrich, Germany
Polyvinyl-pyrrolidone	Sigma-Aldrich, Germany
Potassium chloride	Merck, Germany
Potassium chromosulfate-12-hydrate	Merck, Germany
Propylene oxide	Serva, Germany
Sodium azide	Merck, Germany
Sodium borohydride	Sigma-Aldrich, Germany
Sodium carbonate	Merck, Germany
Sodium chloride	Merck, Germany
Sodium citrate	Merck, Germany
Sodium dihydrogen phosphate	Merck, Germany
Sodium hydroxide	Merck, Germany
Sodium metaperiodic acid	Merck, Germany
Sodium methoxide	Fluka, Germany
Sodium nitrate	Merck, Germany
Sodium thioglyconat	Fluka, Germany
Sucrose	Merck, Germany
Thimerosal	Serva, Germany
Toluol	Merck, Germany
Toluidine blue	Merck, Germany
Trishydroxymethylaminomethane (TRIS)	Merck, Germany
Triton X-100	Sigma-Aldrich, Germany
Uranyl acetate	Merck, Germany
WGA-apo-HRP-gold	E-Y laboratories, USA
X-Gal	Merck, Germany

Xylazine hydrochloride	Bayer Vital, Germany
Xylencyanol	Merck, Germany
Xylol	J.T. Baker, Netherlands

2.2.2 Kits, Enzymes and Buffers

Advantage Taq 2 polymerase	Clontech, Germany
Desoxynucleotidtriphosphate (dNTPs)	Fermentas, Germany
DIG RNA labeling Kit (SP6/T7)	Roche, Germany
DNA - Marker λ-Eco47I	Fermentas, Germany
Elite ABC Kit	Vector Laboratories, USA
E. coli XL1 blue	Promega, Germany
Loading dye 6x	Fermentas, Germany
pGEM-T vector	Promega, Germany
Primers	Qiagen, Germany
Qiagen Midiprep Kit	Qiagen, Germany
Qiagen Miniprep Kit	Qiagen, Germany
QIAquick Gel Extraction Kit	Qiagen, Germany
Silver enhancement kit (Intense M)	Amersham Bioscience, UK
RNeasy Mini Prep Kit	Qiagen, Germany
Rapid Ligation Buffer 2x	Promega, USA
Restriction Buffer (blue)	Fermentas, Germany
Restriction endonucleases	Fermentas, Germany
RNAse-A	Boehringer, Germany
RNAse-free H_2O	Qiagen, Germany
Sensiscript RT Kit	Qiagen, Germany
TaqMan assays	Applied Biosys., Germany
TaqMan Universal PCR Master Mix	Applied Biosys., Germany
T4 DNA Ligase	Promega, USA
tRNA	Roche, Germany

2.2.3 Installations, Equipments and Devices

Anesthesia workstation	Hallowell EMC, USA
Camera CX 9000	MBF Bioscience, USA
Centrifuge Labofuge 400 R	Heraeus, Germany
Centrifuge 5417 C	Eppendorf, Germany
CLSM	Carl Zeiss, Germany
Continuous-current-generator, MVVCS02	NPI electronic, Germany
Controller for XYZ-stage	LudlElectronic, USA
Cryomicrotome (Frigocut 2800)	Reichert-Jung, Germany
Current pulse generator, Master 8	AMPI, Israel
Diamond knife	Diatome, Switzerland
Electron microscope (EM 900)	Carl Zeiss, Germany
Electrophoresis chamber	Kreutz, Germany
Feedback loop rectal sensor	List Medical, Germany
Glass micropipettes (1mm)	Science products, Germany
Heating cabinet	Heraeus, Germany
Heating pad	List Medical, Germany
Incubator	Heraeus, Germany

Leica DMRB microscope	Leica, Germany
Nickel and gold grids	Leica, Germany
Neurolucida software, version 8	MBF Bioscience, USA
PCRmastercycler	Eppendorf, Germany
Power supply unit, Power Pac 200	Bio-Rad, USA
Prism software 4.0	GraphPad software, USA
Puller, P97	Sutter Instruments, USA
Rat anesthesia adaptor	Kopf Instruments, USA
Shaker, Certomat	Biotech, France
Stereotactic frame	Kopf Instruments, USA
Sutures	Ethibond, Germany
Ultramicrotome, Reichert Ultracut S	Leica, Germany
UV-Photometer UV-1202	Shimadzu, Japan
Vibratome VT 1000 S	Leica, Germany

2.2.4 Antibodies and Dilutions

Antigen	**Donor**	**Labeling**	**Manufacturer**	**Cryostat**	**Vibratome**
HCN1	Rabbit	-	Alamone, USA	1.000	x
HCN2	Guinea pig	-	Dr. Shigemoto	5.000	x
HCN3	Rabbit	-	Dr. Shigemoto	1.000	x
HCN4	Rabbit	-	Alamone, USA	100	x
Fluoro Gold	Rabbit	-	Chemicon, USA	5.000	500
Phaseolus	Rabbit	-	Vector, Germany	5.000	500
Phaseolus	Goat	-	Vector, Germany	5.000	500
vGluT 1	Guinea Pig	-	Chemicon, USA	1.000	500
vGluT 2	Guinea Pig	-	Chemicon, USA	2.000	500
vGluT 3	Guinea Pig	-	Chemicon, USA	2.000	500
Orexin	Rabbit	-	Alpha Diagnostik, Ger.	2.000	500
Galanin	Rabbit	-	Peninsula Lab., USA	1.000	500
NPY	Rabbit	-	Peninsula Lab., USA	2.000	500
Vasopressin	Rabbit	-	MBL Int. Corp., USA	2.000	500
MCH	Chicken	-	BMA Biomed., USA	1.000	1000
GAD	Rabbit	-	Chemicon, USA	2.000	500
Digoxigenin	Mouse	-	Vector, Germany	10.000	x
Synaptophysin	Mouse	-	Sigma, Germany	500	x
TMR	Rabbit	-	Mol. Probes, USA	5.000	x
Phaseolus	Goat	Biotin	Vector, Germany	1.000	500
Guinea Pig IGG	Goat	Biotin	Vector, Germany	2.000	500
Mouse IGG	Horse	Biotin	Vector, Germany	2.000	x
Chicken IGG	Goat	Biotin	Vector, Germany	2.000	500
Goat IGG	Horse	Biotin	Vector, Germany	2.000	500
Rabbit IGG	Goat	Biotin	Vector, Germany	2.000	500
Rabbit IGG	Goat	Cy5	Vector, Germany	500	500
Mouse IGG	Donkey	Cy2	Vector, Germany	500	500
Rabbit IGG	Goat	AF488	Vector, Germany	500	500

2.3 Quantitative PCR

cDNA preparations from six rat habenulae were used for quantitative PCR qPCR (kind gifts of Dr. Christian Derst and Dr. Torsten Weiss). RNAs were isolated and purified using RNeasy Mini Prep Kit following the manufacturer's instructions and reverse transcribed using the Sensiscript RT Kit. After 1:10 dilution, the resulting cDNA was used as a template for qPCR. The following TaqMan assays were used for quantitative amplification: HCN1: RN00584498_m1, HCN2: Rn01408575_gH, HCN3: Rn00586666_m1, HCN4: Rn00572232_m1. All assays were used in a duplex PCR reaction with either GAPDH (FG, RAT GAPD MGB) or β-actin (FG, RAT ACTB MGB) as endogenous controls. In a first step the amplification efficiency of each of the four HCN assays was determined using a standard curve generated from dilutions of a positive control (whole brain cDNA). In a second step, qPCR was performed using 10 µl 2× TaqMan Universal PCR Master Mix, 1 µl 20× HCN TaqMan assay, 1 µl 20× endogenous control MGB assay, 3 µl H_2O and 5 µl habenula cDNA. A standard thermal profile was used for quantification (1 precycle for 10 minutes at 95 °C followed by 45 cycles with 15 seconds 95 °C and 1 minute 60 °C). All combinations of habenula cDNA and HCN TaqMan assay were set up in triplicate. For each sample, Ct values were obtained for HCN assay and endogenous control (EC). As a measure for relative expression ΔCt - values, as Ct (EC)-Ct (HCN), were calculated and corrected by a defined efficiency factor for each HCN assay. To enable comparison among experiments, the fluorescence threshold was manually set to a defined value (see also "Relative Quantification Getting Started Guide"; obtainable from Applied Biosystems). Results were plotted and statistically analyzed with GraphPad Prism software 4.0 using "One-way analysis of variance" (ANOVA) and post hoc Tukey Kramer multiple comparison test. The following formula was used to calculate relative fold change: $2^{(Cta-Ctb)}$ in which Cta is cycle threshold average of HCN2, 3 and 4 and Ctb is cycle threshold for HCN1.

2.4 Riboprobe generation

2.4.1 Selection of cDNA sequences for the HCN riboprobes

The cDNA preparations used for qPCR were also used for riboprobe generation. To generate highly specific riboprobes against each of the four HCN mRNAs, it is necessary to select sequences with a minimal overlap to other mRNAs. Using the program NCBI Blast, these sequences were determined by comparing the homologies between the four different HCN mRNAs and all other mRNAs. The smallest overlap exists in the area around the stop-codon. Homologies between the paralogous HCN sequences range between 35% and 48%.

The following primers were used for amplification:

rHCN1/NM_053375 nucleotides: 2411 – 3065	5`tggtagttccacaccgaaaa`3	5`cctttaatggttttaaagaaaggaa`3
rHCN2/AF_247451 nucleotides: 2209 – 2512	5`tacggtgtgcctggctct`3	5`caagggtcacaagttggaaga`3
rHCN3/NM_053685 nucleotides: 1734 – 2169	5`cagagacatggctcgtggta`3	5`ggttgagaggcagagagtgg`3
rHCN4/NM_021658 nucleotides: 2544 – 3284	5`atatggaccccactgatcca`3	5`gggggtaaaggctacaggag`3

2.4.2 PCR amplification of cDNA

During polymerase chain reaction (PCR) the template DNA is denaturized into single strands. At the appropriate annealing temperatures, added primers hybridize to their respective strand and act as the starting point for DNA polymerase, elongating a new complementary strand. Multiple repetitions of this process generate amplification of the selected HCN1-4 cDNA sequences.

PCR cycle:

Step	Temperature (°C)	Time (seconds)
1. Initiation (1x)	94	120
2. Denaturation	94	30
3. Annealing	57	60
4. Elongation	68	120
5. Repetition from 2. (35 cycles)	-	-
6. End	68	180

PCR mixture (50 µl):

10 x Puffer	5 µl
Desoxynucleotidtriphosphate (2.5 mM each)	10 µl
Primer forward (100 pmol/µl)	1 µl
Primer backward (100 pmol/µl)	1 µl
cDNA (rat brain)	3 µl
Advantage Taq 2 Polymerase	1 µl
H_2O	29 µl

2.4.3 Gel electrophoresis of the PCR products

To verify successful amplification, the PCR product was electrophoretically separated in 1% agarose gel in 1 x TAE buffer (40 mM Tris, 20 mM acetate, 1 mM Na_2 EDTA) with 1 µl ethidium bromide added. Ethidium bromide is a fluorescent dye which intercalates with the DNA and makes it visible under ultraviolet light. Electrophoresis was run at 80 V for 40 minutes. As a DNA size marker λ-Eco47I was used and 2 µl 6 x Loading Dye (10 mM Tris-HCl, 0.03% bromophenol blue, 0.03% Xylencyanol FF, 60% Glycerol, 60 mM EDTA) were added to the DNA samples.

2.4.4 Gel-extraction of DNA fragments

DNA was separated by gel-electrophoresis (paragraph 2.4.3) and the band at the expected size of the amplified sequence was cut out of the gel. To extract the DNA from the gel the QIAquick Gel Extraction Kit was used. The gel fragment with the DNA was weighted and completely dissolved in 3 µl QG buffer/mg gel at 50 °C for 10 minutes. After adding 1 µl isopropanol per 1 mg gel the solution was centrifuged through a spin column and the flow-through was discarded. During this process the DNA binds to the column. To remove all traces of agarose 0.5 ml of QG buffer was added to the column and centrifuged for 1 minute again. Then, DNA was washed twice by adding 0.75 ml of PE buffer and centrifugation for 1 minute each. Finally the column was placed into a clean collection tube and the DNA was eluted by adding 50 µl of RNAse-free H_2O to the column and centrifugation for 1 minute at 14,000 rpm. To increase DNA concentration of the sample, the collection tube was placed into a vacuum centrifuge for 15 minutes.

2.4.5 Cloning of DNA fragments into a pGEM-T vector system

pGEM-T is a vector system used for the cloning of PCR products. The plasmid DNA encodes for ampicillin resistance and contains T7- and SP6- RNA polymerase promoters, flanking a multiple cloning region within the α-peptide, coding region for β-galactosidase (lacZ). Insertional inactivation of the α-peptide allows recombinant clones to be directly identified by color screening on indicator plates. cDNA sequences amplified with the Taq polymerase always have an overlapping adenine (A), which easily assembles to the overlapping thymine (T) of the pGEM-T vector. This procedure is known as TA-Cloning. To clone the amplified cDNA sequences into a pGEM-T vector system the following ligation mixture was prepared and incubated overnight at RT:

Ligation mixture (10 µl):

2 x Rapid Ligation Buffer	5 µl
pGEM-T Vector	1 µl
PCR-amplified DNA	3 µl
T4 DNA Ligase	1 µl

2.4.6 Transformation of pGEM-T vectors into *E.coli* XL1 blue

E.coli XL1 blue are endonuclease and recombination deficient bacterial cells, which improves the quality of miniprep DNA and insert stability. A mixture of 100 µl of competent cells (*E. coli*, XL1 blue) and 10 µl ligation mixture was incubated on ice for 1 hour. After transformation, the cells were crossed out on LB agar containing 50 µg/ml ampicillin and 20 µl 2% X-Gal (color indicator, 5-bromo-4-chloro-3-indoyl-β-D-galactopyranoside) dissolved in dimethyl formamide und 20 µl 100 mM IPTG (inductor of lacZ, Isopropyl-β-D-thiogalactopyranoside) were added. Plates were incubated overnight at 37 °C. By adding IPTG to the cells, the expression of galactosidase was induced. This enzyme can be detected with the indicator X-Gal by a color reaction, leading to blue colonies on the agar plate. Because the LacZ-gen was inactivated in plasmids with an insert, cell-clones which took up a successfully ligated plasmid with an insert did not show a color reaction (white colonies). The next day only white colonies were picked under sterile conditions, transferred to 1.5 ml LBA culture medium (25 g/l LB in bidistilled H_2O, autoclaved, 100 µg/ml ampicillin) and incubated overnight at 37 °C on a shaker.

2.4.7 Small scale - preparation of plasmid – DNA (Mini Prep)

For plasmid purification from 1.5 ml overnight cultures of *E. coli,* the Qiagen Miniprep Kit was used. Overnight, LBA cultures of XL1 blue cells containing plasmid DNA were centrifuged for 6 minutes at 6000 rpm and the supernatant was discarded. Pellets of bacterial cells were resuspended in 250 µl buffer P1 (containing RNase) and transferred to a centrifuge tube. After adding 250 µl buffer P2 to the suspension, the tube was inverted 4-6 times to lyse the bacterial cells. Then, 350 µl buffer N3 was added, the tube was again inverted 4-6 times and centrifuged for 10 minutes at 14,000 rpm. The supernatant was decanted to a spin column, centrifuged for 60 seconds and the flow-through was discarded. Columns were again centrifuged for 60 seconds after adding 500 µl PB buffer. Thereafter plasmid DNA was washed twice by adding 0.75 µl ml of PE buffer to the column and centrifugation for 60 seconds each. Finally the column was placed into a clean collection tube and the DNA was eluted by adding 50 µl of RNAse-free H_2O to the column and centrifuged for 1 minute at 14,000 rpm. To increase DNA concentration of the probe, the collection tube was placed into

a vacuum centrifuge for 15 minutes. Concentration of DNA was calculated from the optic density OD_{260nm}, measured against water. Double stranded DNA of a 50 µg/ml concentration has a value of 1. The quotient from OD_{260nm} to OD_{280nm} indicates the purity of the DNA. Values greater than 1.8 are indicative of highly purified DNA.

2.4.8 Restriction analysis and sequencing

To control successful ligation, plasmid DNA was digested with restriction endonucleases, *Not*I in combination with either *Cfr*42i or *Pae*I for 90 minutes at 37 °C and subsequently separated by gel-electrophoresis. Restriction sites were located within the *multiple cloning site* of the plasmid. Double digestions of vectors with an insert resulted in two bands, the vector and the excised insert. Only probes with an insert of the expected size were sent for sequencing (JenaGen, Jena, Germany).

Restriction mixture (10 µl):

Buffer (green or *Bam*H1)	1 µl
*Not*I	1 µl
*Cfr*42i or *Pae*I	1 µl
Plasmid DNA	1 µl
H_2O	6 µl

2.4.9 Intermediate scale - preparation of plasmid DNA (Midi Prep)

To increase the amount of plasmid DNA, 25 ml cultures of sterilely picked *E. coli* XL1 blue colonies containing plasmid DNA were incubated overnight at 37 °C on a shaker. For plasmid purification from 25 ml overnight cultures, the Qiagen Filter Kit was used. LBA cultures of XL1 blue cells were centrifuged for 15 minutes at 6,000 rpm at 4 °C and the supernatant was discarded. Pellets of bacterial cells were resuspended in 4 ml buffer P1 (containing RNAse). After adding 4 ml buffer P2 to the suspension, the tube was inverted 4-6 times and incubated for 5 minutes at RT to lyse the bacterial cells. After 4 ml of chilled buffer P3 was added, the tube was inverted 4-6 times, incubated for 15 minutes on ice and centrifuged for 30 minutes at 20,000 rpm at 4 °C. The supernatant, containing the plasmid DNA was decanted to an equilibrated QiagenTip 100 (filter tube) and allowed to enter the resin by gravity flow. The QiagenTip 100 was washed twice with 10 ml QC buffer and plasmid DNA was eluted with 5 ml QF buffer and collected to a spin tube. DNA was precipitated by adding 3.5 ml isopropanol to the solution followed by a centrifugation for 30 minutes at 14,000 rpm at 4 °C. After decanting the supernatant, DNA was washed with 75% isopropanol and again

centrifuged for 15 minutes at 14,000 rpm. Isopropanol was carefully decanted and pellet was air-dried for 15 minutes at RT. Finally DNA pellet was eluted in H_20.

2.4.10 Linearization of MidiPrep Plasmid DNA

For the linearization of plasmid DNA the following mixture was prepared and incubated at 37 °C for 90 minutes.

Buffer (blue/orange)	1 µl
*Not*I or *Pae*I	1 µl
Plasmid DNA	4 µl
H_2O	4 µl

2.4.11 Digoxigenin labeling of the linearized plasmid

For the preparation of digoxigenin-labeled riboprobes, appropriately linearized vector DNA and the DIG RNA labeling Kit (SP6/T7) were used. This kit labels the RNA with digoxigenin-UTP by in vitro transcription with SP6 or T7 RNA polymerase, to generate antisense and sense riboprobes. For the RNA labeling reaction, 1 µg purified template DNA and 12 µg RNase-free bidistilled water were added to a sterile reaction vial. The reaction vial was placed on ice before adding 2 µl 10x NTP labeling mixture, 2 µl 10x Transcription buffer, 1 µl Protector RNase inhibitor and either 2 µl RNA Polymerase SP6 or T7. After mixing gently and centrifuging briefly, the vial was incubated for 2 h at 37 °C. After the labeling reaction, 2 µl of DNase I was added to the solution to remove the template DNA in another incubation for 15 min at 37 °C. Finally the reaction was stopped by adding 2 µl 0.2 M EDTA (pH 8.0). Labeled riboprobes were stored at – 80 °C until use.

2.5 Tracing Experiments

2.5.1 Anesthesia

Rats were deeply anesthetized by placing them into a plexiglas chamber, ventilated with 5% isoflurane (in 100% O_2). During surgery, anesthesia was continued by application of 3% isoflurane/oxygen through a rat anesthesia adaptor with a flow rate of 0.6 liters/minute. The core body temperature was maintained through a heating pad, connected to a feedback loop rectal sensor.

2.5.2 Stereotactic surgery

Deeply anesthetized rats were put into a stereotactic frame consisting of the rat anesthesia adaptor, fixed on the animal's snout, and two bars fixating the rat's skull at its ear canals. The

head was centered to the frame by adjustment of the ear bars. After removing the hair from the surgery area, skin was sagittally cut in the head's midline. Subcutaneous tissue and periost were removed to bring out the cranial bone sutures for further orientation. Then, the rat's head was readjusted exactly into a horizontal position by moving the anesthesia adaptor up or down until the points Bregma (intersection of sagittal and coronal suture) and Lambda (intersection of sagittal and lambdoid suture) were at equal heights. Coordinates for trepanation were calculated from Bregma and the midline (sagittal suture), according to the Paxinos atlas of the rat brain (Paxinos and Watson, 1998). After drilling the holes into the skull and resetting the third coordinate for the depth of the injection, the dura mater was opened. The glass micropipette, filled with the tracer substance, was then carefully lowered from the surface of the brain to the target area. After injection, the micropipette was left in situ for another 15 minutes to avoid spread of tracer along the injection duct. Finally surgery area was disinfected with 3% H_2O_2 and skin was closed with simple interrupted sutures. Rats were kept warm in single cages until full recovery from anesthesia.

2.5.3 Tracer application

For tracer application, 1 mm glass micropipettes were used. Their tips were created with a puller and broken on a glass block under microscopic control to outer tip diameters between 10 – 15 µm for FluoroGold (FG) and Phaseolus-Leucoagglutinin (PhaL) injections, and 30 - 40 µm for WGA-apo-HRP-gold injections. Tracers with uncharged molecules (WGA-apo-HRP-gold) were pressure-applied and those with charged molecules were iontophoretically injected (FG and PhaL). WGA-apo-HRP-gold pressure application was performed manually with a syringe connected to the injection micropipette over a flexible tube. The amount of injected tracer was controlled by observing the decreasing fluid-level in the micropipette. Iontophoretic application of FG and PhaL was carried out with a positive current generated by a high precision continuous-current-generator and pulsed in a seven second on-off cycle to prevent heating at the tip of the micropipette. FG was applied with an amperage of 1 µA and PhaL with an amperage of 4 µA, both for 15 minutes.

2.5.3.1 Anterograde tracing

As anterograde tracer the Isolectin L (Leucoagglutinin) of Phaseolus vulgaris agglutinin (PhaL, 2% in 0.01 M phosphate buffer, pH 7.4) was used. It was iontophoretically injected unilaterally into the postero-lateral division of the hypothalamus according to the Paxinos

atlas of the rat brain (Paxinos and Watson, 1998) to visualize the axons and terminals originating from the LHA within the LHb.

LHA injection coordinates:
Bregma: -2.7 mm, m-l extent: +1.8 mm, touch-dura: -8.25 mm, injection angle: 0 °

Within the injection area, PhaL is taken up by the dendrites or somata of neurons via an active transport mechanism (binding to N-acetyl-Glucosamine or beta-D-Galactose) or via passive transmembrane diffusion. The tracer is then transported along the microtubules system towards the axons and their terminals. The active transport is mediated by plus-motor proteins like the axonal *Kinesin* and takes about 8-10 days. After immunocytochemical visualization, the terminals demark as so called *buttons,* which appear as clearly distinguishable swellings along the axons (buttons in passing) or at their ends (terminal buttons).

2.5.3.2 Retrograde tracing

As retrograde tracers, the gold-labeled wheat germ agglutinin coupled to a horseradish peroxidase (WGA-apo-HRP-gold) and FluoroGold (FG; 1% 2-hydroxy-4.4-diamino-stilbene in 0.1 M cacodylate buffer, pH 7.4) were used for this study. For visualization of LHb neurons with projections to the VTA, the MnR or the DR a small amount of WGA-apo-HRP-gold was injected unilaterally into these areas according to the Paxinos atlas of the rat brain (Paxinos and Watson, 1998):

VTA:
Bregma: -6.5 mm; m-l extent: +0.5 mm; touch-dura: -7.9 mm; injection angle: 0 °
MnR:
Bregma: -7.8 mm; m-l extent: +0.8 mm; touch-dura: -7.8 mm; injection angle: 6 °
DR:
Bregma: -7.8 mm; m-l extent: +0.9 mm; touch-dura: -5.8 mm; injection angle: 6 °

Within the injection area, FG passively diffuses into the terminals where it is incorporated into lysosomes. From there, tracer filled vesicles are transported along the microtubules system towards the cell soma and their dendrites. Active transport in this direction is mediated by minus-motor proteins like *Dynein*. For both tracers, transport takes about 2-3 days until enough tracer molecules have accumulated in the soma. After immunocytochemical

visualization, FG-filled cell bodies and dendrites appear. WGA-apo-HRP-gold is also taken up by the terminals and transported along the microtubules system within vesicles. As this tracer is coupled to gold particles, it was visualized by silver intensification.

2.5.4 Perfusion fixation

Three (WGA-apo-HRP-gold and FG) to ten days (PhaL) after stereotactic surgery, rats were again deeply anesthetized with isoflurane 5% in a plexiglas chamber, followed by an intraperitoneal injection of 45% ketamine hydrochloride (50 mg/ml), 17.5% xylazine hydrochloride (20 mg/ml,) and 37.5% saline, at a dose of 0.32 ml/100 g body weight. After fixating the rats in supine position on a polystyrene plate, the abdomen was opened by median laparotomy and the skin above the sternum was incised. Thorax was opened by a parasternal incision and held open by a spreader. After preparation of the heart, the left ventricle was incised and the perfusion-cannula was quickly pushed through the left ventricle into the ascending aorta where it was fixed by a clamp. Finally the right auriculum of the heart was opened to allow the blood and perfusion solutions to flow out. To ensure a high tissue quality the hypoxia-time from opening the thorax to the start of the perfusion was kept short (20 to 60 seconds).

Rats were transaortically perfused:

1. with Deltadex 60 plasma substitute at 37 °C for 10 seconds with a pressure of 210 mmHg to remove the blood,
2. followed by the perfusion solution containing 4% paraformaldehyde, 0.05% glutaraldehyde, 0.2% picric acid in 0.1 M phosphate buffer (PB) (pH 7.4) for 5 minutes at a pressure of 210 mmHg and for another 25 minutes at a pressure of 20 mmHg to fix the brain tissue
3. and finally with 0.2 M sucrose in 0.1 M PB (pH 7.4) for another 5 minutes at a pressure of 100 mmHg to cryoprotect the tissue.

Immediately after the perfusion, brains were removed carefully from the skull and adjusted to a plexiglas frame, where they were embedded into 4% agarosis. After hardening of the agarosis, the embedded brains were cut into predefined coronal blocks (4.0 mm to 7.5 mm). The blocks were soaked in 0.4 M and 0.8 M sucrose for cryoprotection over night, then shock frozen in hexane at -70 °C and stored at -80 °C.

2.5.5 Obtaining series of sections

2.5.5.1 Cryomicrotome

On a cryomicrotome, 20-25 µm coronal sections were obtained at a temperature of -20 °C. Sections were collected in ten PBS (150 mM sodium chloride in 10 mM Phosphate buffer (PB, 100 mM NaH_2PO_4 in H_2O; pH 7.4 with NaOH) filled glasses, to produce ten series of sections with a distance of 250 µm between two sections of one series. For storage, series of sections were transferred to an anti-freeze-solution (AFS; 2.2 M Sucrose in 100 mM PB and 42% ethylene glycol, pH 7.4) and stored at -20 °C. For visualization of tracers and Kluever-Barrera staining, whole series were used.

2.5.5.2 Vibratome

Vibratome sections were used for electron microscopy. Due to slicing at room temperature the ultra structure is not damaged in contrast to cryostat sections, where ice crystals form during slicing. On a vibratome 50 µm sections were obtained at a temperature of 4 °C. Sections were collected in five PBS-filled glasses, to produce five series of sections with a distance of 500 µm between two sections of one series. For storage, series of sections were transferred to AFS and stored at -20 °C.

2.6 Immunocytochemistry

2.6.1 Pre - treatment of brain sections

Free floating 25 µm brain sections were rinsed in 0.1 M PBS (3 x 10 minutes), pretreated with 1% sodium borohydride in PBS for 15 minutes to remove excessive aldehydes and thoroughly washed in PBS (2 x 15 minutes). Then, sections were preincubated for 30 minutes in a mixture of 10% normal goat serum (NGS) or 10% normal horse serum (NHS) to block unspecific binding sites, 0.3% Triton X-100 to increase membrane permeability and 0.05% phenylhydrazine in PBS to block endogenous peroxidase activity.

2.6.2 Primary antibodies

After preincubation, sections were transferred to primary antibody solutions (10% NGS, 0.3% Triton, 0.1% sodium azide and 0.1% thimerosal in PBS) for 36 hours at 4 °C. Dilutions of primary antibodies were used as listed in paragraph 2.2.4 (Antibodies and Dilutions).

2.6.3 Secondary antibodies

After washing twice in PBS and preincubating in PBS-A for 60 minutes, sections were incubated with solutions of corresponding biotinylated secondary antibodies as listed in paragraph 2.2.4 (Antibodies and Dilutions) in PBS-A with 0.3% Triton and 0.1% sodium azide for another 24 hours at 4 °C.

2.6.4 Visualization of secondary antibodies

To visualize secondary antibodies, sections were repeatedly rinsed in PBS, preincubated in PBS-A for 60 minutes, followed by 12 hours of incubation in an avidin-biotin-elite complex (ABC) diluted 1:200 in PBS-A. ABC contains streptavidin, which forms an avidin-biotin complex with the biotinylated secondary antibodies. The other component of ABC, a biotinylated peroxidase, then attaches to free binding sites of the streptavidin-antibody complexes. Then, sections were washed again, preincubated in a solution containing 1.4 M 3.3`-diaminobenzidine (DAB) and 10 mM imidazole in a 0.05 M Tris buffer, pH 7.6 for 15 minutes. The color reaction was developed by adding 0.3% ammonium nickel sulfate (ANS) and 0.03% hydrogen peroxide to the DAB solution and stopped after 15 minutes by repeated washes in PBS.

2.6.5 Mounting and coverslipping of brain sections

After the color reaction, sections were washed in PBS and subsequently mounted on gelatin-coated slides, air dried, dehydrated through a graded series of ethanol (70%, 80%, 96% and 100%), transferred into xylene 100%, and coverslipped with Entellan.

2.7 *In Situ* Hybridization

2.7.1 *In situ* hybridization with digoxigenin-labeled riboprobes

Free-floating 25 µm brain sections were rinsed in 0.1 M PBS (3 x 10 minutes), pretreated with 1% sodium borohydride in PBS for 15 minutes and thoroughly washed in PBS (2 x 15 minutes). Thereafter, sections were preincubated in hybridization buffer (HB; 50% formamide, 10 mM Tris, 10 mM phosphate, 600 mM NaCl, 60 mM sodium citrate, 5% dextrane sulfate, 10 mM DL-dithiothreitol, 0.1% ficoll, 0.1% polyvinyl-pyrrolidone, 4 mM 2-mercaptoethanol, 200 µg/ml E. coli t-RNA and 5 mM EDTA, pH 7.0). Slide-mounted sections were incubated in HB containing 1 µg/ml digoxigenin-labeled Riboprobe (HCN1-, HCN2-, HCN3-, HCN4- antisense and sense controls) for 16 hours in a moist chamber (33% formamide in bidistilled water) at 56 °C. After rinsing with PBS (5 minutes), sections were

washed in standard sodium citrate (SSC), pH 7.5 for 30 minutes at 56 °C, followed by RNAse-A digestion (30 ng/ml in 10% bovine serum albumin in PBS (PBS-A) to digest unligated riboprobes for 30 minutes at room temperature (RT). Concentrations of riboprobes for the hybridization and RNAse for the digestion had been optimized in preliminary tests.

2.7.2 Visualization of Digoxigenin

After several rinsing steps in PBS, sections were preincubated with 1% casein, 1% NHS and 1% NaN3 (sodium azide) in PBS for 1 hour and incubated with mouse anti-digoxigenin antibodies overnight at RT. The next day, sections were washed in PBS (3 x 10 minutes), preincubated in PBS-A for 1 hour and incubated with biotinylated horse anti-mouse antibodies in PBS-A for 8 hours, followed by 12 hours of incubation in ABC solution 1:200 in PBS-A. After 24 hours, a CARD reaction (catalyzed-reporter-deposition) was performed for signal amplification. During this reaction the peroxidase of the ABC Kit catalyzes the deposition of biotinyl-tyramide (BT) at the location of the bound riboprobes. After preincubation in 10 µM BT (10 mM imidazole in 0.05 M Tris buffer, pH 7.6) for 15 minutes, the CARD reaction was started by adding 0.03% hydrogen peroxide and stopped after 15 minutes by repeated washes in PBS. To visualize deposited biotin, the slices were again incubated in ABC solution (1:200 in PBS-A) for 12 hours. After rinsing with PBS (3 x 10 minutes), sections were preincubated in a solution containing DAB and 10 mM imidazole in 0.05 M Tris buffer, pH 7.6 for 15 minutes. The color reaction was developed by adding 0.03% hydrogen peroxide, to the DAB solution and stopped after 15 minutes by repeated washes in PBS.

Sections were mounted on gelatin-coated slides, air dried, dehydrated through a graded series of ethanol, transferred into xylene and coverslipped with Entellan.

2.8 Silver intensification and gold toning

To visualize the retrograde tracer WGA-apo-HRP-gold, a silver intensification was performed. During this reaction, the gold particles of the tracer catalyze the reduction of diluted silver ions to metallic silver. The metallic silver deposits on the surface of the gold particles forming a silver shell around them. Once this coat reaches a certain size it becomes visible as a black staining. Free floating 25 µm sections were first rinsed 6 times in 0.1 M PB to remove chloride ions which would interfere with the enhancement. After preincubation in 10% sodium thioglycolate in PB for 30 minutes and rinsing in 0.15 M sodium nitrate, sections were immersed twice for 20 minutes in a mixture of solutions A and B of the Intense M Silver

Enhancement Kit. Residual silver ions were then removed by fixation for 10 minutes in 5% sodium thiosulfate in PB. Finally, sections were washed 3 times in PB.

2.9 Kluever - Barrera staining

Kluever – Barrera is a combination of Luxol fast blue staining of myelin and cellular Nissl counterstaining. Free-floating sections were rinsed in PBS, followed by a lipid extraction in 70% ethanol for 12 hours. Myelinated fibers were stained overnight at 56 °C in a 0.1% Luxol fast blue solution in 96% ethanol and 0.05% acetic acid. Thereafter, sections were washed in bidistilled water and differentiated for 3 minutes in 0.01% lithium carbonate. Subsequently, sections were transferred to 70% ethanol for 3 minutes, washed again, mounted onto gelatin-coated slides, and left to air dry. After two minutes of washing in H_2O, sections were stained in a Cresyl-violet solution (0.2% in 20 mM acetate buffer, pH 4.0) for 30 minutes. After additional washing in H_2O for two minutes, sections were dehydrated through a graded series of ethanol, transferred into xylene, and coverslipped with Entellan.

2.10 Methyl green staining

Methyl green is a basic dye that interacts with RNA and DNA and is used for nuclear staining. Slide mounted sections were left in 70% ethanol overnight for lipid extraction, rinsed in bidistilled water for 2 minutes and stained with methyl green (2% methyl green in 20 mM acetate buffer, pH 5.0) for 30 minutes at RT. After rinsing in bidistilled water, sections were dehydrated and coverslipped in Entellan.

2.11 Coating of slides

Gelatine 15 g and potassium chromosulfate-12-hydrate 1.76 g were diluted in 630 ml H_2O at 70 °C. After adding 300 ml 100% ethanol and 70 ml 100% acetic acid the solution was filtered. Glass slides were washed thoroughly (dishwasher), dipped into warm gelatine solution for 3 minutes and dried for 2-3 hours in a dust-free environment at RT and overnight in a heating cabinet at 60 °C.

2.12 Confocal laser scanning microscopy

2.12.1 Processing of slices for confocal laser scanning microscopy

For confocal laser scanning microscopy (CLSM) either 25 µm cryostat sections or 50 µm vibratome sections were used. Sections were pretreated and incubated as described in paragraph 2.6. Antibody dilutions are shown in Paragraph 2.2.4. After the TMR-CARD reaction, sections were mounted on gelatin-coated slides, coverslipped with "Mount Fluor" and scanned with a confocal laser scanning microscope, Carl Zeiss, Jena, Germany.

2.12.2 Acquiring images with the CLSM

Confocal laser scanning microscopy allows obtaining high resolution images with depth selectivity. Thus, generation of in-focus images of selected depths is possible, a process also known as "optical sectioning". Serial images of individual 2-dimensional scans can then be reconstructed with the help of specific software, resulting in 3-dimensional images of complex morphological objects.

Sections were first visually analyzed using the conventional fluorescence microscope function of the confocal microscope to identify antigen distribution and regions of interest. Subsequently, appropriate laser-, filter- and detector settings of the CSLM served to specifically excite and detect the different fluorescence labeled antigens.

2.13 Electron microscopy

2.13.1 Pre - treatment of the brain sections

Freshly perfused coronal brain blocks were sectioned at 50 µm thickness using a vibratome (paragraph 2.4.5.2). After several rinsing steps in PBS, sections were transferred to 20% sucrose in PB twice for 10 minutes. To increase membrane permeability and antibody penetration, they were placed on a plastic support and freeze-thawed using liquid nitrogen.

2.13.2 Pre - embedding immunocytochemistry

After freeze-thawing, sections were pre-treated and incubated with primary antibodies as previously described (paragraph 2.6). To conserve the ultrastructure of the tissue the following exceptions were made: only 0.1% sodium borohydride and 0.05% triton were used for pre-incubation and incubation. Rinsing, incubation with the secondary antibody and avidin-biotin solutions were carried out as described above (paragraphs 2.5.3; 2.5.4).

2.13.3 Araldite embedding

After immunocytochemistry (ICC) (paragraph 2.6), slices were post-fixed with 1% osmium tetroxide in PB for 10 minutes and washed in PB 3 times for 5 minutes. Thereafter, slices were dehydrated through graded ethanol (2 x 50% EtOH, 2 x 70%) and block stained with 2% uranyl acetate in 70% EtOH for 30 min in the dark. The sections were further dehydrated in graded ethanol (3 x 70% EtOH, 2 x 80%, 2 x 90% and 3 x 100%), transferred into propylene oxide twice for 10 minutes, and incubated overnight in a mixture of 55 g araldite solution (intensively mixed araldite and DDSA (Dodecenyl Succinic Anhydride, araldite hardener) in a ratio of 30:24), 1.5 ml DMP-30 (2,4,6-tris (dimethylaminomethyl-phenol, epoxy accelerator), and 50 ml propylene oxide. The next day, slices were incubated 2 x 2 hours in the embedding solution (100 g araldite solution mixed with 2 ml DMP30, intensively mixed for 30 minutes) and finally embedded between two sheets of Aclar plastic under light pressure. The time for resin polymerization was kept between 24-60 hours at 65 °C.

2.13.4 Preparation of Semi- and Ultrathin sections

Regions of interest were cut out from the embedded sections and glued to a plastic carrier. Semithin (500 nm) and ultrathin (60-70 nm) sections were cut alternately, using a diamond knife and an ultramicrotome. Semithin sections were dried at 70 °C to amino-silanized slides. Ultrathin sections were collected on 300-mesh nickel or gold grids coated with 0.75% pioloform 200.

2.13.5 Post - embedding immunocytochemistry

2.13.5.1 Semithin sections

For post-embedding labeling it is necessary to remove some araldite to unmask the antigens. Therefor, sections were incubated in methanolate etching solution (Sodium methoxide 1 M in a 2:1 mixture of methanol and toluene) for 10 minutes, followed by rinsing in a 2:1 mixture of methanol and toluene for 5 minutes and twice in acetone for 5 minutes. After rinsing with distilled water, slides were transferred in 100 mM acetate buffer (pH 5) for 2 minutes. Afterwards, sections were incubated in 2% hydrogen peroxide for 5 minutes to remove osmium, transferred to acetate buffer for 2 minutes, and finally rinsed in PBS. All following steps were performed in a moist chamber at RT: Sections were pre-incubated in 10% NGS for 30 minutes, followed by incubation with the appropriately diluted primary antibody (Paragraph 2.2.4.) in 10% NGS over-night. After rinsing twice for 5 and 10 minutes in PBS, sections were pre-incubated in PBS-A for 15 minutes and then incubated with the

appropriately diluted secondary antibody (in PBS-A) for 4 hours. After two rinsing steps for 5 and 10 minutes in PBS and pre-incubation in PBS-A, the sections were incubated with the ABC Kit in PBS-A (diluted 1:50) for 1 hour. After washing twice in PBS for 5 and 10 minutes, the sections were pre-incubated in DAB-solution for 15 minutes. Visualization was performed as described in paragraph 2.5.4. In control experiments the primary antibody or ABC Kit was omitted.

2.13.5.2 Ultrathin sections

All steps were performed at RT. Grids were moistened in 50 µl-droplets of bidistilled water on a sheet of parafilm. The grids were then transferred from droplet to droplet. Osmium tetroxide was removed to unmask the antigens by incubation in 1% periodic acid for 7 minutes and washing in H_2O, followed by incubation in 1% sodium metaperiodic acid for another 7 minutes. Subsequently, the grids were jet-rinsed with bidistilled water and transferred to a silicone embedding form with cavities able to hold about 25 µl of solution. Solutions were changed by moving the grids to adjacent cavities. Grids were incubated in TBSX (Tris 50 mM, Triton x-100, Sodium hydrochloride 139 mM) for 10 minutes, followed by pre-incubation in Block 1 (normal goat serum 5%, bovine serum albumin 2%, in TBSX) for 30 minutes. The primary antibody was appropriately diluted in Block 1 and the grids were incubated over night (Paragraph 2.2.4). The next day, sections were jet rinsed with TBSX twice, pre-incubated in Block 2 (Bovine serum albumin 2%, in TBSX) for 10 minutes and incubated in the secondary antibody solution (secondary gold colloid-conjugated antibody, appropriately diluted in Block 2, see Paragraph 2.2.4) for 90 minutes. Grids were then jet-rinsed twice in TBSX, twice in distilled water, and air-dried.

2.13.6 Staining of ultrathin sections

After post - embedding ICC, the air dried grids were incubated in droplets of 2% uranyl acetate in 70% ethanol on a sheet of parafilm for 2 minutes in the dark. Afterwards, grids were jet-rinsed with H_2O twice and air-dried again. Double staining was performed using lead citrate as described by Reynolds et al. (H_20 5 ml, Lead nitrate 133 mg, sodium citrate 200 mg, sodium hydroxide 10 N 80 µl) for 20 seconds, again followed by two jet-rinsing steps with H_20 and air drying.

2.13.7 Toluidine blue staining

To facilitate identification of regions of interest in the electron microscope it is useful to correlate the morphology with a toluidin blue-stained adjacent semithin section. Therefore directly after slicing, the semithin sections were dried on amino-silanized glass slides and stained for 2-5 minutes in toluidin blue solution (Toluidine blue 1%, sodium borohydride 1%, Sucrose 40%) at 70°C. They were then rinsed with H_2O, dried at 70 °C and coverslipped with Entellan.

2.14 Documentation and images

Light microscopic images from brain sections were acquired using a Leica DMRB microscope connected to a MAC 5000 controller for XYZ-stage in combination with a CX 9000 camera driven by Neurolucida software, version 8. This software allows the exact merging of adjacent high magnification images. Thus, high resolution scans, called “virtual slices”, of large regions of interest can be obtained. Minor adjustments of brightness and contrast were made, using Adobe Photoshop CS3. Cells were plotted and counted using the same microscope, using the “meander-scan” tool of the Neurolucida software and the Neurolucida explorer.

3. Results

3.1 Lateral habenular neurons projecting to the monoaminergic systems express HCN channels

The lateral habenula (LHb) exerts a strong continuous inhibition on monoamine release (Lecourtier et al., 2006; Matsumoto and Hikosaka, 2007; Matsumoto and Hikosaka, 2008). It is currently unknown how and where this baseline inhibition is generated. Hypothesizing that this effect is due to spontaneous activity of LHb-projection neurons, the present study was designed to establish whether HCN channels are expressed by neurons in the LHb. Consequently, we examined the regional and cellular expression of HCN subunit mRNAs and proteins in the LHb, especially in those neurons that project to dopaminergic and serotonergic cell groups.

3.1.1 Quantitative PCR analyses confirm high levels of HCN2-4 and low levels of HCN1 mRNA expression

In a first step, the HCN1 to HCN4 mRNA expression levels within the habenula (Hb) were analyzed by quantitative PCR (qPCR) of homogenized rat Hb tissue. These qPCR data allow a better quantification and comparison of HCN expression levels than *in situ* hybridization (ISH) or immunocytochemistry (ICC) alone, because riboprobes or antibodies might have different sensitivities to their targets.

Quantitative PCR analyses of microdissected Hbs from twelve rats produced detectable amounts of mRNAs for all four HCN subunits at different levels. *ANOVA* (**an**alysis **o**f **va**riance) revealed a statistically significant ($p<0.0001$) HCN main expression effect. *Tukey-Kramer posthoc tests* found no significant differences between the expression levels of HCN2 to HCN4 mRNAs, indicating that the expression levels of the three transcripts are almost identical. In contrast, HCN1 mRNA is expressed at significantly ($p<0.001$) lower levels, about 9-fold lower than HCN2 to HCN4 mRNAs (Figure 4). Although these data do not provide information about the distribution of HCN channels within the Hb, they are important for the evaluation and comparison of ISH- and ICC findings.

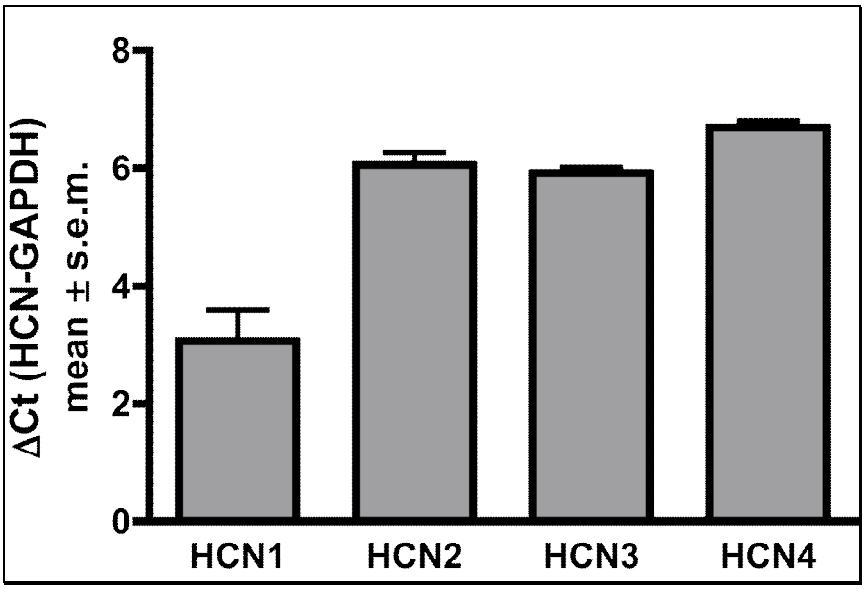

Figure 4: Quantitative PCR analysis of microdissected habenulae (N=12) produced detectable amounts of all HCN subunit mRNAs. Bars show the mean ± s.e.m. of the relative expression of each HCN subunit mRNA compared to GAPDH mRNA as endogenous control (ΔCt (HCN-GAPDH)). *ANOVA* and post hoc *Tukey–Kramer* multiple comparison tests show that HCN1 mRNA expression is about 10-fold lower than expression of HCN2 to HCN4 mRNAs ($F_{3,47} = 36.3$, $P<0.001$). HCN2 to HCN4 mRNAs, however, are expressed at almost identical levels.

3.1.2 Digoxigenin-labeled riboprobes, against HCN1-4 mRNAs are highly specific

3.1.2.1 Selection of HCN1-4 cDNA sequences

Each HCN subunit is encoded by a specific mRNA. Alternative splicing mechanisms for HCN mRNAs are not known (Biel and Michalakis, 2009). For the generation of riboprobes against individual members of the HCN family, specific cDNA sequences are needed. Comparison of the four entire HCN cDNA sequences revealed strong homologies of up to 70% between the different subunits. In general, the largest differences exist towards the non-conserved amino terminus of each channel. Thus, we selected pairs of primers, of a length between 18 to 22 nucleotides, to amplify cDNA sequences within this region. The selected sequences for the HCN riboprobe generation had a size of 303 to 741 nucleotides and they were checked for homologies with the cDNAs of paralogous subunits, as well as with the cDNAs of other unrelated proteins (e.g. GAPDH) using the NCBI-BLAST data base (Table 2).

Subunit Size	HCN 1 cDNA	HCN 2 cDNA	HCN 3 cDNA	HCN 4 cDNA	GAPDH cDNA
HCN1-Ribo 654 bp	100%	35%	35%	35%	40%
HCN2-Ribo 303 bp	37%	100%	38%	48%	43%
HCN3-Ribo 435 bp	37%	45%	100%	38%	41%
HCN4-Ribo 741 bp	37%	42%	39%	100%	35%

Table 2: Sequence homologies between each riboprobe (left column; size in base pairs (bp)) and the other HCN-cDNAs or GAPDH-cDNA (representative for all other proteins) are low, accounting for the specificity of the generated riboprobes.

3.1.2.2 Gel electrophoresis of PCR products

To control the successful amplification of the selected cDNA sequences, the PCR products were electrophoretically separated in 1% agarose gel. Analyses of the stained gels under UV light and comparison with the DNA size markers λ-*Eco*47I and *Bsu*RI revealed a specific band for each amplification product of the expected size (Figure 5). These bands were cut out of the gel and checked for their correct sequence by restriction analyses and sequencing.

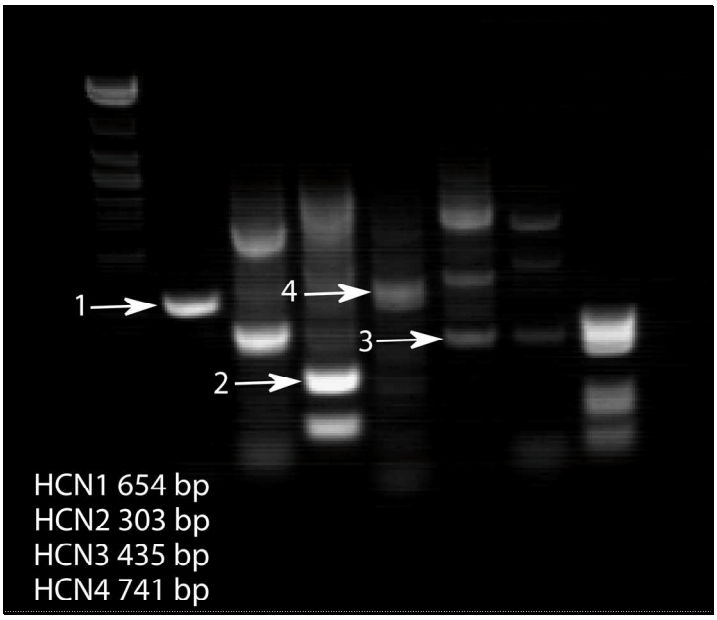

Figure 5: The agarose gel with the electrophoretically separated PCR products under UV light shows a specific band for each HCN subunit at the expected size (white arrows, size denoted in white). These bands were cut out of the gel and used for riboprobe generation. The first lane in the gel represents the DNA size marker λ-*Eco*47I, while the last lane represents the DNA size marker *Bsu*RI.

3.1.2.3 Restriction analysis and Sequencing

To control successful cloning of the amplified products into the pGEM-T vector system, the plasmid DNA was digested with the restriction endonucleases *Not*I in combination with either *Cfr*42i or *Pae*I (depending on HCN-PCR product) for 90 minutes at 37 °C. After digestion the plasmid DNA was separated by gel electrophoresis resulting in two bands, one of the vector DNA and one of the excised insert at their expected sizes (Figure 6). Only probes with an insert of the expected size were sent for sequencing.

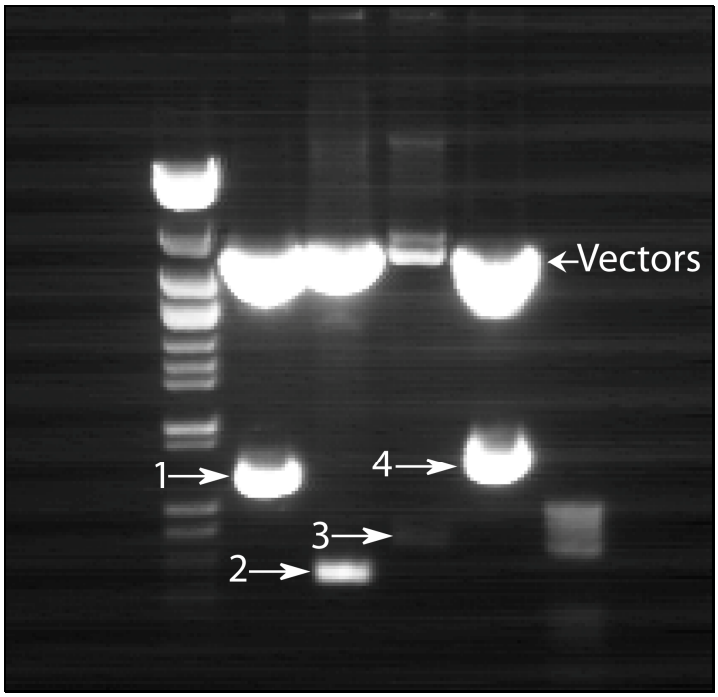

Figure 6: Gel electrophoresis of the digested plasmid DNA resulted in two bands, one of the vector and one of the excised insert. The inserts had the expected size of HCN1: 654 bp; HCN2: 303 bp; HCN3 435 bp; HCN4 741 bp (indicated by white arrows). The first lane in the gel represents the DNA size marker λ-*Eco*47I, while the last lane represents the size marker *Bsu*RI.

3.1.2.4 Specificity of HCN riboprobes

Several tests were performed to optimize the riboprobes before and during the production process and to characterize them regarding their specificity and sensitivity after completion. Prior to the production process, appropriately sized sequences with the lowest homologies to other mRNAs were chosen (see paragraph 3.1.2.1). During the production process the products were repeatedly checked by gel electrophoresis, restriction analyses and finally by sequencing, to make sure that the cDNA sequences were correctly amplified (see paragraphs 3.1.2.2/3.1.2.3).

Thereafter, riboprobes were tested in sections of the rat brain to optimize riboprobe and RNase concentration for *in situ* hybridization. In a first step, riboprobes were checked for unspecific labeling by counterstaining *in situ* hybridized-sections with methyl green, a basic dye that intercalates with the DNA and thereby stains all cell nuclei. These experiments revealed that many cells remain completely negative for HCN *in situ* hybridization signal. Thus, the riboprobes do not unspecifically label all cells (Figure 7). This is supported by the finding, that brain areas without an HCN expression remain unlabeled with our riboprobes.

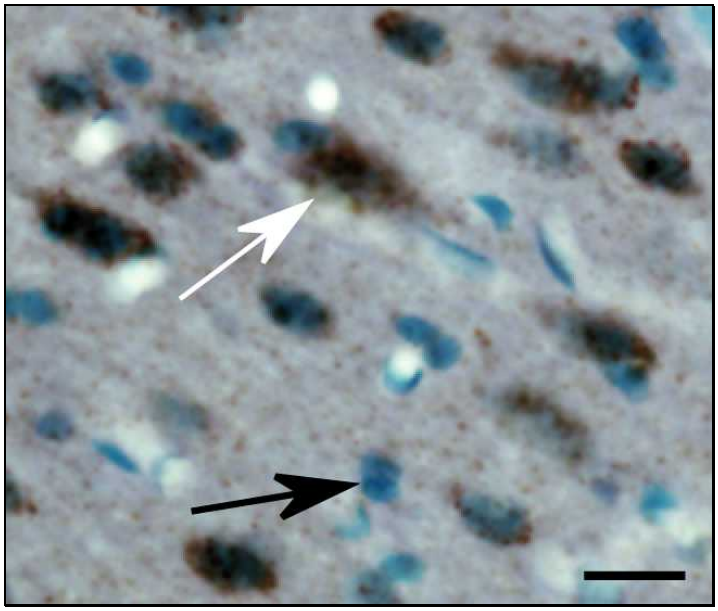

Figure 7: *In situ* hybridization of HCN1 to HCN4 mRNAs with subsequent methyl green (MG) counterstaining shows many HCN-negative cells in sections of the rat brain, thereby excluding an unspecific labeling of all cells. The image shows a double labeling of HCN3 *in situ* signal in brown (white arrow) and methyl green staining in green (black arrow). Bar indicates 10 µm.

In a next step, HCN *in situ* hybridization was accompanied by controls with the corresponding sense riboprobes or without any riboprobe. These controls result in no labeling (negative control) or in a very light unspecific background labeling (sense control) (Figure 8).

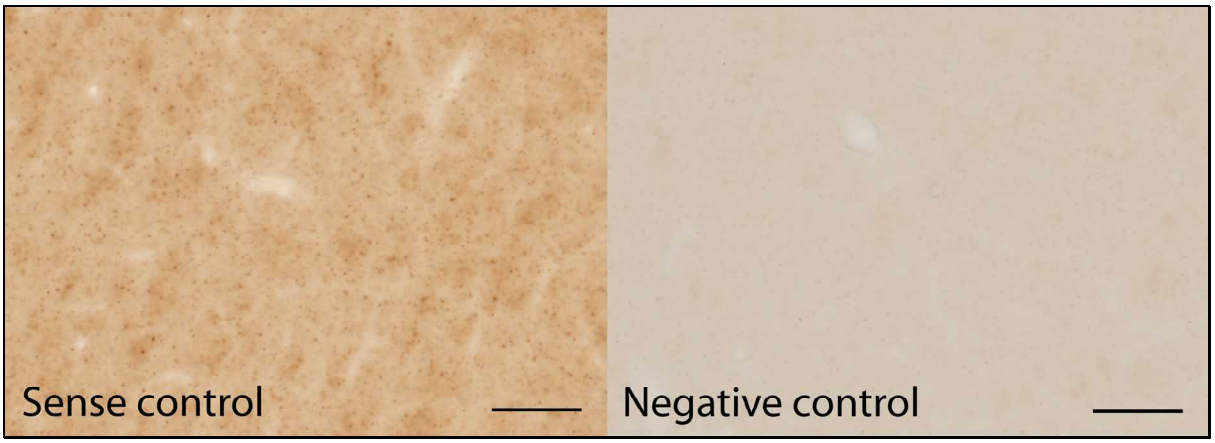

Figure 8: Negative controls of the *in situ* hybridization and HCN sense controls remain negative or show very weak unspecific background labeling. Bars indicate 10 µm.

To evaluate the sensitivity of the riboprobes and to allow an approximate proposition of HCN expression levels by *in sit*u hybridization, the intensity of HCN *in situ* signals was compared with the HCN mRNA levels observed in qPCR analyses. This comparison revealed a good agreement for all four subunits. However, this indicates that the intensity of HCN *in situ* signals may correlate with the actual expression levels of HCN mRNAs in the Hb.

Finally, the distribution and intensity of HCN *in situ* signals was compared with earlier findings (Ludwig et al., 1998; Santoro et al., 1998; Santoro et al., 2000; Moosmang et al., 2001). Therefore, we focused on some specific regions, including neocortex, thalamus, hippocampus and Hb and found good agreement between the distribution described in the literature and the present study. Correlations and comparisons of HCN ISH- and ICC studies are presented and discussed in detail in paragraphs 3.1.4 and 4.2.1.

3.1.3 *In situ* hybridization reveals significant subnuclear differences in the percentages of HCN-positive cells

For qPCR analyses, homogenates of the entire Hb were used. Consequently, qPCR data cannot provide information about the distribution of HCN channels within the Hb complex. Therefore, *in situ* hybridization experiments on sections of the rat Hb were performed to analyze their subnuclear and cellular distribution.

HCN1 mRNA

In good agreement with qPCR data, expression of HCN1 mRNA in the Hb is weak. Only a few cells are labeled throughout the entire LHb. No HCN1 mRNA is expressed in the MHb (Figure 9A). To exclude a false positive result, regions with strong HCN1 expression were checked for labeling. As a positive control for HCN1 *in situ* hybridization, inset 1 in Figure 9A shows a sector of the cerebral pyramidal cell layer, which is known to strongly express HCN1 mRNAs.

HCN2 mRNA

HCN2 mRNA is strongly expressed in cells distributed throughout the entire MHb and LHb. Two different types of HCN-positive cells are distinguishable in the LHb (Figure 9B). The first type is especially strongly labeled, irregularly shaped and exclusively located in the dorsal parts of the LHb, including parts of the *lateral magnocellular subnucleus (LMc)*. Some of these cells are located at the very dorsal border of the LHb, just below the ependym cell layer (9B, inset 1). The second type displays less labeling, is smaller in size, and spread throughout the entire LHb (9B, inset 2). In the MHb, HCN2 mRNA expression levels reveal a decreasing gradient from the medial to the lateral side (Figure 9B).

HCN3 and HCN4 mRNAs

ISH patterns of HCN3 (Figure 9C) and HCN4 (Figure 9D) are similar to HCN2 mRNA staining but are generally less intense. In the MHb, HCN2 to HCN4 mRNAs exhibit a decreasing gradient of expression levels from the medial to the lateral subdivisions.

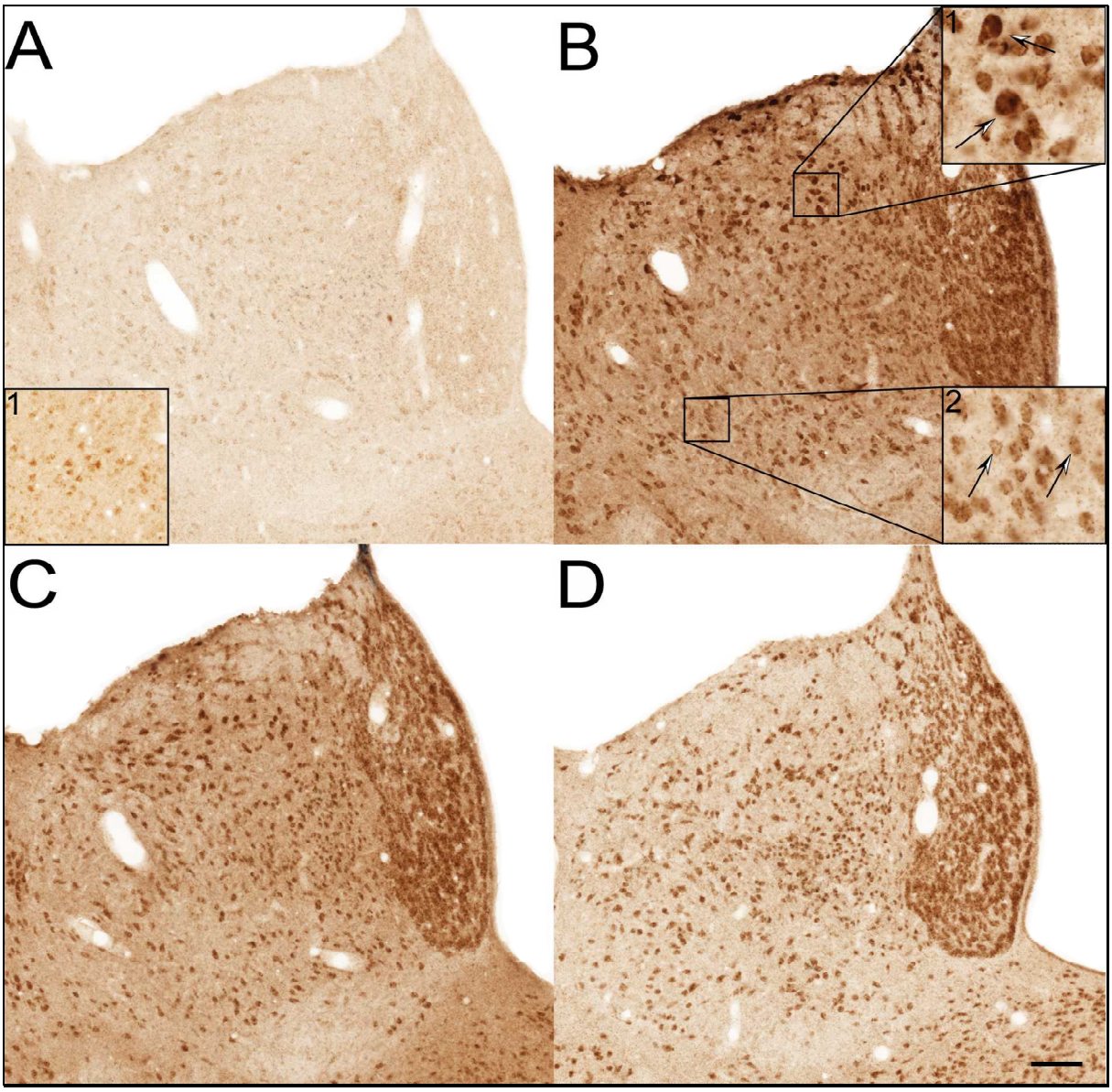

Figure 9: All HCN subunit mRNAs are expressed in the rat habenular complex as visualized by *in situ* hybridization. Consistent with qPCR data, HCN2 to HCN4 mRNAs (B-D) are strongly expressed throughout MHb and LHb with quite similar distribution patterns. Note that HCN2 mRNA is expressed in two different types of LHb cells. The first type is strongly labeled, irregularly shaped and exclusively located in the dorsal parts of the LHb (B, inset 1), while the second type is weaker labeled, smaller in size and spread throughout the entire LHb (B, inset 2). However, HCN1 mRNA (A) expression is much weaker. As a positive control for HCN1 *in situ* hybridization, inset 1 in Figure 9A shows a sector of the cerebral pyramidal cell layer, which is known to express HCN1 mRNAs. Bar indicates 100 µm.

Percentage of HCN-positive cells per subnucleus

The LHb is morphologically and immunocytochemically divided into ten subnuclei (Figure 10A) (Andres et al., 1999; Geisler et al., 2003). To analyze the subnuclear distribution of HCN channels is interesting from a bifocal perspective. First, the delineation of subnuclei was partly based on the distinct and characteristic distribution of selected antigens, including acetylcholinesterase, neurofilament, Kir3.2, GABA-B-receptor and tyrosine hydroxylase (Geisler et al., 2003). From this point of view it might be interesting to know whether or not HCN channels are restricted to some of the subnuclei and might thereby be another antigen to delineate LHb subnuclei. The other important aspect, especially for this study, is that LHb neurons projecting to the monoaminergic brainstem areas are not homogeneously spread throughout the entire LHb, but show regional specificity (Herkenham and Nauta, 1979; Geisler et al., 2003; Brinschwitz et al., 2010). Thus, a predominant expression of HCN channels within those subnuclei, where projections to the monoaminergic systems originate, may indicate a functional role of HCN channels for the generation of spontaneous activity in projection neurons (see paragraph 3.1.5.2).

Consequently, the subnuclear distribution of HCN mRNAs was evaluated combining HCN-ISH with methyl green (MG) counterstaining. LHb subnuclei were delineated in adjacent Kluever-Barrera-stained Hb sections and mirrored on images of ISH-MG sections. By counting the total number of cells (all green-stained cell nuclei) and the number of HCN-positive cells (brown DAB-stained cell bodies), the percentage of HCN-positive cells within each subnucleus was determined (Figure 10B).

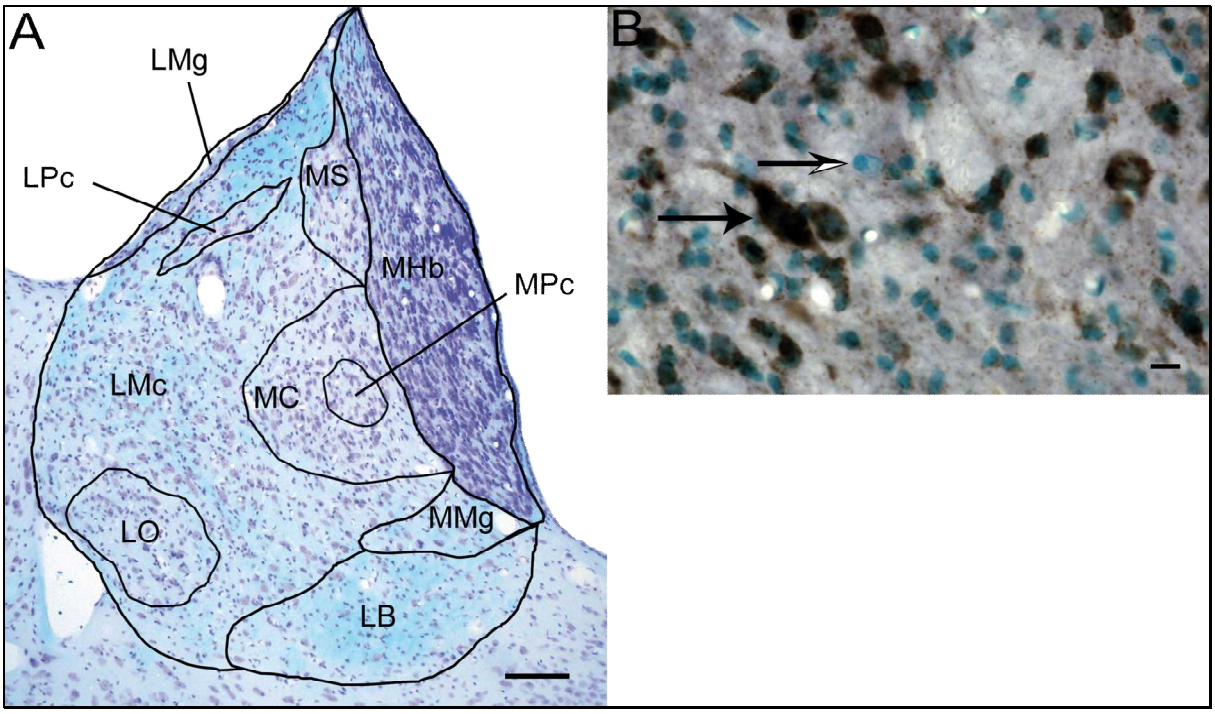

Figure 10: The subnuclear organization of the rat habenular complex is shown in a Kluever-Barrera stained brain section (A). This technique combines cresyl-violet staining of cell bodies with luxol-fast-blue staining of the myelinated fibers. To evaluate the subnuclear distribution of HCN mRNAs, we combined HCN *in situ* hybridization with methyl green staining (B). By counting the total number of cells (methyl green-stained cell nuclei indicated by white arrows) and the number of HCN-positive cells (brown DAB-stained cells indicated by black arrows), we determined the percentages of HCN-positive cells within each subnucleus. The high magnification image (B) shows a representative section of the LHb after HCN2-*in situ* hybridization and methyl green staining. ISH signals for HCN1, HCN3 and HCN4 closely resembled those depicted here and are therefore not shown. Abbreviations: see Figure 1. Bar indicates 100 µm in (A) and 10 µm in (B).

This quantification revealed that HCN2-, HCN3- and HCN4 mRNAs are expressed in cells of all habenular subnuclei in a percentage varying from 20% to 80%. In contrast to that, but consistent with findings from ICC (see paragraph 3.1.4) and qPCR experiments (see paragraph 3.1.1), HCN1 mRNA expression was limited to eight subnuclei with a maximum of 10% positive cells per subnucleus (Figure 11). In general, HCN channel distribution is not specific for any of the LHb subnuclei. Thus, they are not an appropriate antigen to delineate individual LHb subnuclei. Interestingly, the comparison of subnuclear expression levels revealed a decreasing gradient from the medial to the lateral subnuclei of the LHb for all HCN transcripts.

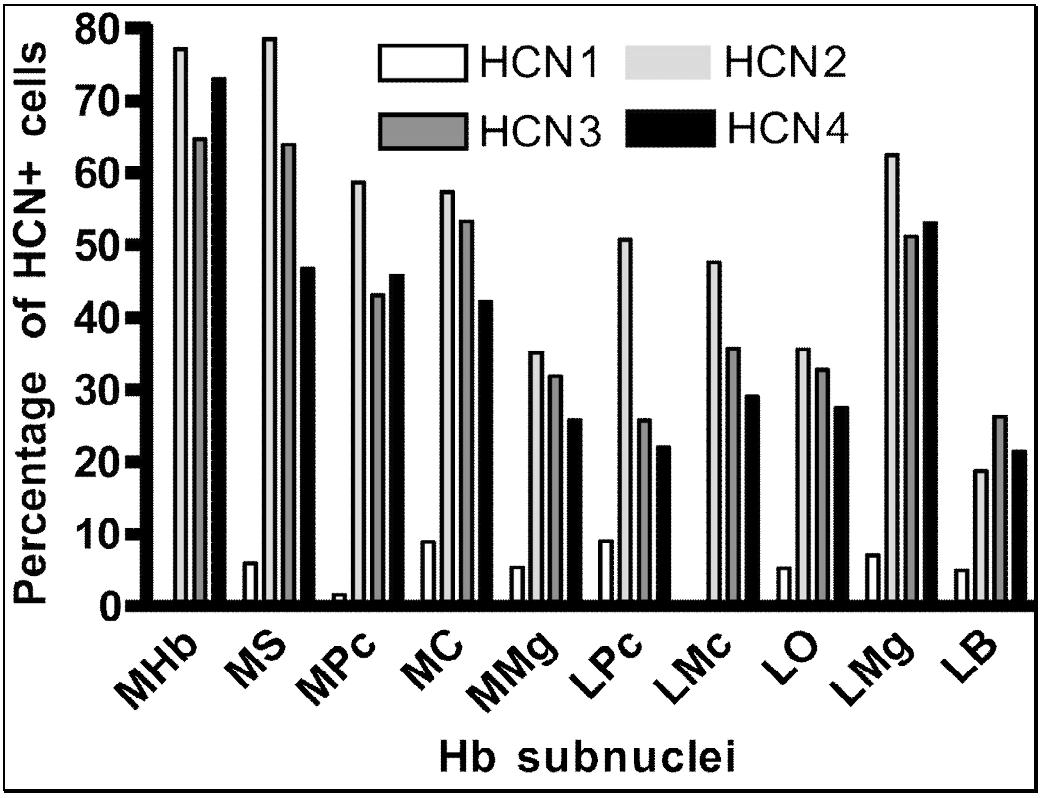

Figure 11: The percentages of HCN1 to HCN4 mRNA positive cells within each subnucleus of the LHb and the MHb are indicated by shaded bars. Note that HCN1 mRNA is expressed in less than 10% of all cells and that the expression is restricted to eight subnuclei of the LHb, emphasizing the special role of this subunit within the habenula. In contrast, HCN2 to HCN4 mRNAs are expressed in all subnuclei of the LHb and the MHb in percentages varying from 20% to 80%. Interestingly, the expression levels show a decreasing gradient from the medial to the lateral subnuclei of the LHb. For abbreviations see Figure 1.

3.1.4 HCN channels are mainly expressed in the habenular neuropil

While HCN mRNAs are restricted to the cell bodies, their corresponding proteins may be transported to dendrites, axons, or even the synaptic terminals. Therefore, immunocytochemical methods were used to analyze the subnuclear distribution of HCN proteins within the Hb and their specific location within individual neurons in order to get an idea of their potential functions within this area. In agreement with previous reports (Notomi and Shigemoto, 2004), all four HCN subunit proteins are expressed within the Hb. In general, HCN-immunoreactivity (ir) is predominantly associated with the habenular neuropil with only a few HCN-positive cell bodies (Figure 12A-D).

HCN1 protein

Consistent with qPCR and ISH data, HCN1-ir is the weakest of all four channels (Figure 12 A1-3). It is restricted to the linear border zone between the MHb and the medial part of LHb (A2, arrows). The labeling in this border zone seems to demark fibers, descending from the dorsal part of the MHb-LHb border to its ventral part. The major LHb fiber tracts, the stria medullaris and the fasciculus retroflexus, remain unstained. Some very weakly stained cell bodies are located in the lateral division of the LHb (Figure 12 A1-3).

HCN2 protein

HCN2-ir is very prominent and unevenly distributed across the entire LHb with the most intense neuropil staining in the areas of the *lateral parvocellular (LPc)- and superior subnucleus (MS)* of the LHb and the *superior subnucleus* of the MHb (Figure 12B). The medial border of the MHb displays moderate HCN2-ir, whereas the rest of the MHb remains almost negative. The major LHb fiber tracts, the stria medullaris and the fasciculus retroflexus, are devoid of reactivity. Consistent with ISH studies, two different types of HCN2-positive cells are distinguishable in the LHb. One type is relatively big, distributed in the dorsal parts of *lateral magnocellular (LMc)*- and *parvocellular subnucleus (LPc)* and surrounded by a strongly labeled, dense neuropil (12B, inset 1). Regarding distribution and shape, these extensively labeled cells seem to be identical with those observed in ISH experiments. The other type is small and spread throughout the entire LHb and might represent the second type of cells observed in ISH studies (12B, inset 2). Both types predominantly display HCN-ir at their cell membranes.

HCN3 protein

HCN3 displays the most intense immunoreactivity of all four HCN subunits, with the most intense staining of the neuropil near the linear border zone between LHb and MHb, the same area that is labeled by HCN1-ir (Figure 12C). In contrast to HCN1 and HCN2, HCN3-ir is also strong in the entire MHb with an especially prominent area at the medial border of the dorsal MHb. Interestingly and unique among the HCN subunits, HCN3 seems to be expressed in axons in the ventral area of the LHb (Figure 12C, inset 1). These fiber bundles, which originate in the LHb and are on their way to the fasciculus retroflexus, do not contain any of the other three subunits.

HCN4 protein

HCN4-ir of the neuropil is weak in the LHb and moderate across the MHb (Figure 12D). The expression intensity decreases from the medial side of the MHb towards the lateral side of the LHb, forming a medio-lateral gradient. While only a few HCN4-positive cells are located in the LHb, many strongly labeled cell bodies are distributed throughout the MHb.

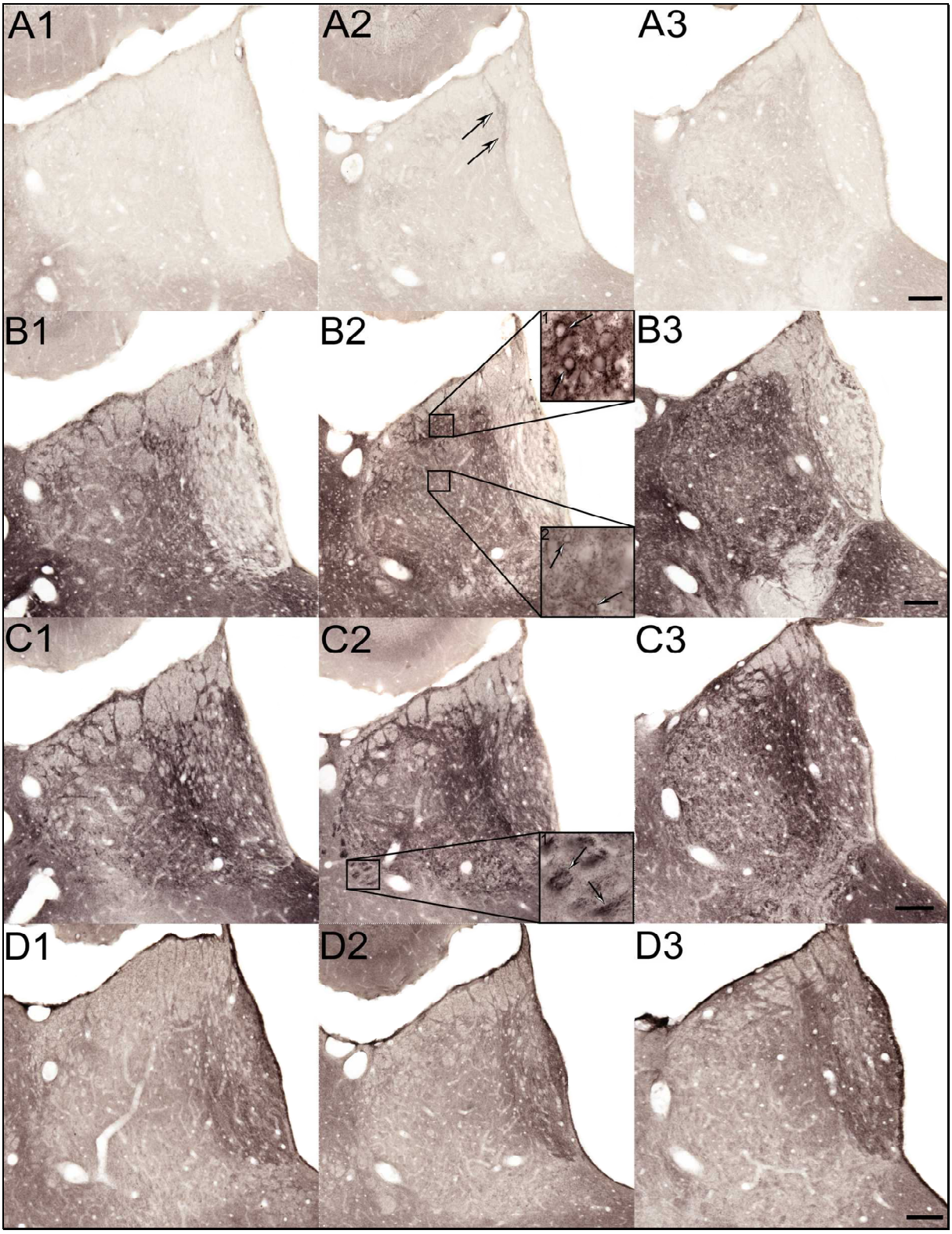

Figure 12: For figure legend see following page.

Figure 12: Immunocytochemical visualization of HCN subunits confirms an expression of all four subunits within the rat habenular complex (HCN1: A1-A3; HCN2: B1-B3; HCN3: C1-C3; HCN4: D1-D3). In general, HCN channels are mostly located within the habenular neuropil with only a few HCN-positive cells, indicating a predominantly dendritic expression. Again, two types of HCN2-immunoreactive cells (B2, insets 1 and 2) are discernible in the LHb, which, regarding shape and distribution, resemble those observed in *in situ* hybridization experiments. Among the four subunits, HCN1 shows a unique expression pattern, which is rather weak and restricted to the linear border zone between MHb and LHb (A2, white arrows). Thus, it is totally different from HCN2 to HCN4, which are widely expressed throughout LHb and MHb, with specific distribution patterns (B to D). Note that HCN2 expression is particularly strong in the areas of the *LPc-* and the *MS subnucleus* of the LHb and the *superior nucleus* of the MHb. Interestingly, HCN3 is the only subunit expressed on axon bundles (2C, inset). For abbreviations of subnuclei, see Figure 3. Bars indicate 100 µm.

In general, HCN channels are predominantly located within the Hb neuropil, with only a few HCN-positive cell bodies. The intensity and distribution of HCN-ir is in good agreement with the mRNA expression levels observed in qPCR and ISH studies. These findings indicate a predominantly dendritic expression and only a weak perikarial localization of HCN channels within the Hb. Interestingly, HCN3 seems to be the only subunit that is expressed on axons in the LHb.

3.1.5 The lateral habenula strongly projects to VTA, DR, and MnR

The LHb is the central part of the dorsal diencephalic conduction system, relaying information from various forebrain areas to monoaminergic nuclei in the mesencephalon (Herkenham and Nauta, 1977; Herkenham and Nauta, 1979; Sutherland, 1982). Major projections of the LHb target the dopaminergic VTA and its GABAergic tail, the RMTg Omelchenko et al., 2009; Brinschwitz et al., 2010), as well as the serotonergic DR and MnR (Phillipson, 1979; Herkenham and Nauta, 1979; Oades and Halliday, 1987). To identify and specifically analyze LHb neurons projecting to these areas, retrograde tracing studies were conducted.

3.1.5.1 Injection sites of the retrograde tracer WGA-apo HRP gold are located in VTA, DR, and MnR

The retrograde tracer WGA-Apo HRP Gold was unilaterally injected into VTA, DR and MnR, resulting in dense black deposits of silver enhanced gold, surrounded by less dense halos of the reaction product. No pronounced tissue damage was observed, as confirmed by normal morphology of cells at the injection site in adjacent Cresyl violet-stained sections (not shown).

VTA injection sites were aimed at the paranigral or parabrachial pigmented nucleus of the VTA at a level of Bregma -6.0 mm. Three animals (VTA-1 to VTA-3) with appropriately localized VTA-injection sites were evaluated for this study. One typical injection site (animal VTA-1) is shown in figure 13A and will be described in more detail.

The injection site in animal VTA-1 is localized in the center of the VTA at a level of Bregma -6.0 mm. It ventrally extends to a level of Bregma -5.0 mm, staining most of the ventral VTA. In a caudal direction, the injection site covers the area of the newly described “rostromedial tegmental nucleus” (RMTg), the GABAergic tail of the VTA. In a coronal axis, the injection site is laterally, ventrally and medially restricted to the VTA, while dorsally a spread of the tracer along the injection duct becomes visible (Figure 13A). While in animal VTA-1 no tracer deposits are located in the interpeduncular nucleus (IP), one of the other VTA-injected animals (animal VTA-2) analyzed for this study shows a minimal spread of tracer into the IP, resulting in some false-positive labeled cells in the MHb.

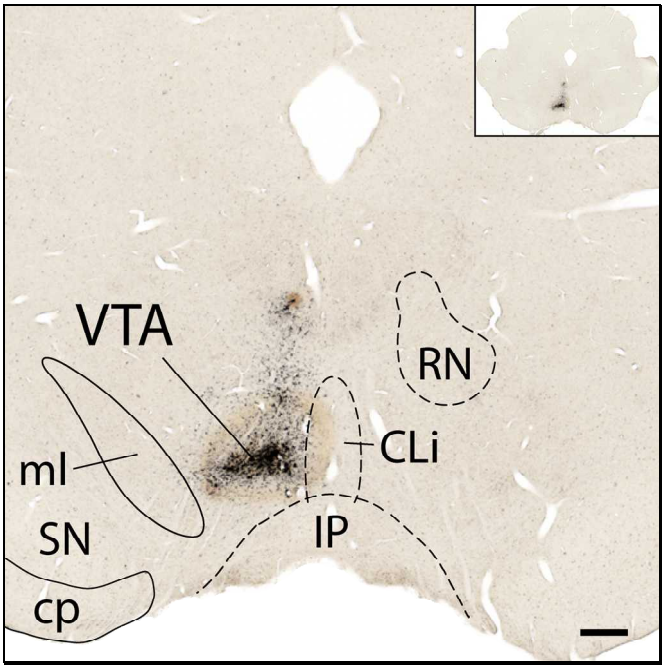

Figure 13A: To identify LHb neurons projecting to the VTA and to analyze their potential expression of HCN subunits, the retrograde tracer WGA-apo HRP gold was unilaterally injected into the VTA. The coronal brain section shows an appropriately localized WGA-apo HRP gold injection site in the VTA with illustrations of the target area and surrounding structures. The injection site shows some spread of tracer into the adjacent RN, which however, is not targeted by the LHb. Abbreviations: RN – red nucleus; ml - medial lemniscus; CLi – central linear nucleus; SN – substantia nigra; IP – interpeduncular nucleus; Bar indicates 250 µm.

DR injections were aimed at the ventral nucleus of the DR at level of Bregma -7.8 mm. In total, two DR-injected (DR-1 and DR-2) animals were analyzed for this study. In the representative animal DR-1 the injection site has its center in the ventral nucleus of the DR at a level of Bregma -7.8 mm, with minimal spread of the tracer into the dorsal and ventrolateral nucleus. In a rostro-caudal axis the injection site reaches from Bregma -7.3 mm to Bregma -8.3 mm and is restricted to the borders of the DR. Other surrounding areas, as well as the injection duct, are devoid of tracer deposits (Figure 13B).

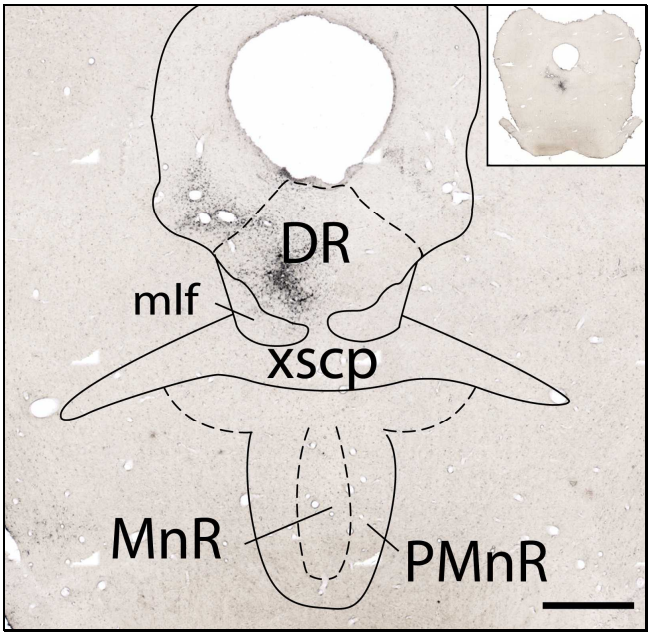

Figure 13B: The coronal brain section shows an appropriately localized WGA-apo HRP gold injection site in the DR with illustrations of the target area and surrounding structures. The injection site is restricted to the DR with no spread of tracer into adjacent areas. Abbreviations: MnR – median raphe; PMnR – paramedian raphe; DR – dorsal Raphe; xscp - decussation of the superior cerebellar peduncle; mlf – medial longitudinal fasciculus. Bar indicates 250 µm.

MnR injections were aimed at the center of the MnR at a level of Bregma -7.8 mm. Two MnR-injected animals (MnR-1 and MnR-2) were evaluated for this study. Animal MnR-1 represents a typical injection site, localized in the midline of the MnR with its center at a level of Bregma -7.8 mm and a rostro-caudal extension from Bregma -7.4 mm to Bregma -8.2 mm. The injection is devoid of any tracer particles in the surrounding paramedian raphe nucleus as well as in the injection duct (Figure 13C).

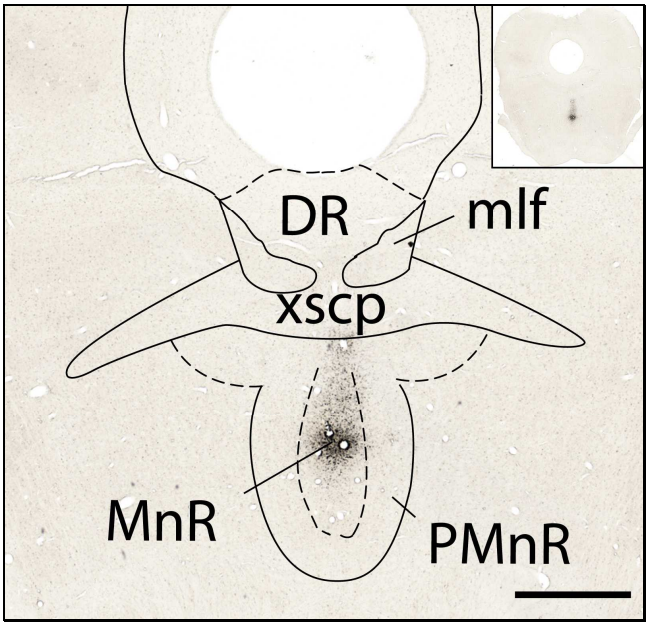

Figure 13C: The MnR injection site is centered to the MnR and shows no tracer deposits in the surrounding PMnR. Abbreviations: MnR – median raphe; PMnR – paramedian raphe; DR – dorsal Raphe; xscp - decussation of the superior cerebellar peduncle; mlf – medial longitudinal fasciculus. Bar indicates 250 µm.

3.1.5.2 Distribution of retrogradely-traced neurons in the lateral habenula

To get an idea whether HCN-positive cells and LHb projection neurons exhibit a similar or completely different distribution pattern within the LHb, the distribution of retrogradely labeled LHb cells was evaluated for each of the three injection areas. In agreement with previous reports (Phillipson, 1979; Herkenham and Nauta, 1979; Oades and Halliday, 1987), we found the highest number of retrogradely labeled LHb neurons after injections into the MnR (Figure 14; MnR: 311 neurons per LHb section). Injections into the VTA and the DR result in lower but comparable numbers of labeled LHb neurons (Figure 14; VTA: 212 neurons; DR: 208 neurons). Retrogradely labeled neurons from the three injection areas are observed in most of the LHb subnuclei and are quite homogeneously distributed, not showing any specific accumulation. They are located with a preference to the medial division of the LHb (Figure 15). Even within the LMc that contains about 50% of all retrogradely labeled neurons, the traced neurons show an increasing density towards the medial side of this nucleus. The contra-lateral LHb regularly displays a few retrogradely labeled neurons in VTA- and DR- injected rats, while after MnR injections, labeled neurons are equally distributed within the LHb on both sides. In general, neurons projecting to VTA, DR and MnR are almost equally distributed throughout the LHb subnuclei (Fig. 15).

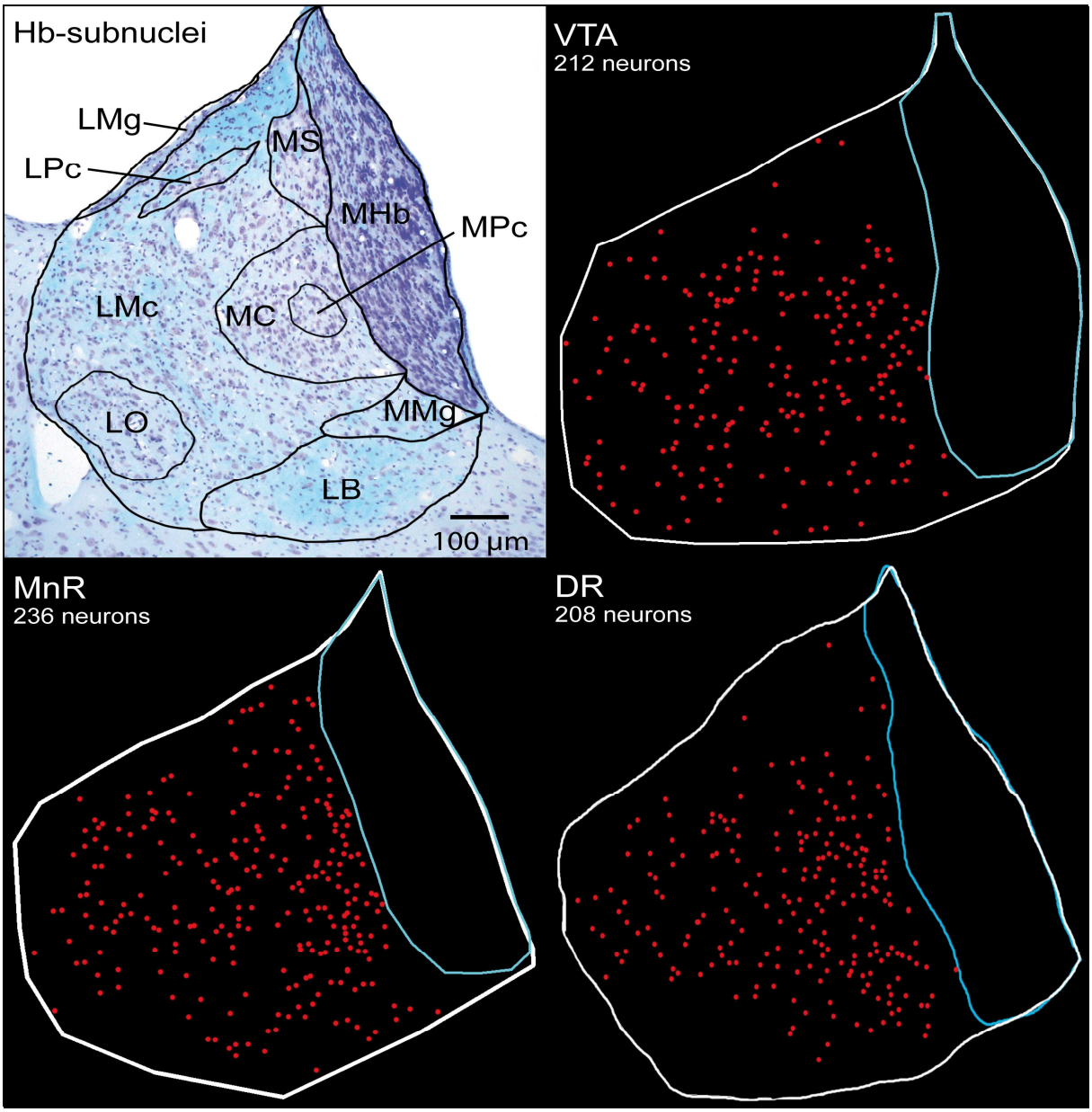

Figure 14: The distribution of retrogradely labeled neurons within the LHb after injections of WGA-apo HRP gold into VTA, DR and MnR is shown. While MnR injections resulted in the highest number of retrogradely labeled neurons, VTA and DR injections resulted in lower but comparable numbers. Each neuron is indicated by a red dot and the total number of retrogradely labeled neurons per section is stated. Note that neurons projecting to the different target areas are similarly distributed, with a preference to the medial division of the LHb. For abbreviations see Figure 1.

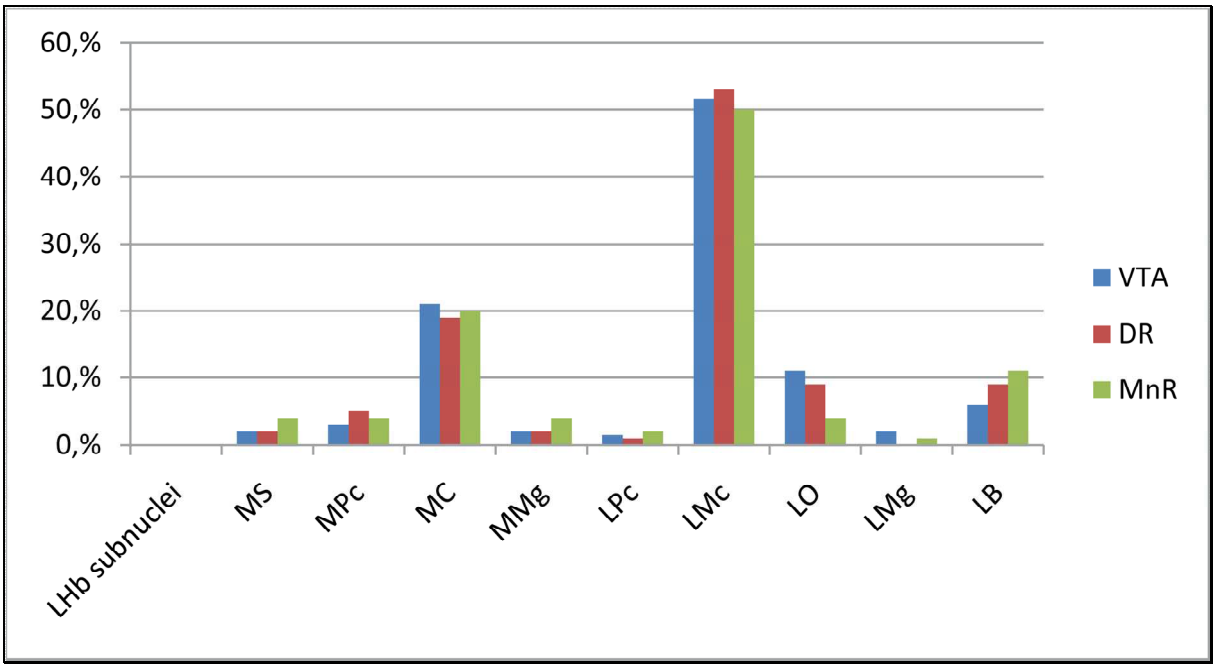

Figure 15: The subnuclear distribution of retrogradely labeled neurons after injections to the VTA, DR and MnR was analyzed. Interestingly, LHb neurons projecting to the different monoaminergic areas are almost similarly distributed throughout the LHb subnuclei. For abbreviations see Figure 1.

3.1.6 Lateral habenular neurons projecting to VTA, DR or MnR strongly express HCN subunits

The expression of HCN channels in retrogradely-traced LHb neurons can be verified by either analyzing the expression of the protein itself or the corresponding mRNA. The detection of mRNAs combined with the tracer labeling is the more promising approach, as retrograde tracers are mainly transported to the cell somata and HCN proteins are mainly located in the neuropil.

The expression of HCN mRNAs in LHb projection neurons was analyzed in coronal brain sections by silver intensification of the tracer and subsequent HCN *in situ* hybridization. Silver intensification of the tracer, accomplished prior to *in situ* hybridization, produced black particles, while the *in situ* hybridization itself resulted in brown deposits of DAB (Figure 16A+B). In these double-labeled sections, LHb cells containing both black particles and brown DAB deposits, were plotted and compared with the total number of retrogradely labeled cells for each of the three injection areas.

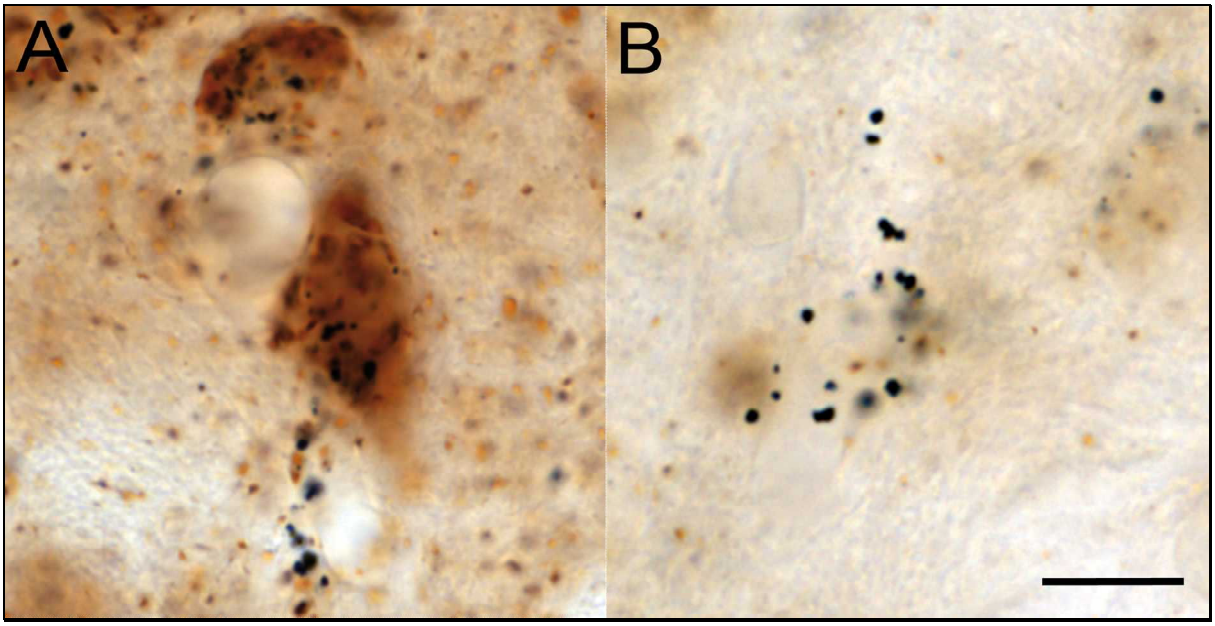

Figure 16: Two retrogradely-traced LHb neurons projecting to the VTA are shown at high magnification (A). Retrograde tracer is visible as black dots in their cytoplasm, representing silver-intensified gold particles. Note that both neurons express HCN2 mRNA, represented by brown DAB deposits. Another retrogradely traced LHb neuron (B) does not express HCN mRNAs, as indicated by the absence of brown DAB deposits. Bar indicates 10 µm.

In general, the evaluation revealed that for all three injection areas, HCN1 mRNA is expressed in less than 10% of all retrogradely labeled LHb neurons, whereas HCN2 to HCN4 mRNAs are found in over 70% (given percentages resemble the "mean" of all evaluated animals per injection area). Subanalysis per injection site demonstrated that in VTA-injected rats, almost all (>95%) retrogradely labeled LHb neurons express HCN2 to HCN4 mRNAs, whereas HCN1 mRNA is only expressed in less than 5% (Figure 17). The HCN expression pattern of LHb cells projecting to the MnR was similar to that of neurons projecting to the VTA. However, slightly more MnR-projecting neurons express HCN1 mRNA (8%), while expression of HCN2 to HCN4 mRNAs is found in about 90% of these neurons. LHb neurons projecting to the DR, unlike those projecting to the VTA, express HCN1 mRNA in a higher percentage (9%), while the percentage expressing HCN2 to HCN4 mRNAs is lower and shows a higher variation between the subunits: HCN2 mRNA with 87%, HCN3 mRNA with 77% and HCN4 mRNA with 88% (Figure 17).

In summary, the majority of LHb neurons projecting to VTA, DR and MnR express HCN2 to HCN4 mRNAs, while only a few express HCN1 mRNA. The expression pattern of the four HCN subunits is quite similar for all three projection areas and there are no subnuclear differences in the percentage of HCN-positive projection neurons.

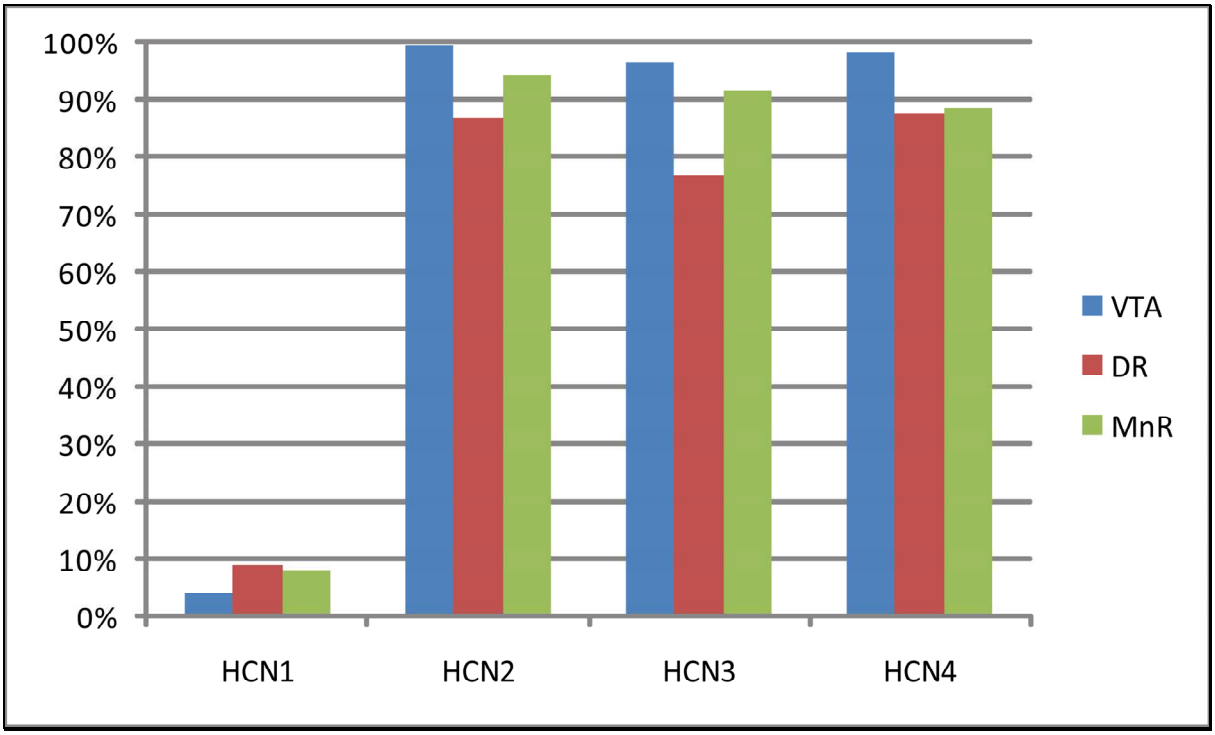

Figure 17: The percentages of LHb neurons projecting to VTA, DR and MnR that express HCN1 to HCN4 mRNAs are indicated by colored bars. Almost all LHb neurons projecting to the monoaminergic areas express HCN2 to HCN4 mRNAs. However, HCN1 mRNA expression is restricted to a few. Overall, the expression pattern of HCN subunits is similar for the different projection areas. Percentages resemble the mean of all evaluated animals per injection site. VTA: 3 rats (87 - 217 retrogradely labeled cells plotted per section); DR: 2 rats (218 - 295 retrogradely labeled cells plotted per section); MnR: 2 rats (243 - 331 retrogradely labeled cells plotted per section)

Considering all experiments collectively, we demonstrated an expression of all four HCN subunits within the LHb subnuclei at mRNA and protein level and within a majority of LHb neurons projecting to the monoaminergic nuclei. We found an expression of HCN2 to HCN4 mRNAs in a high percentage and HCN1 mRNA in a low percentage of LHb cells in general, and within LHb projection neurons in particular. Differences in the expression pattern of subunits between the different LHb projection neurons are very small.

3.2 A glutamatergic projection from the lateral hypothalamus directly targets VTA-projecting neurons in the lateral habenula

The lateral habenula (LHb) exerts a strong continuous inhibition on monoamine release (Lecourtier et al., 2006; Matsumoto and Hikosaka, 2007; Matsumoto and Hikosaka, 2008). The results presented so far suggest that the molecular mechanism underlying this baseline inhibition is an HCN channel-mediated spontaneous activity of LHb projection neurons. This spontaneous activity is subject to changes in response to positive and negative rewards (Ullsperger and von Cramon, 2003; Matsumoto and Hikosaka, 2007; Matsumoto and Hikosaka, 2008). Currently, less is known about the pathways that deliver reward-related information to the LHb and about their effects on the activity of LHb neurons. However, a promising candidate to provide this reward-related information is the lateral hypothalamus (LHA). The LHA measures or receives data about various homeostatic parameters and their changes in response to behaviors and rewards. The LHA is the superior regulator of the homeostatic system and strongly projects to the LHb (Herkenham and Nauta, 1977; Sutherland, 1982; Kowski Dissertation, 2010). To get a better idea of the function of this major link between the homeostatic system and the reward system, we analyzed the neurotransmitters and the cellular targets of the hypothalamic projection to the LHb.

3.2.1 The lateral hypothalamus strongly projects to the lateral habenula

3.2.1.1 Neurons projecting to the lateral habenula are distributed throughout many hypothalamic subnuclei

The LHA is a large heterogeneous field consisting of various subnuclei. Since LHA neurons projecting to the LHb were found in most of these subnuclei (Kowski et al., 2010), big injection sites were generated to label as many LHA axons projecting to the LHb as possible. The injections were aimed at the center of the LHA at a level of Bregma -2.7 mm. Of the total number of six LHA injected rats (LHA-1 to LHA-6), one representative injection site (animal LHA-1) is shown and described in more detail (Figure 18).

In animal LHA-1, a large injection site is located in the center of the LHA at a Bregma level of -2.7 mm. Tracer deposits nearly completely cover the area of the LHA, while almost no spread of tracer into adjacent structures, including capsula interna, tractus opticus, or medial hypothalamus is observable. In a rostro-caudal extent the injection site reaches from Bregma -2.1 mm to Bregma -3.1 mm (Figure 18).

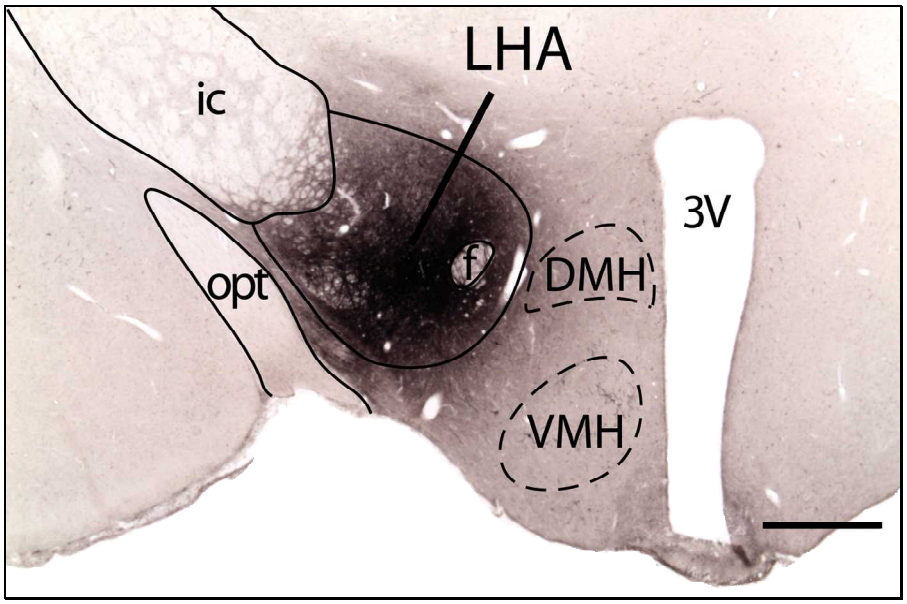

Figure 18**:** The coronal brain section at Bregma -2.7 mm shows a representative Pha-L injection site (black DAB/Ni deposits) in the LHA with illustrations of the target area and surrounding structures. The injection site has only minimal spread of tracer into adjacent structures. Abbreviations: VMH - ventromedial hypothalamus; DMH - dorsomedial hypothalamus; 3V - third ventricle; ic - internal capsule; opt - optic tract; f – fornix. Bar indicates 500 µm.

3.2.1.2 Lateral hypothalamic axons mainly target the medial division of the lateral habenula

Axons from the LHA reach the LHb via two different pathways. Axons from the rostral parts of the LHA proceed rostrally within the medial forebrain bundle and join the stria medullaris to get to the LHb. However, the majority of LHA axons, especially from the caudal areas, initially follow the medial forebrain bundle in a caudal direction before turning dorsally to reach the LHb via the paraventricular fiber system and the fasciculus retroflexus (Herkenham and Nauta, 1977; Sutherland, 1982; Kowski Dissertation, 2010).

Anterograde tracing experiments display a very dense plexus of LHA axons and terminals within the LHb (Figure 19A (rostral LHb) - 19D (caudal LHb)). While ascending in the LHb, these axons form multiple *in passing*- and *terminal buttons*. In general, labeled axons from the LHA target almost all subnuclei with a preference to the medial division of the LHb. The only exception from that is the *oval subnucleus (LO)*, which is completely devoid of traced axons. Interestingly, in some sections an area consistent with the *medial parvocellular subnucleus (MPc)* is completely omitted by LHA axons (Figure 19C+D, asterisks). In contrast to the unstained MHb, the contra-lateral LHb regularly displays a few labeled axons.

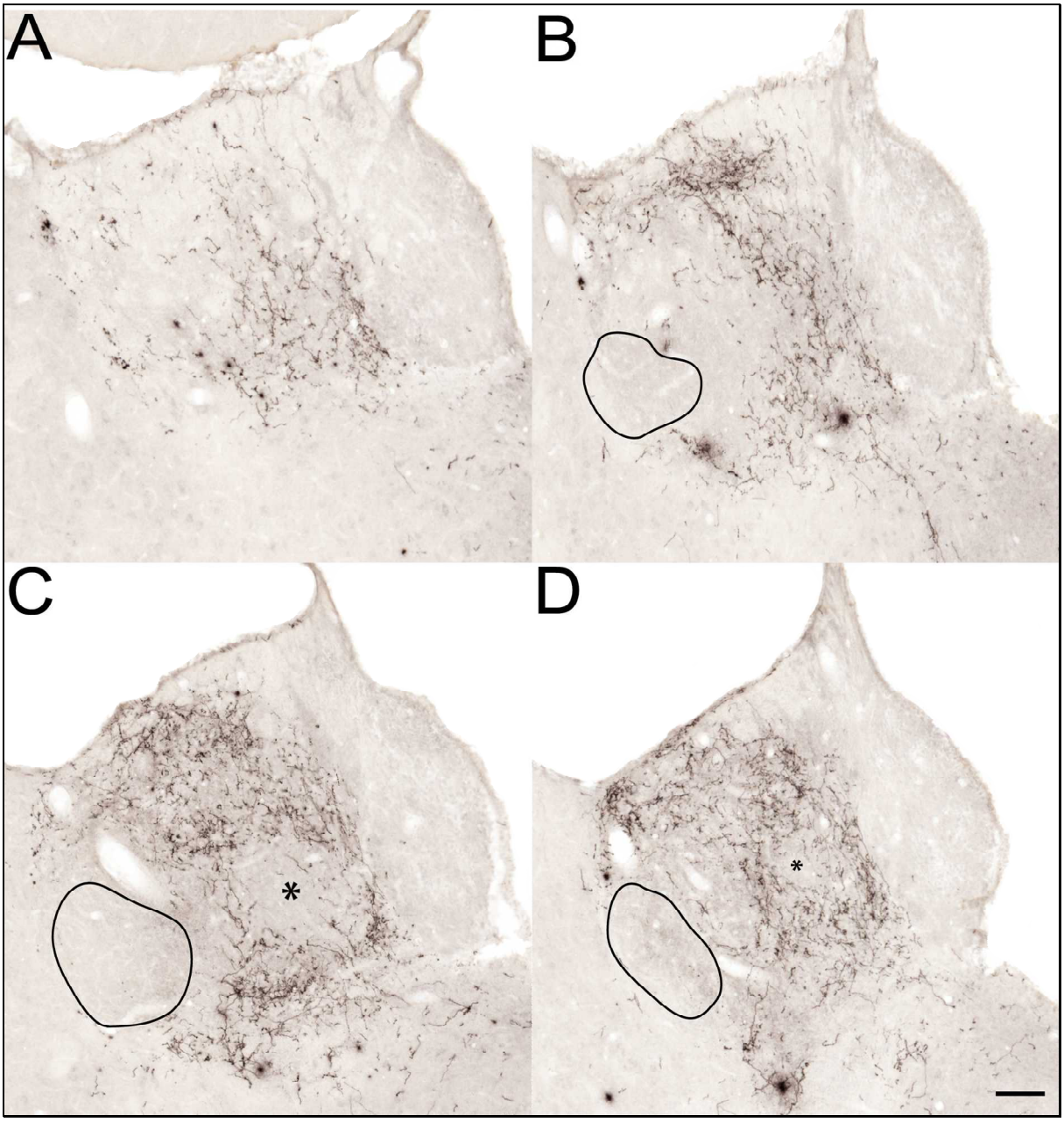

Figure 19: Anterogradely traced axons and terminals (black DAB/Ni deposits) from the LHA appear widespread within the LHb with the most intense staining in the medial division (A-rostral LHb to D-caudal LHb). An exception from that is the *oval subnucleus (LO)*, which is completely devoid of LHA axons (framed area in C-D). Note, that an area consistent with the *medial parvocellular nucleus (MPc)* is also not targeted by the LHA projection (C and D, asterisks). Bar indicates 100 µm.

3.2.1.3 Projections from the lateral hypothalamus to the lateral habenula are glutamatergic

All mRNAs for the vesicular glutamate transporters (vGluT1 to vGluT3) are expressed within the LHA (Geisler et al., 2007) (Allen Brain Atlas). Hence, we hypothesize that this widespread excitatory neurotransmitter may be used by the LHA projection that targets the LHb. The three different isoforms of the vesicular glutamate transporters (vGluT1 to vGluT3) are used for the transport of glutamate into the synaptic vesicles of glutamatergic terminals. Thus, vGluTs are well suited for the identification of glutamatergic terminals (Bellocchio et al., 2000). Data from *in situ* studies of the mouse brain, as presented by the Allen Brain Atlas, reveal a very weak expression of vGluT1 throughout the LHA, a strong expression of vGluT2 in most areas of the LHA and a vGluT3 expression restricted to a few cells distributed in the lateral parts of the LHA (Allen Brain Atlas).

Immunocytochemical analyses of vGluT1-3-expression in the habenula

In a first step, to analyze which types of vGluTs are actually expressed by terminals in the LHb, vGluT1, vGluT2 and vGluT3, were immunocytochemically visualized in LHb sections. These experiments reveal a strong expression of vGluT1 within the MHb, facing a weak expression throughout the LHb. Stronger signals within the LHb are restricted to some fibers in the *basal subnucleus (LB)* and in an area consistent with the *superior subnucleus (MS)* (Figure 20 A, arrows).

The expression of vGluT2 is very intense throughout MHb and LHb, leaving only the major fiber bundles unstained. Cell bodies exhibiting vGluT1- or vGluT2 immunoreactivity are undetectable (Figure 20 B). Since vGluT2 expression is extraordinarily strong, a detailed analysis of the cellular distribution in 25 µm thick LHb sections is difficult. Therefore, semithin sections of the LHb were labeled with vGluT2 antibodies. In these semithin sections many neurons and their dendrites are densely surrounded by vGluT2 positive terminals (Figure 21, arrows).

Immunoreactivity for vGluT3 is moderate throughout the MHb and displays a very heterogeneous pattern within the LHb. The neuropil is intensively stained, preferentially in the area of the *lateral magnocellular subnucleus (LMc)*. In contrast to vGluT1 and vGluT2, many vGluT3-positive cells are distributed throughout the lateral division of the LHb (Figure 20 C).

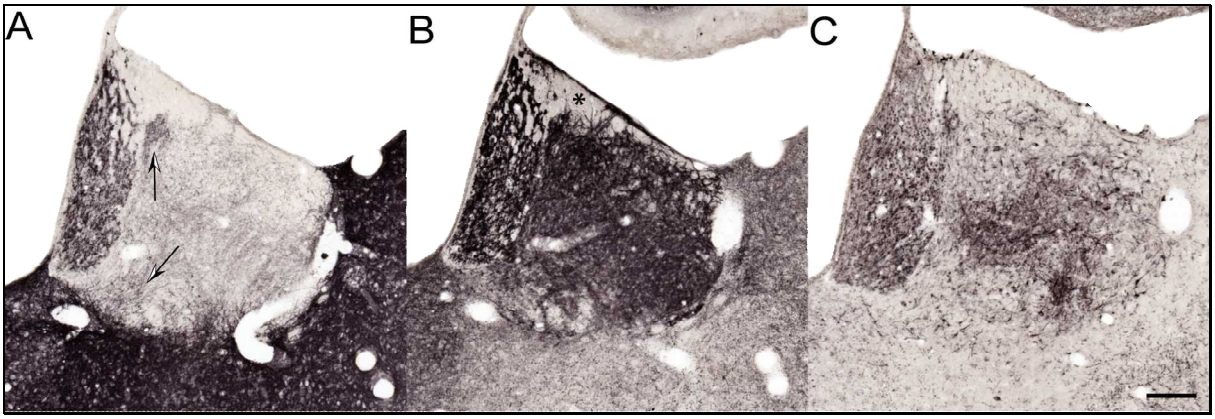

Figure 20: All three vGluTs are expressed within the rat Hb. VGluT1 is mainly localized in the MHb, with only a weak staining in the LHb. An exception from that is the area of the *superior nucleus (MS)* and parts of the *basal subnucleus (LB)*, which are more strongly labeled (arrows in A). VGluT2 shows a very strong expression throughout MHb and LHb, leaving only the major fiber bundles unstained (asterisk in B). VGluT3 displays a heterogeneous pattern within the LHb, with the strongest label in the *lateral magnocellular subnucleus (LMc)* (C). It is the only subunit that is expressed on cell bodies in the LHb. Bar indicates 100 µm.

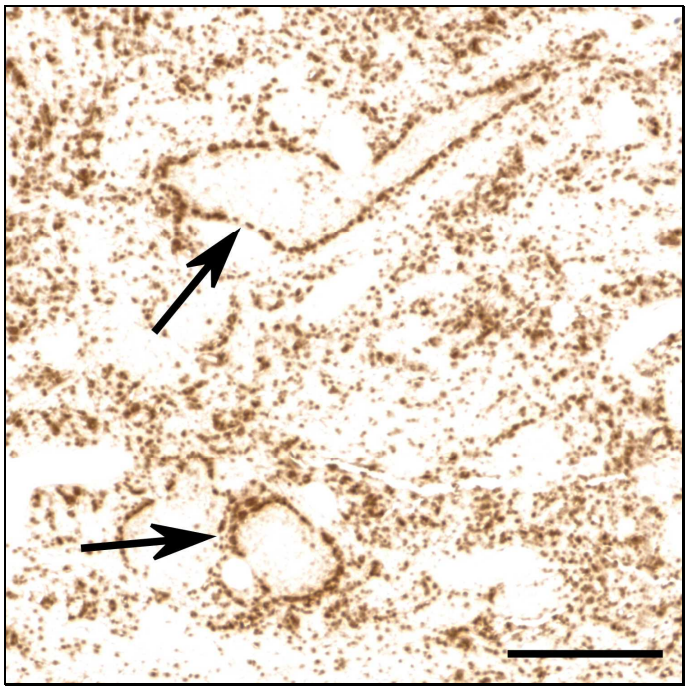

Figure 21: VGluT2 expression is extremely strong throughout the LHb, making it difficult to analyze the cellular distribution in detail (Figure 20 B). Therefore, vGluT2 was visualized in semithin sections. In these sections, many LHb neurons are surrounded by vGluT2-ir, indicating that they are densely targeted by glutamatergic terminals (black arrows). These terminals are localized at the cell body, as well as along their big dendrites. Bar indicates 10 µm.

In summary, all vGluT mRNAs are produced by cells in the LHA (Allen Brain Atlas, Geisler et al., 2007) and their corresponding proteins are expressed within the LHb. Hence, all three vGluTs are potential candidates for an expression in LHA terminals. Consequently, labeling of PhaL was combined with the visualization of all three vGluTs in LHb sections. In a first set of experiments, these double-labeled sections were scanned at the confocal laser scanning microscope (CLSM) to check whether LHA terminals in the LHb display immunoreactivity for vGluT1, vGluT2 or vGluT3. In CLSM scans of the LHb, the green fluorescence indicating vGluT1- or vGluT3- positive synapses (Figure 22, blue arrows) and the red fluorescence indicating LHA axons (white arrows) display segregated distribution patterns. In particular no fluorescence overlays are found in traced terminals, indicating that neither vGluT1 (Figure 22, A1+2) nor vGluT3 (Figure 22, B1+2) is expressed in LHA terminals in the LHb. Compared to vGluT1-ir, and consistent with light microscopic findings, vGluT3-ir is more concentrated in and around cell bodies, with only a few solitary signals.

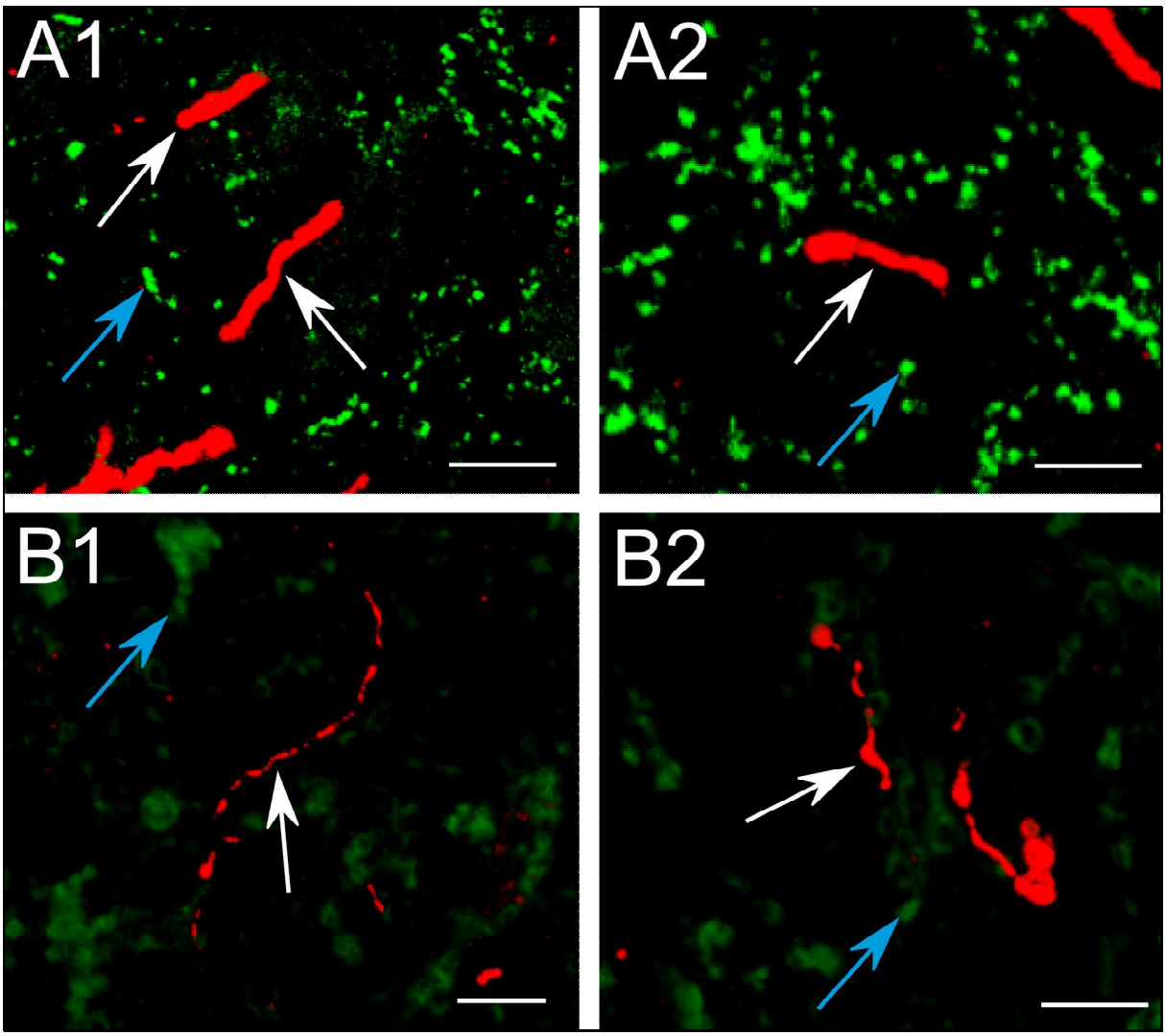

Figure 22: For figure legend see following page.

Figure 22: In highly magnified CLSM-images of the LHb, the green spots either indicate vGluT1- (A1+A2) or vGluT3- (B1+B2) expression (blue arrows). The red structures represent anterogradely traced LHA axons (white arrows). The green and red fluorescences are separated and do not show any overlap, indicating that neither vGluT1 nor vGluT3 is expressed in LHA axons. In agreement with ICC studies, vGluT3 is expressed in cell bodies in the LHb (B1). VGluT1 in contrast is mainly located in terminals, while no cell bodies are stained (A1+A2). Bars indicate 10 µm in A1 and B1 and 5µm in A2 and B2.

vGluT2

In contrast to vGluT1 and vGluT3, several LHA terminals throughout the LHb seem to contain vGluT2 (Figure 23). This is indicated by overlapping fluorescences, resulting in yellow colored terminals (Figure 23A, white arrows). Interestingly, some green spots are directly located along the LHA axons, suggesting that these axons may themselves be the target of vGluT2-positive terminals from unknown origin (Figure 23B, white arrows). Double-labeled terminals are located mainly in the medial division of the LHb. Surprisingly, only a comparatively small number of retrogradely labeled LHA terminals display vGluT2 fluorescence.

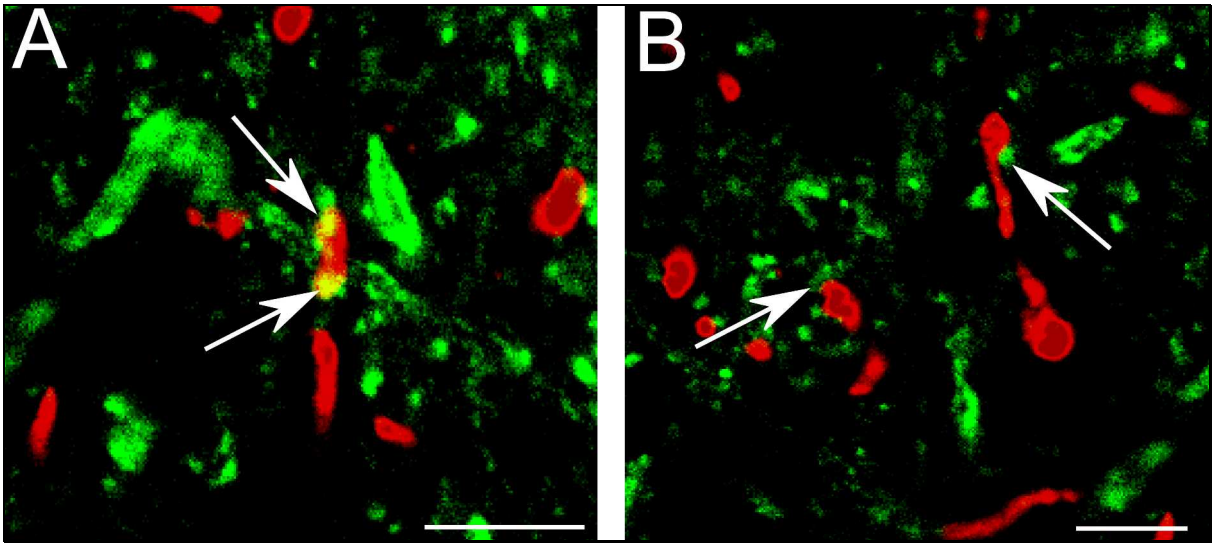

Figure 23: Highly magnified 2D - CLSM images of double-labeled LHb sections show vGluT2 signals in green and LHA terminals in red. Note, that some LHA terminals contain vGluT2 signal, resulting in yellow colored terminals (A, white arrows). Overlapping fluorescences in CLSM2-D scans strongly indicate that these terminals are glutamatergic. Interestingly, axons from the LHA are themselves targeted by vGluT2 - positive synapses of unknown origin (B, white arrows). Bars indicate 5 µm.

Electron microscopic analyses of vGluT2 expression in the habenula

Results from the CLSM indicate that vGluT2 is the only isoform that is expressed in LHA terminals. To evidence this expression and evaluate the fraction of vGluT2-positive terminals among all LHA terminals, electron microscopic (EM) analyses were performed. Therefore, a DAB-visualization of PhaL was combined with a virtual preembedding technique to label vGluT2 with nanogold particles (see methods, paragraph 2.13). These double-labeled ultrathin sections were checked for terminals containing both black deposits of DAB and nanogold. Each ultrathin section was accompanied by an adjacent semithin section to get a better overview and to simplify navigation (Figure 25). To test the specificity of VGluT2-/Pha-L- double labelings for the EM, several controls were performed. Accounting for the selectivity of the vGluT2 labeling, many terminals in the LHb remain completely unstained with vGluT2 antibodies (Figure 24A), while others are intensively stained (Figure 26 B+C). Consistent with the exclusive expression of vGluT2 in terminals, EM analyses never display immunoreactivity for vGluT2 in axons (Figure 24B).

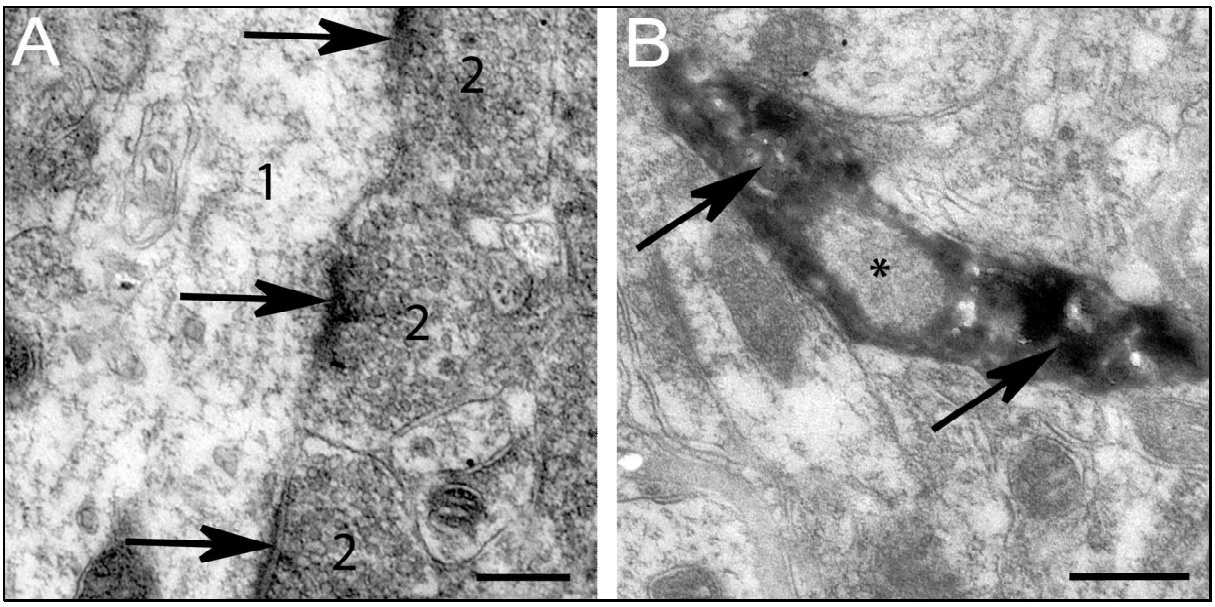

Figure 24: In vGluT2-labeled ultrathin sections, many terminals remain completely unstained (A, 2), while others show a very strong signal (Figure 26, B+C), accounting for the specificity of the vGluT2- visualization. The vGluT2-negative terminals in A are located along a big dendrite (1), which they synaptically target (A, black arrows). B shows an anterogradely traced axon from the LHA (black arrows indicate DAB deposits) in the same LHb section that is also devoid of vGluT2 signal. This is in agreement with the exclusive expression of vGluT2 in terminals. Bars indicate 500 nm in A and 1000 nm in B.

In contrast to axons, most of the actual LHA terminals contain densely packed vGluT2-positive vesicles, as indicated by at least ten nanogold particles (Figure 26 B2+C2). Some vGluT2-positive vesicles are even located within the preterminal regions of the axon (Figure 26 A2). Most of the LHA terminals observed in these experiments form axo-dendritic synapses (Figure 26, arrows). Interestingly, none of the terminals or axons analyzed in this study contains dense-core vesicles, which are typical for the storage of neuropeptides. The localization of the terminals (shown in Figure 26) within the habenular complex is delineated in an adjacent semithin section (Figure 25).

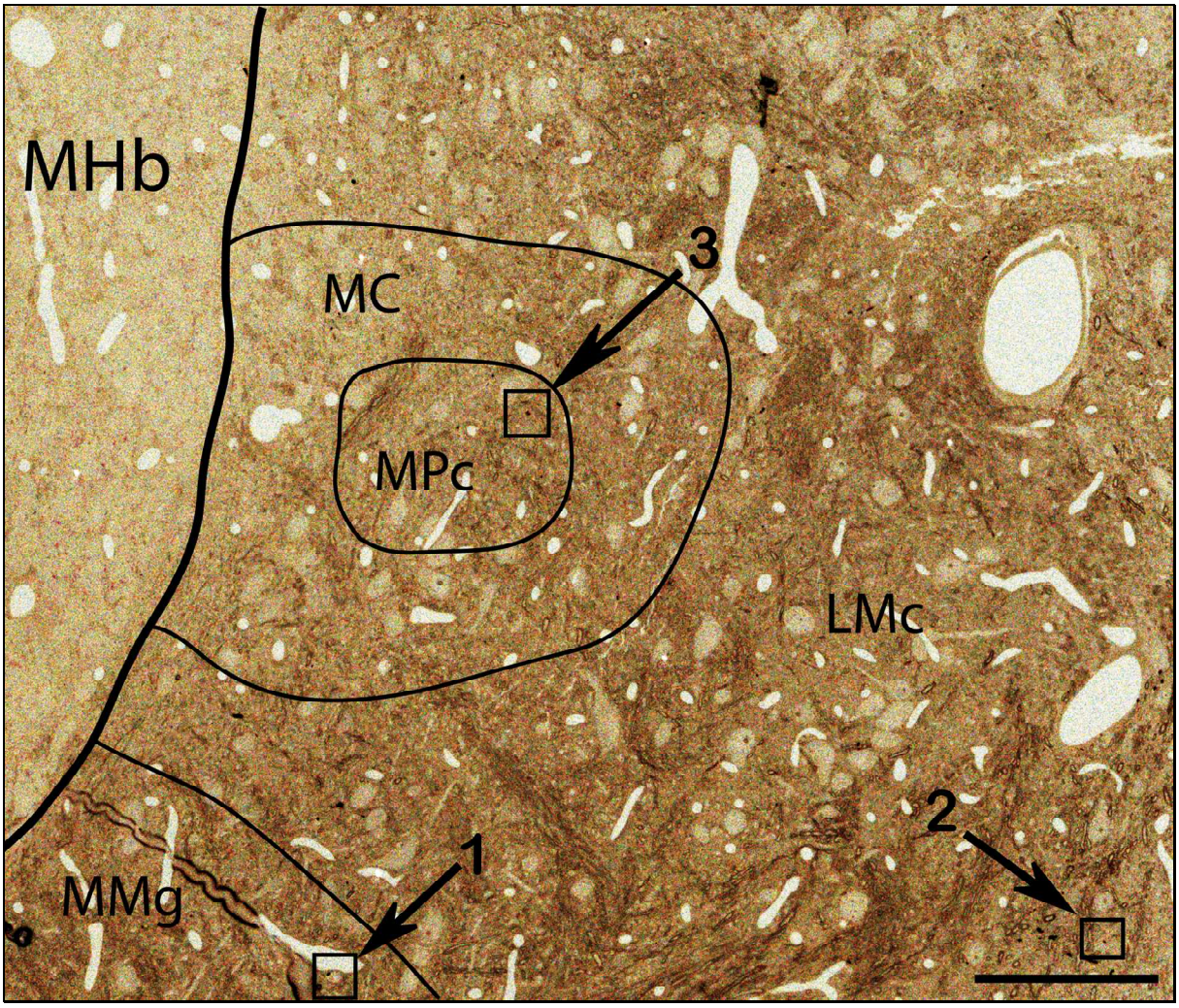

Figure 25: In semithin sections of the LHb, anterogradely traced axons and terminals are indicated by brown DAB deposits. These semithin sections were used to identify regions of interest (ROIs) that were subsequently analyzed in adjacent ultrathin sections at the electron microscope. Electron microscopic images of the three boxed areas (1-3) are presented in Figure 26. Abbreviations: MHb – medial habenula; LHb – lateral habenula; MC – central subnucleus; MPc- medial parvocellular subnucleus; MMg – marginal subnucleus. Bar indicates 100 µm.

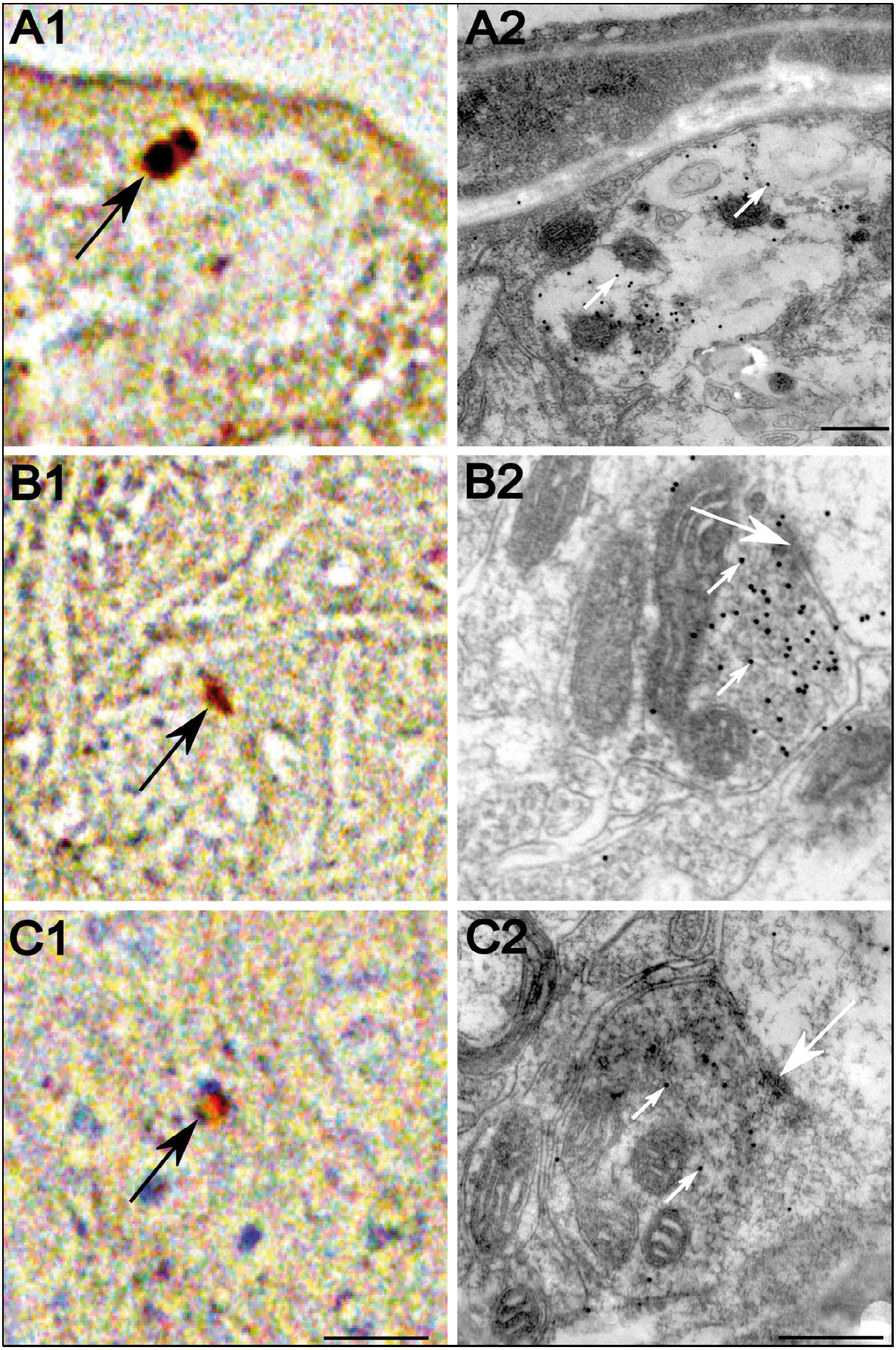

Figure 26: For figure legend see following page.

Figure 26: The regions of interest (ROIs) that were identified in the semithin section (boxed areas in Figure 25) are now presented at high magnification. Images (A1-C1) on the left side display magnified images of the semithin section, with brown DAB deposits indicating traced LHA terminals (black arrows). Electron microscopic images of the same terminals were acquired from adjacent ultrathin sections and are arranged on the right side (A2-C2). These terminals contain both anterograde tracer (black deposits of DAB) and 15 nm nanogold particles, indicating vGluT2 reactivity (small white arrows). VGlut2-positive vesicles are sometimes located in preterminal axons (A2), but mainly in the actual terminals (B2 and C2) close to the synaptic contacts (indicated by big white arrows in B2 and C2). The targeted structures are dendrites. Thus, the LHA projection seems to be predominantly glutamatergic. However, not all labeled LHA terminals express vGluT2. Other neurotransmitters might be involved. Bars indicate 5 µm in A1-C1 and 500 nm in A2-C2.

3.2.1.4 GAD is not expressed in lateral hypothalamic terminals

The GABA-synthesizing enzyme glutamate decarboxylase (GAD) is a protein routinely used for the identification of GABAergic synapses. Since GAD mRNA is detectable in neurons in the LHA (Allen Brain Atlas) and GAD protein is strongly expressed in LHb terminals (Figure 27), we also asked, whether the LHA projection may be GABAergic.

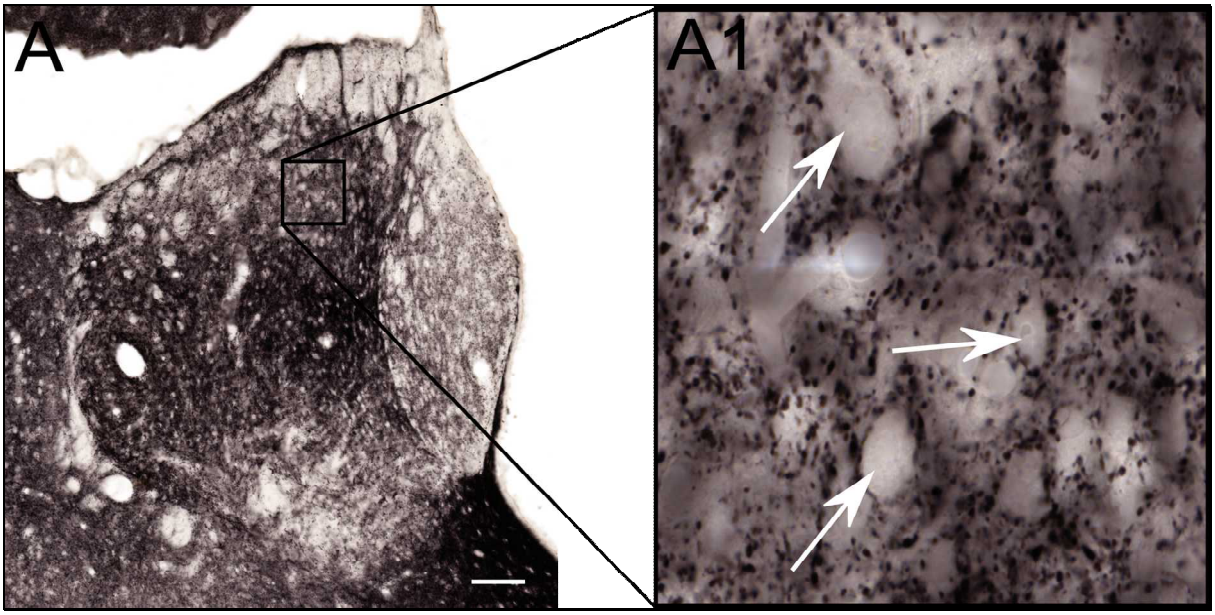

Figure 27: Immunocytochemical analyses reveal a strong and widespread expression of GAD throughout the LHb and a weaker expression within the MHb (A). In a high magnification image of the LHb (A1), many cell bodies are surrounded by GAD signal, indicating that these cells are strongly targeted by GABAergic terminals (white arrows). Bar indicates 100 µm.

Therefore, GAD and PhaL were simultaneously fluorescence double-labeled and scanned in the CLSM. However, these analyses found no GAD signal in LHA terminals. Both fluorescences are clearly detectable but exhibit no overlays, thereby excluding GABAergic synapses of this projection (Figure 28).

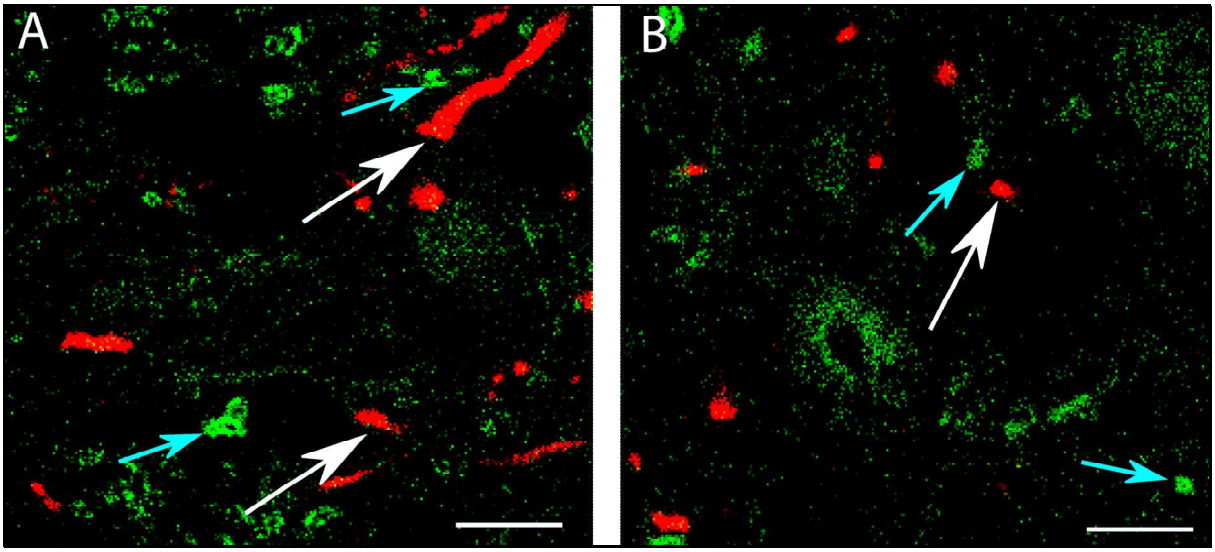

Figure 28: CLSM scans of double-labeled LHb sections display GAD signal in green (blue arrows) and LHA axons and terminals in red (white arrows). However, the two fluorescences are not collocated in any terminal, indicating that the LHA projection is not GABAergic. Bars indicate 5 µm.

3.2.1.5 Lateral hypothalamic axons in the lateral habenula do not contain the neuropeptides Orexin and Galanin

The LHA is a very heterogeneous area with different cell types expressing various neuropeptides (Melander et al., 1986; Miller et al., 1993; Nambu et al., 1999). Neuropeptides are also detectable in axons within the LHb (Figures 29 and 30). Hence, we analyzed the LHA projection for the potential use of neuropeptides. Only those neuropeptides that are expressed in cells of the LHA, as well as in terminals or axons within the LHb came into consideration. Appropriate neuropeptides include melanocyte-stimulating hormone (MCH), neuropeptide Y (NPY), Arginin-Vasopressin (Arg-VP), Orexin and Galanin. The distribution of these peptides within the LHb is shown in Figures 29 and 30.

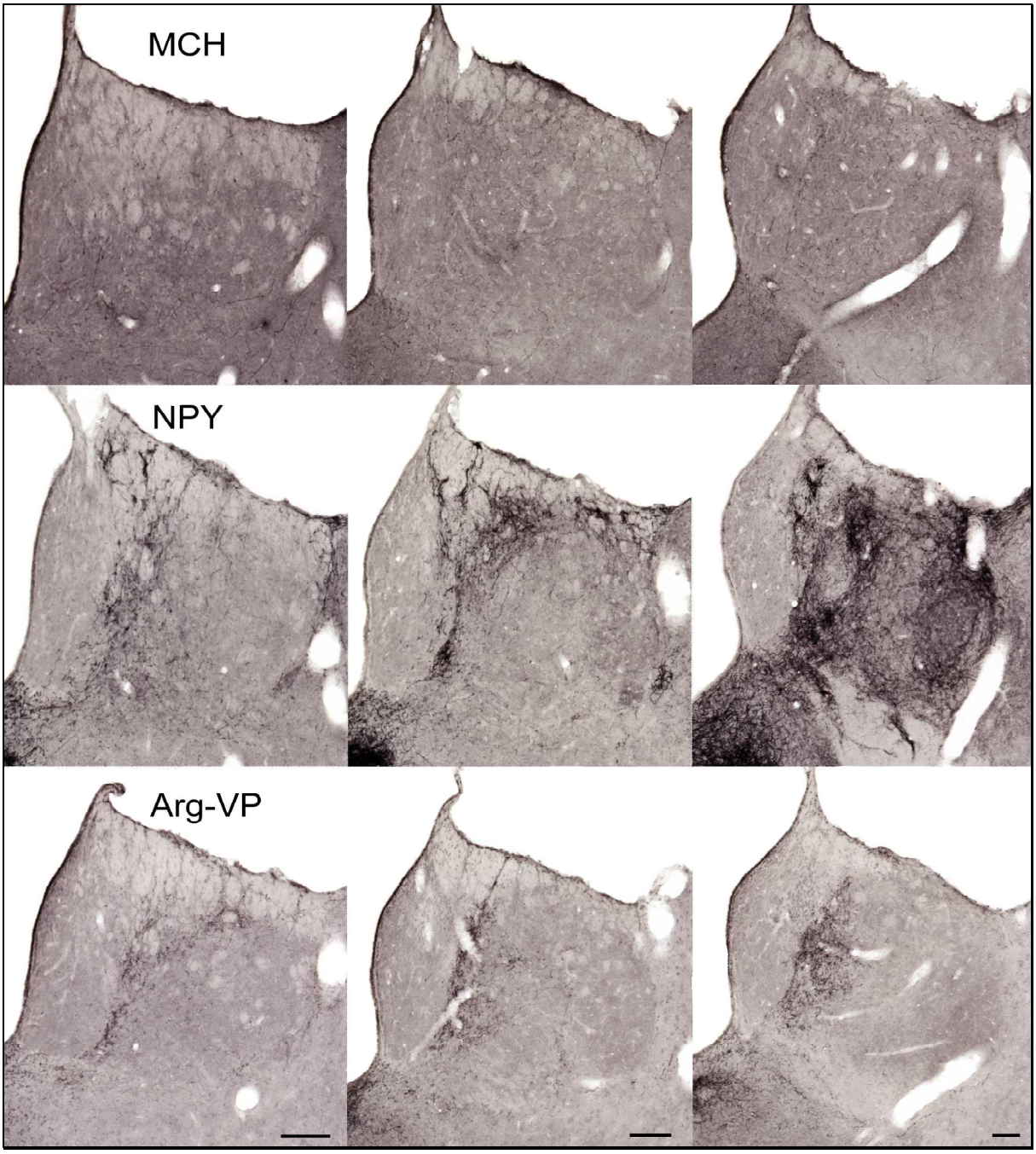

Figure 29: Several neuropeptides, including MCH, NPY and Arg-VP are expressed in axons and terminals within the LHb. MCH expression is rather weak and restricted to some scattered axons distributed throughout the entire LHb. NPY is expressed mainly within the medial division of the anterior and mid LHb. Towards the caudal end, NPY expression becomes stronger, also covering the lateral division. Axons containing Arg-VP are restricted to the medial division of the LHb. Interestingly, all three neuropeptides completely omit the MHb. Bars indicate 100 µm.

Here, we exemplarily analyzed the expression of Galanin and Orexin in LHA axons in the LHb. Orexin seemed promising since many Orexin producing cells are located in the LHA. Galanin mRNA producing cells are also present within the LHA (Allen Brain Atlas) and the distribution of Galanin peptide resembles the distribution of traced LHA terminals (Figure 27 B1-3).

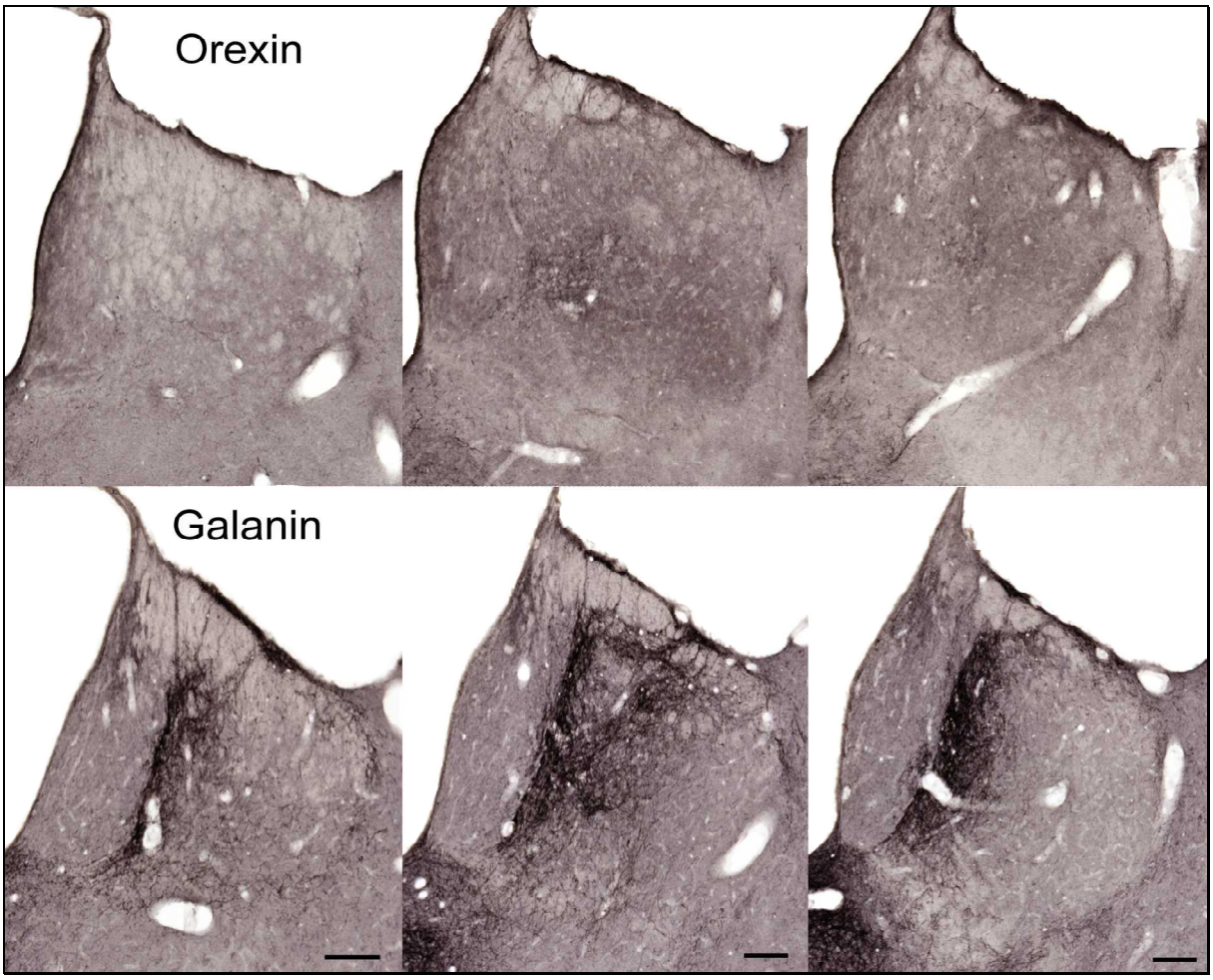

Figure 30: The expression of Orexin is restricted to some thin axons distributed throughout the LHb. Stronger signals are located in the area of the *medial parvocellular (MPc)* and *central subnucleus (MS)*. Galanin is strongly expressed in axons and terminals within the medial division of the LHb. The MHb and the lateral division of the LHb are mostly free of Galanin signal. Regarding distribution and shape, Galanin-positive axons are similar to the traced LHA terminals (see figure 19). Bars indicate 100 µm.

Both fluorescence signals are clearly detectable in the LHb, however, they are not co-localized in the same axons (Figure 31). Orexin-containing axons mostly run completely separated from the LHA axons and do not exhibit any contacts to them (Figure 31).

In contrast to Orexin, many Galanin-positive axons are located directly beside LHA axons (Figure 31). These galaninergic axons display various enlargements that actually seem to be attached to the traced LHA axon (Figure 31, arrows).

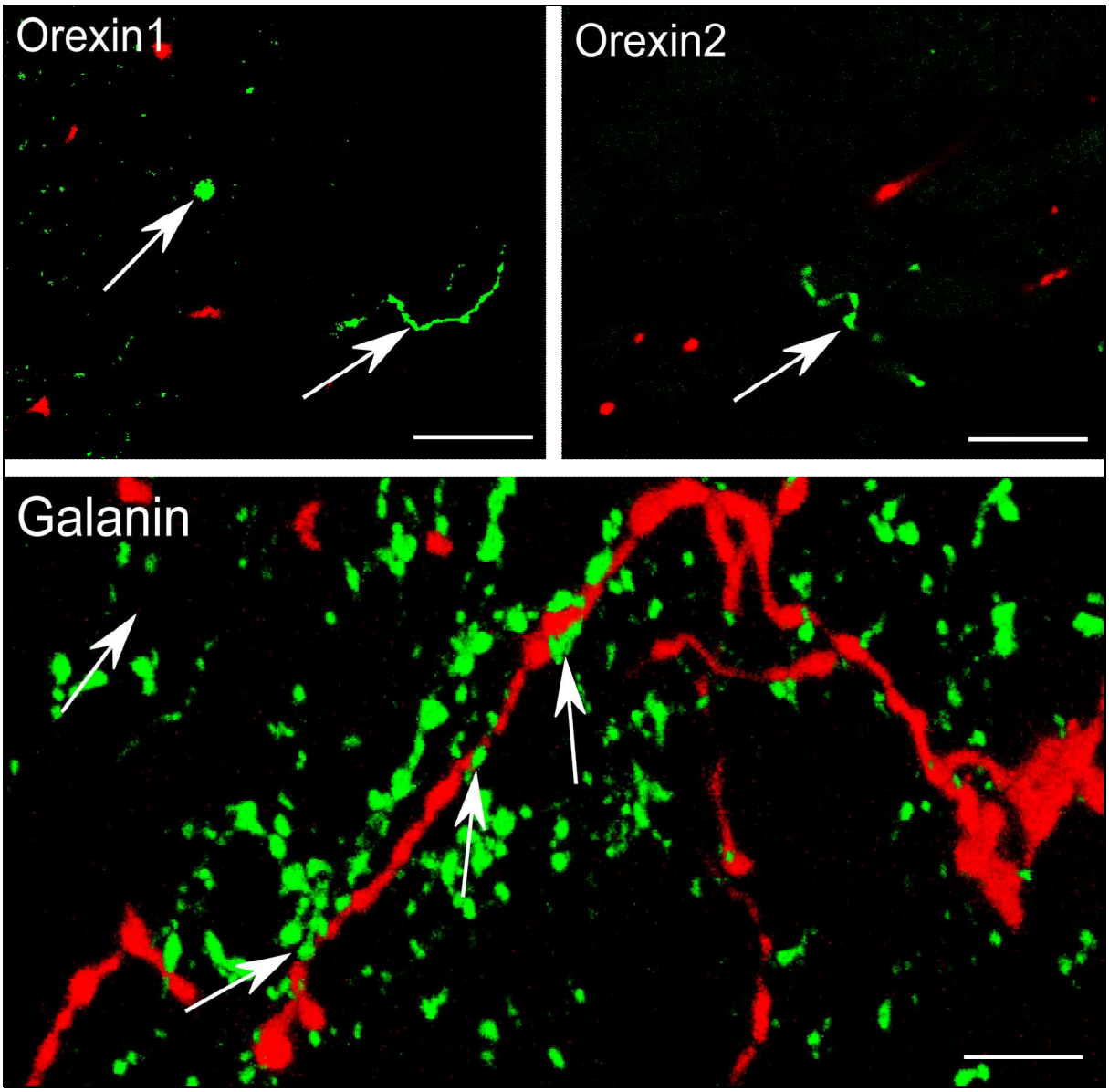

Figure 31: CLSM scans of double-labeled LHb sections display neuropeptides in green and LHA axons in red. Orexin-positive axons appear as thin green structures with some enlargements (Orexin1+2, white arrows). However, they are completely separated from the LHA axons, not showing any fluorescence overlap. In contrast to that, Galanin-positive axons partly run parallel to the LHA axons. Enlargements of these galaninergic axons are closely attached to the LHA axon (Galanin, white arrows). Bars indicate 5 µm.

3.2.2 Lateral hypothalamic terminals directly target VTA-projecting neurons in the lateral habenula

Due to its strong projection that nearly targets all LHb subnuclei, the LHA seems to play an important role in the regulation of LHb activity. Given the expression of vGluT2 in LHA terminals, this projection seems to be predominantly excitatory. To analyze the potential effects of this projection on LHb baseline inhibition, it is important to know which cells are targeted and how the information is further processed. As the LHA projection may transmit reward-encoding information, we hypothesize that LHA terminals directly contact VTA-projecting LHb neurons, thus changing their baseline activity. In this model the LHA would be able to modulate monoamine release via the LHb. To prove our hypothesis, we performed double-tracing studies injecting the anterograde tracer PhaL into the LHA and the retrograde tracer FG into the VTA of adult male rats. Subsequently, both tracers were visualized in the LHb.

3.2.2.1 VTA-projecting neurons and axons from the lateral hypothalamus are similarly distributed within most of the lateral habenular subnuclei

Double-tracing experiments were carried out with the same coordinates as those used for VTA- and LHA injections in the previous experiments. Injection sites were similarly located as specified in these experiments, so that they are not again described in detail. Overall, four double- injected animals were evaluated for this study. In good agreement with findings from single-tracing experiments (paragraphs 3.1.5 and 3.2.1), the distribution of retrogradely-traced cells from the VTA and anterogradely-traced axons from the LHA reveals a big regional overlap within most of the LHb subnuclei, with a preference to the medial division of the LHb (Figure 32) (see also figures 14 and 19).

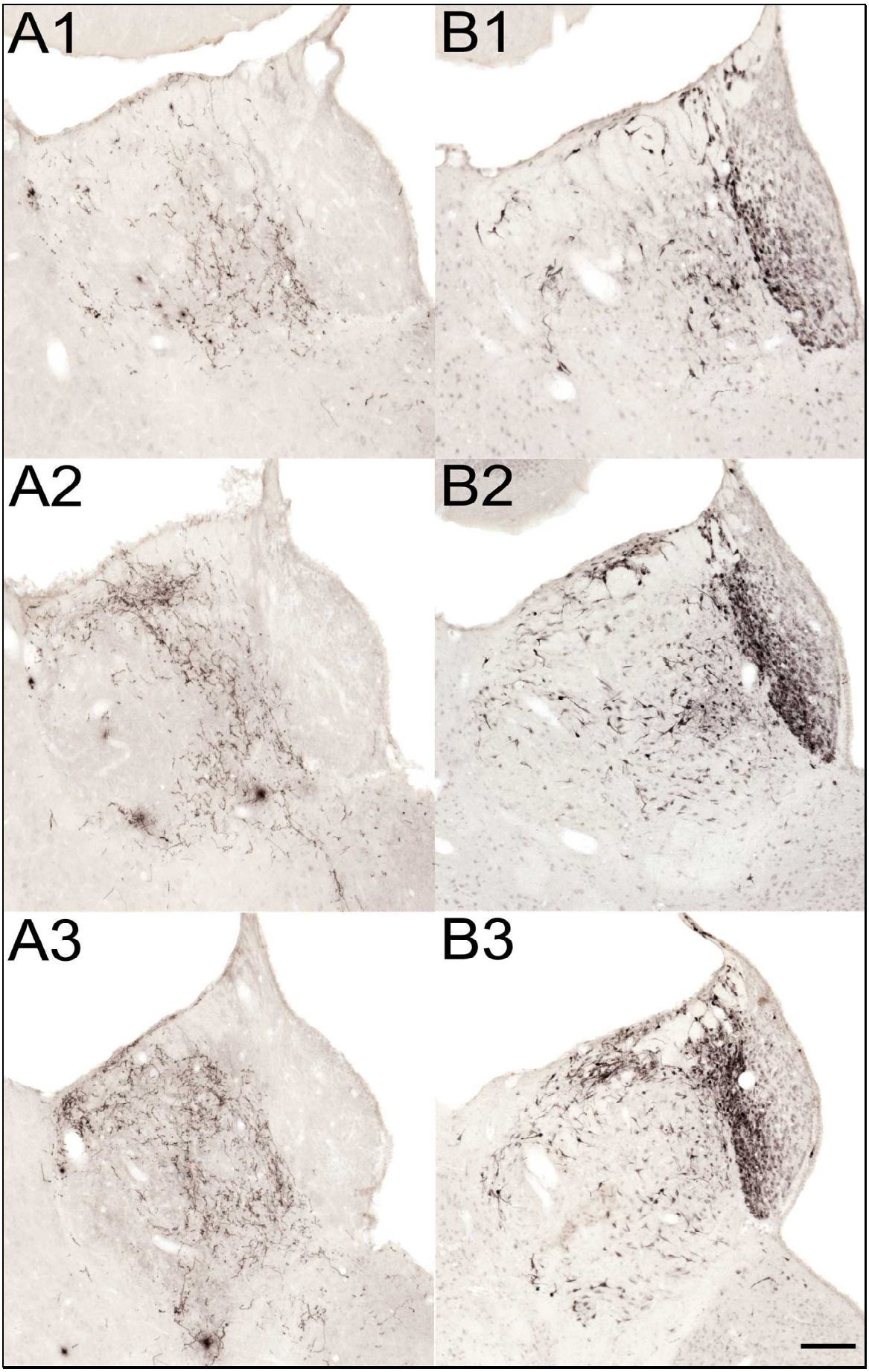

Figure 32: For figure legend see following page.

Figure 32: Double tracing experiments reveal that LHA terminals (A1-3) and neurons projecting to the VTA (B1-3) are similarly distributed throughout the LHb, with a preference to the medial division. Bar indicates 100 µm.

LHb neurons retrogradely traced from the VTA show strongly stained cell bodies and one to three weaker stained dendrites, traceable over a distance up to 50 µm (Figure 33 A). In high magnification images, some LHA terminals actually seem to surround cells, targeting them from all sites (Figure 33 B).

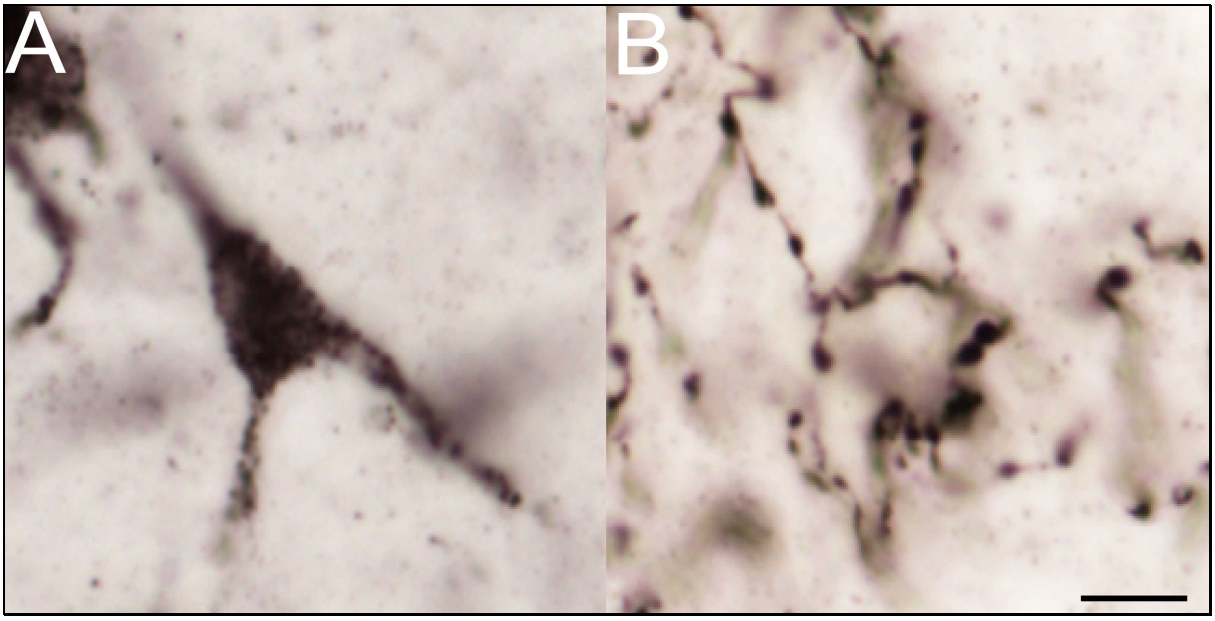

Figure 33: LHb neurons projecting to the VTA show a strongly stained cell body with one to three weaker stained dendrites (black DAB/Nickel deposits in A). Axons from the LHA form multiple terminal- and in passing- buttons (black DAB/Nickel deposits in B). These terminals actually seem to surround individual LHb neurons targeting them from all sides. Bar indicates 10 µm.

3.2.2.2 Lateral hypothalamic terminals directly contact VTA-projecting neurons in the lateral habenula

To analyze LHb sections of double-traced animals for potential contacts of LHA terminals on VTA-projecting neurons, both tracers were visualized using fluorescence-labeled secondary antibodies. Sections were scanned in the CLSM, first at a low magnification to find potential contacts and thereafter at a high magnification to generate detailed 3-D scans of potential contact sites.

These scans show several VTA-projecting neurons that are contacted by axons from the LHA. Contacted cells are mostly located within the medial division of the LHb. Most of them are found in the area of the *central subnucleus (MC)*, but also in all other areas where both tracers are colocalized.

Cells with three different types of contacts are discriminable. The first type of cells is contacted on large dendrites close to the cell body (Figure 34, A1). The second type achieves contacts of LHA terminals directly on the cell body (Figure 34, A2). The third type of cells is densely surrounded by LHA terminals that target the cell body from all sides (Figure 34, B). The contact sites are usually formed by enlarged terminals of a labeled axon sitting directly and broadly-based on VTA-projecting neurons, indicating the actual existence of synaptic contacts.

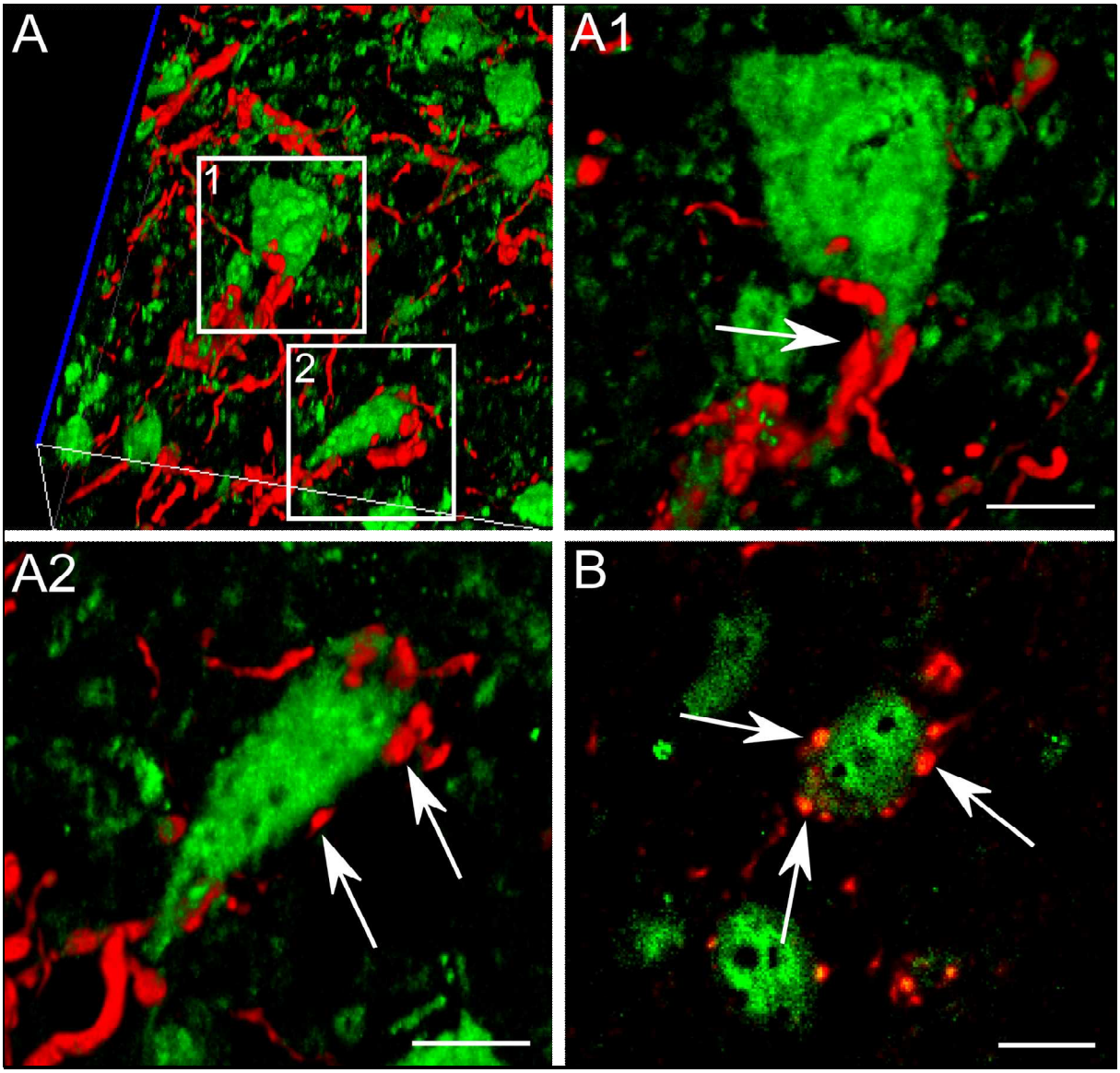

Figure 34: Reconstructed 3-D CLSM images of double-labeled LHb sections show various contact sites (white arrows) of anterogradely-traced LHA terminals (red fluorescence) on cell bodies and big dendrites of retrogradely-traced VTA-projection neurons (green fluorescence). While some cells only achieve contacts on big dendrites, others are densely surrounded and contacted by LHA terminals from all sides. Bars indicate 10 µm.

To ensure the existence of synapses at these contact sites, the double-fluorescence was combined with the detection of synaptophysin. Synaptophysin is a synaptic vesicle glycoprotein, exclusively expressed in synapses. In CLSM scans of fluorescence triple-labeled sections, the green fluorescence indicating synaptophysin is located within LHA terminals opposing VTA-projecting cells, evidencing the existence of synaptic contacts at these locations (Figure 35).

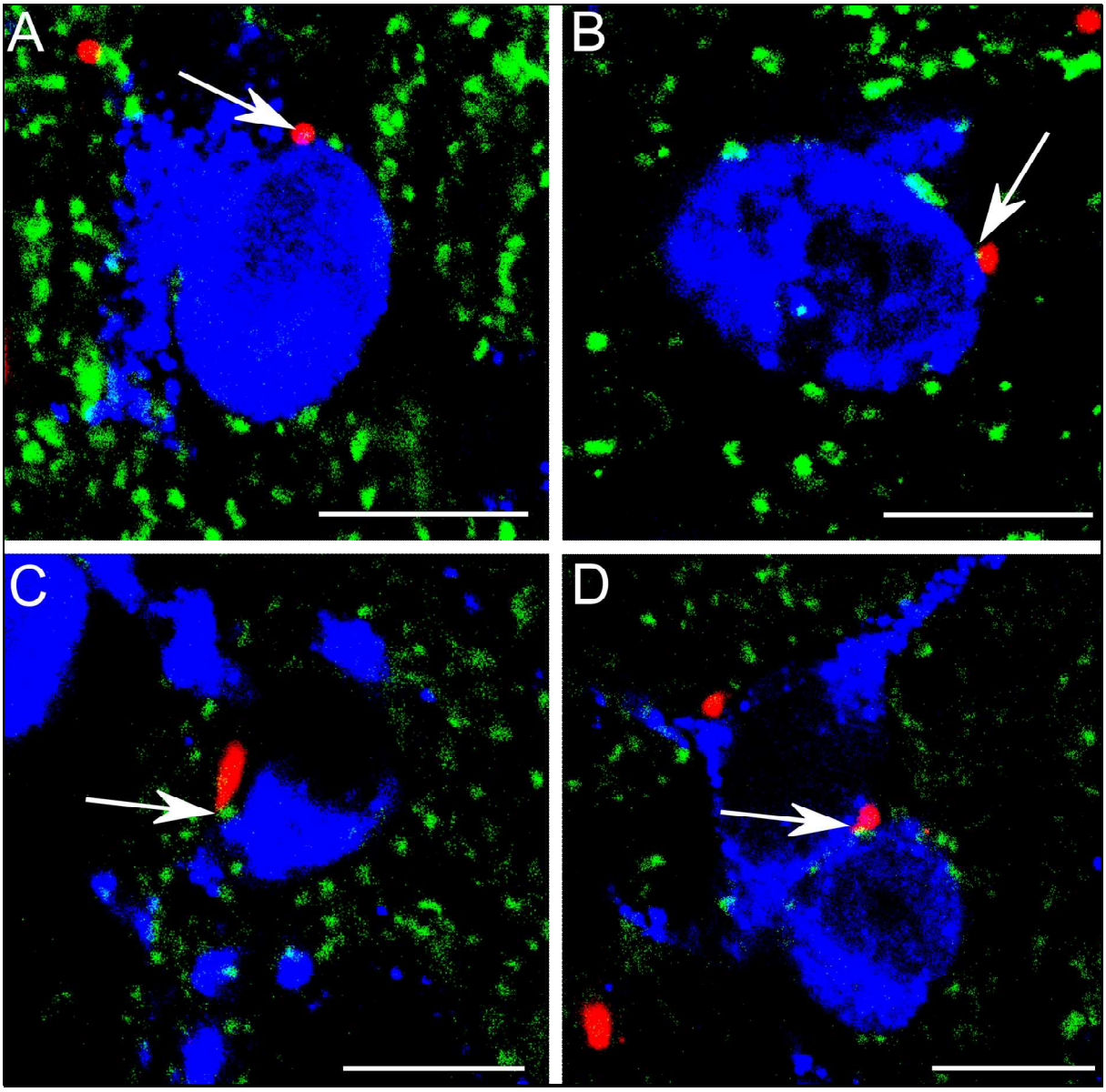

Figure 35: 2-D CLSM scans of triple-labeled LHb sections evidence the existence of synaptophysin (green fluorescence) at the contact sides between LHA terminals (red fluorescence) and VTA-projection LHb neurons (blue fluorescence). Bars indicate 10 µm.

In summary, many VTA-projecting neurons in the LHb are contacted by LHA terminals. These terminals form multiple synapses either on their dendrites or cell bodies, indicating a strong and direct influence of the LHA on LHb projection neurons. These contacts are located in all regions of the LHb, where both tracers are colocalized. However, many LHA terminals terminate on other, so far unidentified, structures. The projection is mainly glutamatergic, hence having an excitatory effect on LHb projection neurons. GABA or neuropeptides seem not to be involved.

4. Discussion

In a basic state, when neither negative nor positive rewards are processed, the LHb exerts a strong tonic inhibition on monoamine release (Kim and Chang, 2005; Lecourtier et al., 2008; Matsumoto, 2009). Currently it is unknown, whether this inhibition is the result of a continuous external activation of LHb projection neurons or if it is due to a spontaneous intrinsic activity.

In the first part of this study, the widespread expression of HCN channels within the LHb and specifically in those LHb neurons projecting to the monoaminergic nuclei was demonstrated. Interestingly, LHb neurons projecting to VTA, DR and MnR exhibit a similar expression pattern of HCN subunits. While most of these neurons contain HCN2 to HCN4 mRNAs, HCN1 mRNA expression is restricted to a few. This neuroanatomical evidence indicates that HCN-mediated spontaneous activity of LHb projection neurons is responsible for the tonic inhibition of monoamine release.

Positive and negative situations induce major changes in the activity of LHb neurons, resulting in either increased or decreased inhibition of monoamine release (Matsumoto and Hikosaka, 2007; Ji and Shepard, 2007; Matsumoto and Hikosaka, 2009). To cause these effects, the reward-encoding information needs to reach the LHb and to finally modulate the activity of LHb projection neurons. The second part of this study demonstrates the existence of a strong glutamatergic projection from the lateral hypothalamic area (LHA) that directly targets VTA-projecting LHb neurons. Thus, the LHA is in a position to modulate the baseline activity of LHb projection neurons, thereby exerting an indirect effect on monoamine release.

4.1 Methodical considerations

The reliability of techniques is essential for valid analysis of any scientific subject and was therefore repeatedly controlled in this study. Thus, before proceeding to the actual results, the skills in and limitations of critical techniques are discussed. Thereby the reader is provided with the essential information to better evaluate the results presented in the following paragraphs.

Riboprobe and antibody specificity

The specificity of the antibodies used in this study was verified in addition to the characterization known from the producer. These tests included positive and negative controls

as well as the comparison with the antigen distribution described in the literature and with other antibodies targeting the same antigen.

The riboprobes were extensively tested (see paragraph 3.1.2). In summary, the riboprobes have cDNA sequences with minimized homologies to other cDNAs, do not unspecifically stain all cells, and show a labeling consistent with findings from previous studies. Sense and negative controls always remain negative. In addition, qPCR experiments are consistent with the signal intensity of *in situ* hybridization studies of the LHb.

Single and double tracing studies

Neuronal tracing is a well established technique to investigate neuronal connectivity. A problem that can never be completely excluded is an injury of passing fibers at the injection site. This could lead to a subsequent uptake of tracer into these fibers, resulting in some false-positive labeled neurons or terminals. Injury of passing fibers can be caused by high pressure during pressure application or by heating around the tip of the injection pipette during iontophoretic application.

In general, PhaL is a tracer without a "fibers of passage" problem. In contrast, the retrograde tracers WGA-Apo HRP gold and FG are known to be affected by this problem when inaccurately injected. Thus, to minimize the tissue damage at the injection site, pressure applicated tracers are slowly injected and iontophoretical injections are pulsed in a 7 sec on-off rhythm. Adjacent Cresyl-Violet stained sections never showed any tissue damage and the retrograde labeling is in general consistent with findings from the literature and earlier experiments in our lab. Thus, we are convinced that the "fibers of passage" problem is not relevant in our experiments.

Another problem is a spread of tracer outside the perimeter of the targeted nucleus. Therefore small tracer injections are aimed for selected nuclei and every injection site is evaluated to verify that the injection has no significant spread into adjacent areas (see paragraph 3.1.5.1 and 3.2.1.1). Only minimal spread of tracer into areas with well known projections is accepted, e.g. the IP which is known to exclusively project to the MHb (Herkenham and Nauta, 1979). To get a strong tracer transport, a period of four days for retrograde tracers and ten days for anterograde tracers is consistently maintained.

Combination of retrograde tracing and *in situ* hybridization

To analyze the expression of HCN mRNAs in LHb projecting neurons, a combination of non-isotopic *in situ* hybridization and retrograde tracing with WGA-Apo HRP gold is used.

Combination of these techniques was discussed recently (Jongen-Relo and Amaral, 2000) (Geisler and Zahm, 2006). Consistent with our observations, these investigators used silver intensification of the tracer prior to *in situ* hybridization and concluded that the inert deposited silver does not interfere with subsequent tissue processing. Using light microscopy, black silver particles are clearly distinguishable from the brown deposits of *in situ* hybridization. To avoid counting of small labeled dendrites, only structures containing at least five aggregated silver particles are counted as retrogradely labeled neurons.

4.2 HCN channels might be the molecular mechanism underlying lateral habenular baseline inhibition of monoamine release

HCN channels are known to generate pacemaker activity in neurons and heart cells. The genes encoding this family of four subunits have been cloned a decade ago (Ludwig et al., 1998; Santoro et al., 1998). Since then, several studies investigated the distribution of HCN mRNAs (Ludwig et al., 1998; Santoro et al., 1998; Moosmang et al., 2001) and proteins (Notomi and Shigemoto, 2004) throughout brains of rats and mice. However, none of them specifically focused on the habenular expression of HCN channels, explaining that available data present only one image or even just a table indicating the intensity of HCN immunoreactivity within LHb and MHb. The present work aimed to perform a set of experiments focusing on the detailed localization of HCN channels within the LHb.

4.2.1 All HCN subunits are expressed within the lateral habenula

Localization of HCN proteins within LHb neurons

HCN channels in neurons are mainly localized along the plasma membrane of dendrites, but are also expressed in myelinated and unmyelinated axons (Notomi and Shigemoto, 2004). The most impressive result when analyzing LHb sections is an intense HCN immunoreactivity (HCN-ir) of the neuropil. While LHb areas with a dense dendritic plexus (Geisler et al., 2003) are intensively stained, the major fiber tracts of the LHb, the stria medullaris and the fasciculus retroflexus, mostly remain free of HCN signal. This indicates that HCN channels in the LHb are predominantly expressed in dendrites. The only exception is HCN3, which is observed on fiber bundles ventrally in the LHb that represent axons joining the fasciculus retroflexus. Thus, HCN3 is the only subunit expressed in LHb axons, indicating a specific role of HCN3 in the modulation of axonal signal transmission. Furthermore, HCN channels seem to be localized in the perikarial plasma membrane of several types of LHb cells, as various differentially shaped cells display a ring of immunoreactivity surrounding them.

Perikarial HCN signal is mostly restricted to the membranes, whereas the cell interior largely remains unlabeled. This indicates that only minor amounts of protein are expressed or stored within the cells. In general, the number of cells containing HCN mRNAs is by far higher than the number of cells actually expressing the protein on their cell body, suggesting that in the majority of cells the protein is effectively transported towards the dendrites.

Comparison of HCN mRNA and protein distribution

The riboprobes and antibodies used in this study display a similar distribution pattern of HCN channels in the rat brain as observed in previous reports, accounting for their specificity and sensitivity (Ludwig et al., 1998; Santoro et al., 1998; Moosmang et al., 1999; Notomi and Shigemoto, 2004). The localization and intensity of HCN mRNA and protein (HCN-ir) expressions in the Hb are well correlated and supported by qPCR data, confirming differences in their expression levels.

Among the four subunits, HCN1 seems to play a unique role in the habenula as only weak HCN1-ir is located at some fibers in the border zone between MHb and LHb. This might represent dendritically transported protein, translated in the few HCN1 mRNA positive cells, which exist throughout the LHb. However, HCN1 seems not to be responsible for the generation of pacemaker activity in the majority of LHb cells, but instead fulfill other so far unknown functions in a subpopulation of LHb cells.

HCN2-ir is strong throughout the entire LHb and weak within the MHb. Beside the intense neuropil staining two types of cells are discriminable in the LHb. Some strongly labeled big cells in the dorsal LHb, including parts of the parvocellular and the magnocellular subnucleus and some weaker labeled small cells within all subnuclei. The big cells have labeled dendrites and are thereby presumably neurons. The majority of the small cells also seem to be neurons as they regularly contain silver particles in retrograde tracing experiments. However, at least some of the small cells might be oligodendrocytes, especially since HCN2 was found to be expressed on oligodendrocytes throughout the brain (Notomi and Shigemoto, 2004). This idea is supported by the fact that in some LHb subnuclei, up to 80% of all cells express HCN2 mRNAs, indicating that HCN2 is partly expressed in glia cells.

The distribution of HCN2 protein and HCN2 mRNA within the LHb reveals a great regional overlap. Interestingly, MHb cells strongly express HCN2 mRNA, whereas only little HCN2-ir is visible. This might be due to a transport of the translated protein towards the axons or even the terminals. Supporting this hypothesis, the expression of HCN2 is strong in the IP, the major projection area of the MHb (Herkenham and Nauta, 1979).

The distribution of HCN3 protein and HCN3 mRNA is similar to that of HCN2, however HCN3 protein expression is also strong in the MHb. HCN4 protein and HCN4 mRNA signals are more prominent in the MHb, but also present throughout the LHb with no subnuclear preference, but an impressive medio-lateral gradient. This gradient observed for all HCN subunits, but particularly for HCN4, was also described for many other neuronal markers (Geisler et al., 2003) and might thereby reflect a general concept of functional differences between the medial and the lateral divisions of the LHb.

Expression of HCN channels on LHb projection neurons

Experiments combining retrograde tracing and *in situ* hybridization demonstrate that HCN subunits are expressed in LHb projection neurons. Therein over 90% of the LHb neurons projecting to VTA, DR and MnR express HCN2, HCN3 and HCN4 mRNAs, whereas only a few express HCN1 mRNA. Thus, even without specific double- or triple- labeling it is numerically evident, that many of the projection neurons coexpress at least two or even three different HCN subunit mRNAs. More than one type of HCN mRNA in a single cell either indicates the simultaneous expression of several homomeric channels or the formation of heteromeric HCN channels. Heteromerization of HCN subunits is known from cell culture experiments. In HEK293 cells almost all dimeric combinations, except for HCN2/HCN3 dimers, have been observed (Much et al., 2003). However, so far only HCN1/HCN2 heteromers have been identified in vivo (Chen et al., 2001; Ulens and Tytgat, 2001). Hence, our data suggest that the LHb may also contain heteromeric HCN channels, including HCN2, HCN3 and HCN4 subunits. In this respect, the LHb may be regarded as a potentially useful object to study the presence and the properties of heteromeric HCN channels with novel subunit combinations in vivo.

Similar HCN expression patterns of LHb projection neurons throughout all subnuclei indicate that their basic function as pacemaker cells may be identical, in whatever subnuclei they are located. In summary, the majority of projection neurons in the LHb expresses up to three different HCN mRNAs in their cell body, indicating the potential formation of heteromeric HCN channels. As observed in immunocytochemical analyses, these channels are mostly transported towards the dendrites, while only few are actually expressed at the cell body.

4.2.2 HCN channels explain electrophysiological characteristics of lateral habenular neurons

Cells with three different types of resting activity have been described in the LHb. Type one cells spontaneously generate tonic firing in a frequency range of 1-20 Hz, whereas type two cells generate burst oscillations of action potentials (AP). The third type of cells is silent (Kim and Chang, 2005; Weiss and Veh, 2010). These three types of resting activities have recently been confirmed by in vivo experiments in the rat (Kowski et al., 2009). In vitro, type one cells still exhibit tonic trains of APs after blockade of all synaptic input, suggesting their ability to generate APs independently of synaptic activation (Kim and Chang, 2005). Furthermore, different responses to membrane hyperpolarization are observed in LHb cells. A subpopulation of cells from the first group alters the mode of spontaneous firing from tonic to burst oscillations in response to a brief hyperpolarization of the membrane potential. Cells from the first and the third group generate long-lasting intense discharges of APs triggered by membrane hyperpolarization (Kim and Chang, 2005).

The expression of HCN channels on a high percentage of LHb cells may be consistent with these electrophysiological findings. HCN channel activity would explain most of these phenomena. HCN subunits form ion channels, which conduct slow inward non-selective cation currents and are activated by the hyperpolarization following each AP, as well as by the accumulation of hyperpolarizing IPSPs (Ludwig et al., 1998; Santoro et al., 1998; Luthi and McCormick, 1998). These currents, called Ih currents, slowly depolarize the cell towards the action potential threshold.

Given their ability to generate intrinsic pacemaker activity, HCN channels are likely responsible for the tonic firing of the type one LHb cells, especially since this firing persisted in the absence of synaptic input, meaning that no other cells are involved. The burst oscillations of APs generated by the second group of LHb cells might reflect an activation of HCN channels in response to the accumulation of incoming IPSPs. The non-pacing cells from the third group might either represent the HCN-negative cells observed in our experiments, or carry HCN channels with other functions.

Potential roles of HCN channels on non-pacing cells include the resetting of voltage threshold if overwhelming inhibitory inputs would otherwise silence the neuron (Magee, 2000; Nolan et al., 2007). In the case of the LHb, an inhibitory input may come from forebrain regions such as the internal pallidum (entopeduncular nucleus in rats) (Herkenham and Nauta, 1977; Hikosaka et al., 2008). Reset would permit small excitatory inputs on LHb dendrites to generate an AP in these neurons. Such excitatory inputs partly come from the lateral

hypothalamus or other limbic input areas of the LHb and might transmit important reward-encoding information (Herkenham and Nauta, 1977) (unpublished observations from our lab).
Differential expression of HCN subunits may be responsible for the different responses of LHb cells to membrane-hyperpolarizing stimuli. HCN subunits are able to form homo- or hetero-tetrameric channels with different functional properties. While HCN1 tetramers show the fastest activation kinetics and the lowest sensitivity to cAMP (Santoro et al., 1998), HCN4 tetramers are slowly gating and highly sensitive to cAMP (Ishii et al., 1999). HCN2 and 3 have intermediate properties (Ludwig et al., 1998; Moosmang et al., 2001).
Given the differences in their cAMP sensitivity, the high percentage of HCN4-positive projection neurons in the LHb may reflect a strong influenceability of LHb pacemaker activity via synaptic transmission. As an important intracellular substrate in various receptor pathways elevated cAMP levels induce a faster membrane depolarization resulting in an increased firing rate. Since many neurotransmitters target G-Protein coupled receptors, this might be one mechanism of how pacemaker activity in LHb cells is regulated by synaptic transmission from other brain areas. To specify the effect of different HCN subunit patterns on LHb baseline activity, further experiments are necessary.

4.2.3 The lateral habenula is in a perfect position to control monoaminergic circuitry

The LHb is part of the dorsal diencephalic conduction system, which is composed of the stria medullaris, the LHb and the fasciculus retroflexus. This system provides an important route for information flow from forebrain regions to regulatory midbrain nuclei (Sutherland, 1982)
Projections from the LHb to VTA, DR and MnR are well known (Phillipson, 1979; Herkenham and Nauta, 1979; Oades and Halliday, 1987). In good agreement with these reports, we found the highest number of retrogradely labeled LHb neurons after injections to the MnR, followed by injections to the VTA and the DR. The distribution of retrogradely labeled neurons from the three injection areas visually reveals a great regional overlap, with localization of traced neurons in all LHb subnuclei with a preference to the medial division of the LHb.
Electrophysiological studies of the dorsal diencephalic conduction system reveal that LHb stimulation results in an almost complete inhibition of dopaminergic cells in the VTA (Christoph et al., 1986; Matsumoto, 2009; Hikosaka et al., 2008) and serotonergic cells in the DR (Wang and Aghajanian, 1977). Furthermore, other studies suggested a strong tonic inhibition of the LHb on dopamine release (Lisoprawski et al., 1980; Nishikawa et al., 1986;

Lecourtier et al., 2008). These data are based on lesion experiments of the LHb and the fasciculus retroflexus. Both interventions result in strongly increased dopamine release in forebrain regions, consistent with a disinhibition of the VTA. The tonic inhibition seems to be near-maximal as stimulation of the LHb produced only minimal further decreases of extracellular dopamine levels compared to the baseline situation (Lecourtier et al., 2008). The suggestion of a tonic inhibition on dopamine release is supported by recent electrophysiological experiments that found spontaneously active cells in the LHb (Kim and Chang, 2005; Matsumoto, 2009; Weiss and Veh, 2010).

Taken these findings, the expression of HCN channels observed in a majority of LHb projection neurons strongly supports the hypothesis that spontaneously active cells in the LHb are responsible for a tonic inhibition of monoamine release.

4.2.4 Lateral habenular projections to VTA, MnR and DR have a lot in common

The comparison of LHb neurons projecting to the VTA with those projecting to the DR and the MnR reveals many similarities. First, they are almost equally distributed within the LHb. Whether this is due to dual projections of single LHb neurons to VTA and raphe nuclei, or to the formation of functional groups within the LHb has still to be investigated.

Furthermore, all of these neurons express HCN channels and are known to inhibit their target areas via GABAergic interneurons. Thus, their basic function in the regulation of monoamine circuitry may be similar as well, especially since even the pattern of HCN subunit expression is identical. Whether and how input and regulation of these two systems are different needs further investigation.

4.2.5 Conclusions and future prospects

HCN channels are widely expressed throughout the entire LHb and their activity explains many of the observed electrophysiological phenomena. The expression of HCN channels in almost all LHb projection neurons primarily supports the hypothesis that their spontaneous activity is intrinsically and only regulated via synaptic input. The inhibition of the different monoaminergic systems may basically follow the same principles, as we found important similarities between those systems. To obtain actual evidence for HCN channels to be responsible for the baseline inhibition, *in vivo* experiments combining stereotactical application of HCN channel blockers like Cesium or ZD-7288 into the LHb and simultaneous electrophysiological measurement of dopaminergic cell activity in the VTA could be a promising approach.

However, the widespread distribution and intensity of HCN expression in those LHb neurons, which directly inhibit monoamine release, suggests an important role of HCN channels in the regulation of dopamine and serotonin levels in the brain. Disturbances in monoamine neurotransmission are found in drug addiction as well as in various psychiatric diseases, including major depression, bipolar disorder and schizophrenia, HCN channels may be involved in their pathophysiology. Further studies have to investigate whether and how the expression of HCN subunits in the LHb is altered in these diseases and whether HCN channels are a potential target for treatment.

4.3 The lateral hypothalamus seems to be an important source of modulatory input to lateral habenular projection neurons

4.3.1 A strong lateral hypothalamic projection preferentially innervates the medial division of the lateral habenula

In a first approach to analyze how reward-encoding information reaches the LHb and how it modulates the HCN-mediated tonic inhibition of monoamine release, we focused on the lateral hypothalamic area (LHA). This decision was mostly based on two arguments. The functional one was the outstanding role of the LHA as a sensor of multiple internal states and their potential changes in response to reward. The anatomical one was the extraordinarily strong projection from the LHA to the LHb (Swanson, 1976; Herkenham and Nauta, 1977; Berk and Finkelstein, 1982).

This projection and its subnuclear specificity have been excessively investigated by Kowski et al. in our lab (manuscript in preparation). In summary, they found that the projection from the LHA is partly related to individual LHb subnuclei. While the lateral zone of the LHA preferentially targets the *magnocellular (LMc)* and *basal (LB) subnucleus* of the lateral division of the LHb, the medial zone of the LHA, mainly projects to the *anterior (MA), marginal (MMg)* and *central (MC) subnucleus* of the medial division of the LHb. The anterodorsal cell group of the LHA is the only exception, as it exclusively targets the *oval subnucleus (LO)*. Neurotransmitters and cellular targets of this projection are currently completely unknown and the anatomical data do not highlight any region within the LHA to be specifically important for the LHb projection. Consequently, we initially focused on the projection in general and generated big injection sites to cover a large fraction of the LHA projection.

In good agreement with previous reports, our tracing experiments reveal that the LHA mainly projects to the medial division of the ipsilateral LHb, with only a few fibers in the

contralateral LHb and no labeling in the MHb (Swanson, 1976; Herkenham and Nauta, 1977; Berk and Finkelstein, 1982). Large injection sites covering the lateral and the medial zone, but omitting the anterodorsal cell group of the LHA, result in the expected labeling of all subnuclei within the LHb, except of the *oval subnucleus (LO)*. In some sections the untraced area around the *oval subnucleus (LO)* is bigger than expected. This might be due to variable dimensions of the immunocytochemically defined *LHbLO*, when looking at other functional aspects of this area. Also noticeable among the subnuclei is that an area consistent with the *parvocellular nucleus (MPc)* is repeatedly, but not always, free of traced terminals. The *parvocellular nucleus (MPc)* is predominantly targeted by the caudal LPOA (Kowski et. al manuscript in preparation). Thus, this phenomenon may be due to a spread of minor amounts of tracer into this adjacent area, resulting in an incomplete labeling of the *parvocellular nucleus (MPc)*. However, our tracing results are in good agreement with previous reports (Swanson, 1976; Herkenham and Nauta, 1977; Berk and Finkelstein, 1982), do not show any evidence for unspecific labeling and cover a major fraction of LHA fibers projecting to the LHb. Thus, they are well suited for further investigations.

4.3.2 Lateral hypothalamic terminals in the lateral habenula mainly use glutamate as neurotransmitter

To analyze the biological effects of the strong LHA projection to the LHb, the neurotransmitters used by its terminals were determined.

Glutamate

The three known “vesicular glutamate transporters” (vGluT1-3) are exclusively expressed in glutamatergic terminals. Hence, they are appropriate for the identification of glutamatergic terminals (Bellocchio et al., 2000). Due to the existence of vGluT1-3 mRNAs in the LHA (Geisler et al., 2007; Allen Brain Atlas) and vGluT1-3 proteins in the LHb (own observations), we initially focused on the expression of vGluT1-3 in traced terminals in the LHb. Compared to the other vGluTs, vGluT2 mRNA shows the strongest expression within the LHA by far (Allen Brain Atlas). Some authors even describe vGluT2 mRNA to be the only isoform expressed in the LHA (Geisler et al., 2007). The same applies for the proteins` expression in the LHb, as a vGluT2 expression in the LHb is extraordinarily strong. VGluT1, with only a very weak labeling, seems to play a minor role in the LHb. VGluT3 is not only expressed on axons and terminals, but also within the cell bodies of some LHb neurons. These neurons might be projection neurons, since Herzog et al. demonstrated an expression of vGluT3 in projection neurons in various brain regions (Herzog et al., 2004).

However, these data suggest that vGluT2 is the predominant glutamate transporter expressed within LHA terminals in the LHb.

This suggestion is confirmed by CLSM and EM analyses, evidencing vGluT2 to be the only isoform expressed by LHA terminals within the LHb. While the number of vGluT2-positive LHA terminals appears comparatively low at the CLSM level, EM analyses demonstrated an expression of vGluT2 in the majority of LHA terminals. This underestimation of vGluT2 expression at the CLSM might be due to difficulties in differentiating between small cross-cut axons and actual terminals and the high density of vGluT2 signal in the LHb. However, results from the EM are doubtlessly more representative, since they allow a clear identification of synaptic sites.

CLSM scans further revealed the existence of vGluT2-positive terminals that contact LHA axons from the side. These vGluT2-positive terminals are so broadly-based sitting directly on the axons that a synaptic contact seems likely. The terminals from unknown origin could exert modulatory effects on the LHA axon activity. However, vGluT2-positive terminals targeting LHA axons from the side have not yet been detected in the EM. Thus, the close relation of these terminals to LHA axons in the CLSM might also be by chance, as vGluT2 signals are extremely dense in the LHb.

GABA

GAD as the GABA-synthesizing enzyme is obligatorily expressed in GABA-ergic synapses. Although GAD mRNA is produced in cells of the LHA (Allen Brain Atlas) and GAD protein is widely expressed in LHb terminals, detailed CLSM analyses do not provide any evidence for an expression of GAD in traced terminals. This suggests that GABA is not used by the LHA projection. These findings may on the one hand be explained by the existence of Calbindin-positive neurons in the LHA (Kowski et al. manuscript in preparation), which are thought to be GABAergic interneurons and might thereby be identical with the GAD mRNA producing cells observed in the LHA of mice (Allen Brain Atlas). On the other hand GAD-positive terminals in the LHb may derive from various other areas. These areas include the Globus pallidus internus (entopeduncular nucleus in rats), which is thought to send GABAergic projections to the LHb (Lecourtier and Kelly, 2007).

Orexin and Galanin

The LHA is an area that produces various neuropeptides and strongly projects to the LHb (Swanson, 1976; Berk and Finkelstein, 1982; Melander et al., 1986; Miller et al., 1993; Nambu et al., 1999). The LHb however, contains many neuropeptidergic axons. Consequently, we hypothesized that at least some of these axons may derive from the LHA.

Neurons producing the two exemplarily analyzed neuropeptides Galanin and Orexin are located in areas of the LHA that are covered by our injection sites. Thus, the tracer should theoretically be taken up by the neuropeptidergic cells in the LHA and be anterogradely transported to the LHb, where it should be detectable in their peptidergic axons. Since neuropeptides usually exert their effects via volume transmission, they are not restricted to specific terminals, but are located in the axon itself, particularly in some swellings along the axon.

Such peptidergic axons are clearly detectable in light- and fluorescence- labeled LHb sections and display the expected shape with a thin axon interrupted by strongly labeled swellings. However, CLSM analyses reveal that these peptidergic axons never contain tracer, indicating that they do not derive from the LHA. Another explanation for the absence of tracer in these axons could be a specific problem with the tracer uptake or transport in peptidergic LHA cells. So far such problems have not been described in the literature and we also do not have any evidence for an adverse effect of the tracer on these cells.

Thus, a different origin of peptidergic axons in the LHb seems more likely. This hypothesis is supported by the complete absence of dense-core vesicles in traced LHA terminals, as evidenced by EM analyses.

In contrast to orexin, galanin-positive axons run directly beside LHA axons and even seem to contact them. Thus, they might have a modulatory effect on them, although the three known Galanin receptors have not yet been described to be expressed on axons.

Further experiments analyzing the expression of other neuropeptides are still in progress. However, their expression in LHA axons in the LHb is unlikely. On the one hand, they are also stored in dense-core vesicles and, on the other hand, their distribution patterns within the LHb do not resemble the pattern of LHA axons within this area.

Taken together, some neuropeptides, especially Galanin, may be involved in the modulation of LHA input to the LHb. Such peptidergic axons do not originate in the LHA. Thus, neuropeptides in the LHb seem to derive from other input areas than the LHA.

4.3.3 VTA-projecting lateral habenular neurons are directly targeted by the lateral hypothalamic projection

Single tracings reveal a widely overlapping distribution of LHA terminals and VTA-projecting neurons in the LHb, indicating a potential relationship between the two systems. Although these experiments are not a sufficient proof for the actual existence of synaptic contacts, they increase the pre-test probability for them to exist. However, to analyze the exact

anatomical relation between LHA terminals and VTA-projecting neurons in the LHb and to prove our hypothesis of direct synaptic contacts between them, double-tracing studies were performed.

The injection sites of the two tracers are correctly located and both tracers are effectively transported to the LHb, where they show the distribution pattern, already known from our single tracing studies and other previous reports (see paragraphs 3.1.5.2 and 3.2.1.2). Double-labeling of both tracers in the LHb does not show any evidence for adverse effects between the two tracers. The retrograde tracer FG, which is usually analyzed three to four days after tracing, is still strongly detectable in LHb neurons. Thus, the double-tracings do correctly reflect both projections and are qualified for the analyses of potential synaptic contacts.

CLSM analyses of fluorescence double-labeled LHb sections reveal the existence of multiple synaptic contacts of LHA terminals on VTA-projecting neurons. These contacts are preferentially found within the medial division of the LHb, which might simply be due to the dense plexus of LHA terminals and VTA-projecting neurons within this area. Furthermore, contacts are also observed in almost all other areas, where traced terminals and neurons are co-located, suggesting that the connectivity between the two systems is not restricted to specific subnuclei.

High magnification scans of potential contact sites demonstrate that LHb projection neurons are targeted by LHA terminals in three different fashions. The first type of projection neurons only achieves contacts on their dendrites. The second type is sporadically contacted at the cell body, while the third type of projection neurons is densely targeted so that their cell bodies are actually embedded between LHA terminals. However, these findings are in good agreement with the targeting pattern of vGluT2-positive terminals observed in semithin sections. Therein vGluT2-positive synapses target large dendrites, as well as individual cell bodies. The morphological differences between the contact sites might be due to differential intensities of LHA influence on individual VTA-projecting neurons. Another explanation could be an incomplete labeling of LHA axons leaving some of the terminals targeting an individual VTA-projecting neuron unlabeled.

However, all three types of contacts are formed by enlargements, potentially terminal- or in passing buttons, of labeled LHA axons sitting directly and broadly-based on VTA-projecting neurons. By their shape, these contacts are clearly discriminable from small axons just passing a projection neuron, which are generally round and not as closely attached to the cell. Thus, the existence of synapses at the contact sites seems likely, however not fully evidenced.

Finally, the combination of tracer double-labeling with the detection of synaptophysin confirmed the existence of synapses at the contact sites described. Synaptophysin is a widely used, highly specific marker for the detection and counting of synapses. The fluorescence of synaptophysin is exactly localized within the LHA terminals that directly contact the VTA-projecting cells, evidencing the existence of synaptic contacts.

In summary, the high number and intensity of contacts and the widespread distribution throughout the entire LHb, suggest an outstanding role of the LHA in the regulation of the tonic activity of VTA-projecting LHb neurons.

4.3.4 The lateral hypothalamus might be a major provider of reward-encoding information

Homeostasis describes the ability of a system to regulate its internal states and to maintain stable conditions. Like in any regulatory circuit, this requires a permanent measurement of various actual parameters, a comparison with target parameters and the initiation of appropriate reactions. In the body of mammals, the superior regulator of this system is the hypothalamus. It collects information from pivotal systems, including body temperature, blood pressure, blood glucose concentration, and many others, either via direct measurement or via neuronal inputs. After comparison with target parameters it induces an appropriate reaction to readjust the divergent parameter. These reactions might either be internal adjustments or changes in the behavior of an individual.

Most of the hypothalamic mechanisms that cause internal reactions are located within the medial hypothalamic area (MHA), including the production of releasing- or inhibiting-hormones and the activation of the vegetative nervous system. These mechanisms are comparatively well understood. Much less is known about the effects of the hypothalamus on behavior. For this regulation the LHA seems to be more relevant, as it is strongly linked to areas of the limbic system, including the LHb (Swanson, 1976; Berk and Finkelstein, 1982; Kowski et al., 2008). The present study indicates that the LHA is able to directly influence the baseline activity of LHb neurons projecting to the VTA. Thus, via increasing or decreasing the dopamine levels in the brain, information from the LHA might be able to regulate the motivation of an individual to perform behaviors necessary for homeostasis. These abilities would allow the LHA to promote or reward certain behaviors that are currently necessary to keep the body homeostatically balanced. A simplified example of how this system might work should be exemplarily explained on the basis of thirst. The increased osmolarity of the blood is measured in the hypothalamus. The hypothalamus, as the regulator of the osmolarity,

now induces reactions to readjust the parameter to the normal level. On the one hand, these reactions are internal, including the secretion of anti diuretic hormone (ADH) from the MHA via the neurohypophysis. On the other hand, drinking needs to be induced. According to our example this behavioral reaction could be induced via the LHA projection. As this projection is mainly glutamatergic it could increase the LHb baseline inhibition on the VTA, resulting in decreased dopamine levels and a removal of reward. This would force the individual to drink, in order to regain the detracted reward. While the individual is drinking, the osmolarity is coming back to normal. The LHA would be able to measure this process and to stop the activation of LHb projection neurons. Although this model is highly simplified and neglects cortical aspects of reward, it might be sufficient to understand the importance of the LHA and its projection to the LHb in the maintenance of constant internal conditions.

4.3.5 Conclusions and future prospects

A glutamatergic projection from the LHA directly targets VTA-projecting neurons throughout the LHb. The distinct connectivity indicates an important influence of the LHA on the LHb-mediated tonic inhibition of monoamine release and suggests the LHA to be a major source of reward-encoding information to the LHb.

Our data indicate a direct influence of the LHA on the LHb and on dopamine release. To support this suggestion, electrophysiological studies could in a first step investigate the actual effects of LHA stimulation on LHb- and VTA cell activity. Further experiments could analyze whether and which rewards actually have an effect on LHA activity, and whether these effects explain the changes of LHb activity.

Taken the extraordinary strength of the LHA projection to the LHb, it appears obvious that many other LHb neurons, beside those projecting to the VTA, are targeted. These could include unlabeled distal dendrites of VTA-projecting neurons, as well as LHb neurons projecting to other monoaminergic areas. The hypothesis that other projection neurons might also be targeted is supported by findings from the first part of this study. These experiments found many similarities between the different populations of projection neurons, including similar distribution, HCN expression and mechanism of inhibition on monoamine release. Thus, the idea of similar input and regulation becomes attractive. According to it, the LHA would modulate the baseline activity of LHb neurons projecting to all monoaminergic systems. To prove this hypothesis, similar double-tracing experiments, but with an injection of FG into the DR, MnR or other monoaminergic areas would be necessary.

5. Summary

Homeostasis describes the fundamental biological ability of individuals to maintain stable internal conditions in a changing environment. The homeostatic system is pivotal for the survival of individuals but also for the survival of entire species. It requires complex regulatory mechanisms to appropriately react to internal and external changes. These reactions include internal adjustments as well as behavioral responses. In vertebrates, the coordination of these mechanisms is primarily managed by phylogenetically old structures in the diencephalon and the brainstem. These structures include the hypothalamus, the habenula as a part of the epithalamus, and several brainstem nuclei.

While the hypothalamus is responsible for the measurement of homeostatic parameters and induces appropriate internal responses, the monoaminergic brainstem nuclei, as the origin of the reward system, seem to be involved in the regulation of behavior. The precise relation between the homeostatic system and the reward system remains mostly unknown at present. Recently, the lateral habenular complex (LHb) has come into focus, as it provides an important anatomical link between homeostatic areas and the reward processing monoaminergic brainstem nuclei.

Major projections of the LHb target the dopaminergic ventral tegmental area (VTA) and the serotonergic dorsal (DR) and median raphe nuclei (MnR). Both monoaminergic neurotransmitter systems play a central role in reward processing and reward-related decision-making. Glutamatergic LHb efferents terminate on inhibitory GABAergic neurons in the VTA, and the raphe nuclei, thereby suppressing monoamine release when required by the present behavioral context. Recent studies suggest that the LHb exerts a strong tonic inhibition on monoamine release, when no reward is to be obtained. It is yet unknown whether this inhibition is the result of a continuous external activation by other brain areas, or if it is intrinsically generated within the LHb projection neurons.

Hypothesizing that the tonic inhibition is intrinsically generated by an HCN channel - mediated pacemaker activity of LHb projection neurons, retrograde tracing in rats was combined with *in situ* hybridization of HCN1 to HCN4 mRNAs. In fact, nearly all LHb neurons targeting VTA or raphe nuclei are equipped with HCN subunit mRNAs. While HCN1 mRNA is scarce, most neurons display strong expression of HCN2 to HCN4 mRNAs. These results are supported by quantitative PCR and immunocytochemical analyses. Thus, our data suggest that the tonic inhibition of monoamine release is intrinsically generated in LHb projection neurons and that their activity may only be modulated by synaptic inputs.

In the second part of the study, the regulation of LHb activity was analyzed. A major input to the LHb comes from the lateral hypothalamus (LHA), the superior regulator of the homeostatic system. This projection is thought to transmit homeostatic information to the habenula, thereby inducing changes in the activity of the reward system. These changes could finally force the individual to perform or desist from certain behaviors currently necessary to keep the body homeostatically balanced. However, less is known about the effects of the intense hypothalamic projection on the activity of lateral habenular neurons.

Consequently, we analyzed the neurotransmitters and the cellular targets of the hypothalamic projection within the LHb. Therefore, anterograde tracing into the LHA was combined with subsequent double-labeling of neurotransmitters and tracer in LHA terminals with the confocal laser scanning- and electron microscope. These analyses revealed that the hypothalamic projection to the LHb is mainly glutamatergic, using vGluT2 to fill its synaptic vesicles. Other neurotransmitters, including GABA and various neuropeptides, are not involved. Thus, the projection exerts an excitatory effect on the targeted cells.

These cellular targets were analyzed in a second step. Hypothesizing a direct contact of hypothalamic terminals on LHb neurons projecting to the VTA, we combined anterograde tracing from the LHA with retrograde tracing from the VTA. After visualization of both tracers, LHb sections were scanned for these potential contacts with the confocal laser scanning microscope. In fact, many LHb neurons projecting to the VTA are densely targeted by the LHA projection. The existence of synaptic contacts is evidenced by covisualization of synaptophysin at these contact sites.

In summary, the first part of this study demonstrates a strong expression of HCN channels on LHb projection neurons. Thus, an intrinsically generated pacemaker activity of LHb neurons that is only modulated by synaptic input seems to be responsible for the tonic inhibition of monoamine release. In the second part of this study, the existence of a strong glutamatergic projection from the LHA that directly targets LHb neurons projecting to the reward system is demonstrated. This is the first description of a synaptic mechanism for the modulation of the tonic LHb inhibition of monoamine release. As the hypothalamus is the homeostatic center of the brain, this study also emphasizes the role of the LHb as a major link between the homeostatic system and the reward system.

6. Zusammenfassung

Der Begriff „Homöostase“ beschreibt die grundlegende biologische Fähigkeit von Lebewesen stabile innere Bedingungen in einer sich ständig verändernden Umwelt aufrecht zu erhalten. Das homöostatische System ist unabdingbar für das Überleben einzelner Lebewesen, genauso wie für das Bestehen der gesamten Spezies. Es erfordert komplexe regulatorische Mechanismen, um adäquat auf innere und äußere Veränderungen zu reagieren. Diese Mechanismen umfassen sowohl interne Anpassungen, als auch Änderungen des Verhaltens. In Wirbeltieren werden diese Mechanismen durch phylogenetisch alte Strukturen im Zwischenhirn und Hirnstamm koordiniert. Beteiligte Strukturen sind der Hypothalamus, die Habenula als Teil des Epithalamus, sowie verschiedene Hirnstammkerne.

Während der Hypothalamus für die Messung homöostatischer Parameter und die Auslösung innerer Anpassungen verantwortlich ist, scheinen die monoaminergen Hirnstammkerne, als Ursprung des Rewardsystems, Änderungen im Verhalten zu bewirken. Über das genaue Zusammenspiel zwischen homöostatischem System und Rewardsystem ist momentan wenig bekannt. In letzter Zeit ist die laterale Habenula (LHb) vermehrt in den Fokus gerückt, da sie eine wichtige anatomische Verbindungsstelle zwischen den homöostatischen Arealen und den Reward verarbeitenden Hirnstammkernen darstellt.

Die Hauptprojektionen der LHb erreichen die dopaminerge ventral tegmental area (VTA) und die serotonerge dorsale- (DR) und mediane Raphe (MnR). Beide monoaminergen Neurotransmittersysteme spielen eine zentrale Rolle in der Verarbeitung von Reward sowie der Reward-basierten Entscheidungsfindung. Glutamaterge Projektionen der LHb enden dabei auf inhibitorischen GABAergen Neuronen in der VTA und den Raphe Kernen, wodurch eine Unterdrückung der Monoamin-Freisetzung in entsprechenden Situationen möglich ist. Aktuelle Studien zeigen, dass die LHb auch dann eine starke kontinuierliche Hemmung der Monoamine-Freisetzung vermittelt, wenn gerade kein Reward zu verarbeiten ist. Es ist momentan nicht bekannt, ob diese kontinuierliche Hemmung das Resultat einer andauernden externen Aktivierung der LHb durch andere Hirnregionen ist, oder ob sie intrinsisch in den Projektionsneuronen der LHb selbst erzeugt wird.

In der vorliegenden Arbeit wurde die Hypothese aufgestellt, dass die kontinuierliche Hemmung intrinsisch, durch eine HCN-Kanal vermittelte Spontanaktivität der LHb Projektionsneurone, generiert wird. Zur Überprüfung dieser Hypothese wurde die Technik des retrograden Tracing in Ratten mit *In Situ* Hybridisierungen von HCN1 bis HCN4 mRNAs kombiniert. Tatsächlich exprimieren beinahe alle Projektionsneurone der LHb, die zur VTA oder den Raphe Kernen projizieren HCN mRNAs. Während HCN1 mRNA nur in wenigen

Zellen nachweisbar ist, zeigen die meisten Neurone eine starke HCN2-, HCN3- und HCN4-Expression. Diese Ergebnisse werden durch quantitative PCR und immunzytochemische Analysen bestätigt. Insgesamt sprechen unsere Daten dafür, dass die kontinuierliche Hemmung der Monoamin-Freisetzung intrinsisch in LHb Projektionsneuronen generiert wird und dass ihre Aktivität lediglich durch synaptische Eingänge moduliert wird.

Im zweiten Teil der Studie wurde die Regulation der LHb Aktivität untersucht. Eine Hauptafferenz der LHb kommt aus dem lateralen Hypothalamus (LHA), dem obersten Steuerungszentrum des homöostatischen Systems. Es wird angenommen, dass diese Projektion homöostatische Informationen zur Habenula übermittelt, wodurch Veränderungen in der Aktivität des Rewardsystems ausgelöst werden. Diese Veränderungen könnten das Lebewesen letztendlich zu Verhaltensweisen veranlassen, die momentan zur Aufrechterhaltung des homöostatischen Gleichgewichts nötig sind. Allerdings ist wenig über die genauen Effekte der hypothalamischen Projektion auf die Aktivität der Neurone in der LHb bekannt.

Um diese Effekte zu charakterisieren, untersuchten wir die Neurotransmitter und die Zielzellen der hypothalamischen Projektion in der LHb. Dazu wurde anterogrades Tracing aus dem lateralen Hypothalamus mit anschließendem Doppelnachweis von Tracer und Neurotransmittern in hypothalamischen Terminalen in der LHb, mittels Konfokalem Laser Scanning- und Elektronen Mikroskop, kombiniert. Diese Analysen zeigten, dass die hypothalamische Projektion zur LHb hauptsächlich Glutamat als Neurotransmitter verwendet. Andere Neurotransmitter, wie GABA oder Neuropeptide scheinen keine Rolle zu spielen. Aus diesen Ergebnissen ergibt sich, dass die hypothalamische Projektion einen exzitatorischen Effekt auf ihre Zielzellen vermittelt.

Diese Zielzellen wurden in einem nächsten Schritt untersucht. Wir stellten dazu die Hypothese auf, dass es direkte Kontakte der hypothalamischen Terminalen zu LHb Neuronen mit Projektion zur VTA gibt. Um dies zu belegen wurde anterogrades Tracing aus dem LHA und retrogrades Tracing aus der VTA kombiniert. Nach Visualisierung beider Tracer wurden Schnitte der LHb im Konfokalen Laser Scanning Mikroskop auf mögliche Kontaktstellen hin untersucht. In der Tat werden zahlreiche LHb Neurone mit Projektion zur VTA dicht von hypothalamischen Terminalen innerviert. Die Existenz von Synapsen wurde durch den Nachweis von Synaptophysin an den Kontaktstellen bewiesen.

Zusammengefasst zeigt der erste Teil der Arbeit die starke Expression von HCN Kanälen in der Mehrzahl der LHb Neurone mit Projektionen zur VTA und den Raphe Kernen. Daher erscheint eine intrinsisch generierte Spontanaktivität dieser Neurone für die kontinuierliche Hemmung der Monoamin-Freisetzung verantwortlich zu sein. Im zweiten Teil der Untersuchung wird die Existenz einer starken glutamatergen Projektion vom Hypothalamus mit direkten Kontakten zu LHb Projektionsneuronen gezeigt. Dies ist die erste Beschreibung eines synaptischen Mechanismus für die Modulation der kontinuierlichen, LHb-vermittelten Hemmung der Monoamine-Freisetzung. Mit dem Hypothalamus als homöostatischem Zentrum des Gehirns, hebt die vorliegende Arbeit die Bedeutung der Habenula als entscheidende Verbindungsstelle zwischen homöostatischen Arealen und dem Rewardsystem hervor.

7. Abbreviations

3V	third ventricle
Acc	accumbens nucleus
ADH	anti diuretic hormone
ADHD	attention deficit hyperactive disorder
AP	action potential
AVP	arginin-vasopressin
BST	bed nucleus of the stria terminalis
CLi	central linear nucleus of the raphe
CLSM	confocal laser scanning microscope
CNG	cyclic nucleotide gated channel
cp	cerebellar peduncle
DMH	dorsomedial hypothalamus
DR	dorsal raphe nucleus
EM	electron microscope
EPN	entopeduncular nucleus
f	fornix
FG	fluoro gold
fr	fasciculus retroflexus
GAD	glutamate decarboxylase
Hb	Habenula
HCN	hyperpolarization-activated cyclic nucleotide gated cation channel
HDB	nucleus of the horizontal limb of the diagonal band of broca
ic	internal capsula
Ih	hyperpolarization-activated current
IP	interpeduncular nucleus
ir	immunoreactivity
Kv	voltage-gated potassium channel
LDTg	laterodorsal tegmentum
LHA	lateral hypothalamic area
LHb	lateral habenula
LHbL	lateral habenula, lateral division
LHbLB	basal subnucleus of the lateral division of the LHb
LHbLMc	magnocellular subnucleus of the lateral division of the LHb

LHbLMg	marginal subnucleus of the lateral division of the LHb
LHbLO	oval subnucleus of the lateral division of the LHb
LHbLPc	parvocellular subnucleus of the lateral division of the LHb
LHbM	lateral habenula, medial division
LHbMC	central subnucleus of the medial division of the LHb
LHbMMg	marginal subnucleus of the lateral division of the LHb
LHbMPc	parvocellular subnucleus of the medial division of the LHb
LHbMS	superior subnucleus of the medial division of the LHb
LPOA	lateral preoptic area
LV	left ventricle
MCH	melanocyte-stimulating hormone
mfb	medial forebrain bundle
MG	methyl green
MHA	medial hypothalamic area
MHb	medial habenula
ml	medial lemniscus
mlf	medial longitudinal fasciculus
MnR	median raphe nucleus
mPFC	medial prefrontal cortex
NPY	neuropeptide Y
opt	optic tract
PBP	parabrachial pigmented area of the VTA
PFR	parafasciculus retroflexus area of the VTA
Pha-L	phaseolus-leucoagglutinin
PMnR	paramedian raphe nucleus
PN	paranigral nucleus of the VTA
RMTg	rostromedial tegmental nucleus
RN	red nucleus
RV	right ventricle
sm	stria medullaris
SN	substantia nigra
SNc	substantia nigra, pars compacta
Th	thalamus
VMH	ventromedial hypothalamus

Vpa	ventral pallidum
VTA	ventral tegmental area
VTT	ventral tegmental tail
xscp	decussation of the superior cerebellar peduncle

8. References

Aghajanian, G. K. and Wang, R. Y., 1977. Habenular and other midbrain raphe afferents demonstrated by a modified retrograde tracing technique. Brain Res. 122, 229-242.

Andres, K. H., von During, M. and Veh, R. W., 1999. Subnuclear organization of the rat habenular complexes. J Comp Neurol. 407, 130-150.

Bal, T. and McCormick, D. A., 1997. Synchronized oscillations in the inferior olive are controlled by the hyperpolarization-activated cation current I(h). J Neurophysiol. 77, 3145-3156.

Beaumont, V. and Zucker, R. S., 2000. Enhancement of synaptic transmission by cyclic AMP modulation of presynaptic Ih channels. Nat Neurosci. 3, 133-141.

Behzadi, G., Kalen, P., Parvopassu, F. and Wiklund, L., 1990. Afferents to the median raphe nucleus of the rat: retrograde cholera toxin and wheat germ conjugated horseradish peroxidase tracing, and selective D-[3H]aspartate labeling of possible excitatory amino acid inputs. Neuroscience. 37, 77-100.

Bellocchio, E. E., Reimer, R. J., Fremeau, R. T., Jr. and Edwards, R. H., 2000. Uptake of glutamate into synaptic vesicles by an inorganic phosphate transporter. Science. 289, 957-960.

Berk, M. L. and Finkelstein, J. A., 1982. Efferent connections of the lateral hypothalamic area of the rat: an autoradiographic investigation. Brain Res Bull. 8, 511-526.

Biel, M. and Michalakis, S., 2009. Cyclic nucleotide-gated channels. Handb Exp Pharmacol, 111-136.

Biel, M., Schneider, A. and Wahl, C., 2002. Cardiac HCN channels: structure, function, and modulation. Trends Cardiovasc Med. 12, 206-212.

Blander, A. and Wise, R. A., 1989. Anatomical mapping of brain stimulation reward sites in the anterior hypothalamic area: special attention to the stria medullaris. Brain Res. 483, 12-16.

Brinschwitz, K., Dittgen, A., Madai, V. I., Lommel, R., Geisler, S. and Veh, R. W., 2010. Glutamatergic axons from the lateral habenula mainly terminate on GABAergic neurons of the ventral midbrain. Neuroscience.

Bromberg-Martin, E. S., Hikosaka, O. and Nakamura, K., 2010. Coding of task reward value in the dorsal raphe nucleus. J Neurosci. 30, 6262-6272.

Carboni, L., Carletti, R., Tacconi, S., Corti, C. and Ferraguti, F., 1998. Differential expression of SAPK isoforms in the rat brain. An in situ hybridisation study in the adult rat brain and during post-natal development. Brain Res Mol Brain Res. 60, 57-68.

Chen, J., Mitcheson, J. S., Tristani-Firouzi, M., Lin, M. and Sanguinetti, M. C., 2001. The S4-S5 linker couples voltage sensing and activation of pacemaker channels. Proc Natl Acad Sci U S A. 98, 11277-11282.

Christoph, G. R., Leonzio, R. J. and Wilcox, K. S., 1986. Stimulation of the lateral habenula inhibits dopamine-containing neurons in the substantia nigra and ventral tegmental area of the rat. J Neurosci. 6, 613-619.

Concha, M. L. and Wilson, S. W., 2001. Asymmetry in the epithalamus of vertebrates. J Anat. 199, 63-84.

Conrad, L. C. and Pfaff, D. W., 1976. Efferents from medial basal forebrain and hypothalamus in the rat. II. An autoradiographic study of the anterior hypothalamus. J Comp Neurol. 169, 221-261.

Craven, K. B. and Zagotta, W. N., 2006. CNG and HCN channels: two peas, one pod. Annu Rev Physiol. 68, 375-401.

Curran, C., Byrappa, N. and McBride, A., 2004. Stimulant psychosis: systematic review. Br J Psychiatry. 185, 196-204.

Curzon, G., 1990. Serotonin and appetite. Ann N Y Acad Sci. 600, 521-530; discussion 530-521.

DiFrancesco, D., 1993. Pacemaker mechanisms in cardiac tissue. Annu Rev Physiol. 55, 455-472.

Dugovic, C., 2001. Role of serotonin in sleep mechanisms. Rev Neurol (Paris). 157, S16-19.

Ellison, G., 1994. Stimulant-induced psychosis, the dopamine theory of schizophrenia, and the habenula. Brain Res Brain Res Rev. 19, 223-239.

Elmquist, J. K., 2001. Hypothalamic pathways underlying the endocrine, autonomic, and behavioral effects of leptin. Int J Obes Relat Metab Disord. 25 Suppl 5, S78-82.

Ferraro, G., Montalbano, M. E., Sardo, P. and La Grutta, V., 1996. Lateral habenular influence on dorsal raphe neurons. Brain Res Bull. 41, 47-52.

Gallistel, C. R., Gomita, Y., Yadin, E. and Campbell, K. A., 1985. Forebrain origins and terminations of the medial forebrain bundle metabolically activated by rewarding stimulation or by reward-blocking doses of pimozide. J Neurosci. 5, 1246-1261.

Gauss, R., Seifert, R. and Kaupp, U. B., 1998. Molecular identification of a hyperpolarization-activated channel in sea urchin sperm. Nature. 393, 583-587.

Geeraedts, L. M., Nieuwenhuys, R. and Veening, J. G., 1990. Medial forebrain bundle of the rat: IV. Cytoarchitecture of the caudal (lateral hypothalamic) part of the medial forebrain bundle bed nucleus. J Comp Neurol. 294, 537-568.

Geisler, S., Derst, C., Veh, R. W. and Zahm, D. S., 2007. Glutamatergic afferents of the ventral tegmental area in the rat. J Neurosci. 27, 5730-5743.

Grace, A. A. and Bunney, B. S., 1984. The control of firing pattern in nigral dopamine neurons: burst firing. J Neurosci. 4, 2877-2890.

Graeff, F. G., 2004. Serotonin, the periaqueductal gray and panic. Neurosci Biobehav Rev. 28, 239-259.

Graeff, F. G., Guimaraes, F. S., De Andrade, T. G. and Deakin, J. F., 1996. Role of 5-HT in stress, anxiety, and depression. Pharmacol Biochem Behav. 54, 129-141.

Gruber, C., Kahl, A., Lebenheim, L., Kowski, A., Dittgen, A. and Veh, R. W., 2007. Dopaminergic projections from the VTA substantially contribute to the mesohabenular pathway in the rat. Neurosci Lett. 427, 165-170.

Herkenham, M. and Nauta, W. J., 1977. Afferent connections of the habenular nuclei in the rat. A horseradish peroxidase study, with a note on the fiber-of-passage problem. J Comp Neurol. 173, 123-146.

Herkenham, M. and Nauta, W. J., 1979. Efferent connections of the habenular nuclei in the rat. J Comp Neurol. 187, 19-47.

Herzog, E., Gilchrist, J., Gras, C., Muzerelle, A., Ravassard, P., Giros, B., Gaspar, P. and El Mestikawy, S., 2004. Localization of VGLUT3, the vesicular glutamate transporter type 3, in the rat brain. Neuroscience. 123, 983-1002.

Hikosaka, O., Sesack, S. R., Lecourtier, L. and Shepard, P. D., 2008. Habenula: crossroad between the basal ganglia and the limbic system. J Neurosci. 28, 11825-11829.

Hong, S. and Hikosaka, O., 2008. The globus pallidus sends reward-related signals to the lateral habenula. Neuron. 60, 720-729.

Howes, O. D., Montgomery, A. J., Asselin, M. C., Murray, R. M., Valli, I., Tabraham, P., Bramon-Bosch, E., Valmaggia, L., Johns, L., Broome, M., McGuire, P. K. and Grasby, P. M., 2009. Elevated striatal dopamine function linked to prodromal signs of schizophrenia. Arch Gen Psychiatry. 66, 13-20.

Ikemoto, S. and Panksepp, J., 1999. The role of nucleus accumbens dopamine in motivated behavior: a unifying interpretation with special reference to reward-seeking. Brain Res Brain Res Rev. 31, 6-41.

Ikemoto, S., Witkin, B. M. and Morales, M., 2003. Rewarding injections of the cholinergic agonist carbachol into the ventral tegmental area induce locomotion and c-Fos expression in the retrosplenial area and supramammillary nucleus. Brain Res. 969, 78-87.

Ishii, T. M., Takano, M., Xie, L. H., Noma, A. and Ohmori, H., 1999. Molecular characterization of the hyperpolarization-activated cation channel in rabbit heart sinoatrial node. J Biol Chem. 274, 12835-12839.

Jacobs, B. L. and Fornal, C. A., 1993. 5-HT and motor control: a hypothesis. Trends Neurosci. 16, 346-352.

Ji, H. and Shepard, P. D., 2007. Lateral habenula stimulation inhibits rat midbrain dopamine neurons through a GABA(A) receptor-mediated mechanism. J Neurosci. 27, 6923-6930.

Jongen-Relo, A. L. and Amaral, D. G., 2000. A labeling technique using WGA-apoHRP-gold as a retrograde tracer and non-isotopic in situ hybridization histochemistry for the detection of mRNA. J Neurosci Methods. 101, 9-17.

Kaufling, J., Veinante, P., Pawlowski, S. A., Freund-Mercier, M. J. and Barrot, M., 2009. Afferents to the GABAergic tail of the ventral tegmental area in the rat. J Comp Neurol. 513, 597-621.

Kim, U. and Chang, S. Y., 2005. Dendritic morphology, local circuitry, and intrinsic electrophysiology of neurons in the rat medial and lateral habenular nuclei of the epithalamus. J Comp Neurol. 483, 236-250.

Kowski, A. B., Geisler, S., Krauss, M. and Veh, R. W., 2008. Differential projections from subfields in the lateral preoptic area to the lateral habenular complex of the rat. J Comp Neurol. 507, 1465-1478.

Lecourtier, L., Defrancesco, A. and Moghaddam, B., 2008. Differential tonic influence of lateral habenula on prefrontal cortex and nucleus accumbens dopamine release. Eur J Neurosci. 27, 1755-1762.

Lecourtier, L., Deschaux, O., Arnaud, C., Chessel, A., Kelly, P. H. and Garcia, R., 2006. Habenula lesions alter synaptic plasticity within the fimbria-accumbens pathway in the rat. Neuroscience. 141, 1025-1032.

Lecourtier, L., Neijt, H. C. and Kelly, P. H., 2004. Habenula lesions cause impaired cognitive performance in rats: implications for schizophrenia. Eur J Neurosci. 19, 2551-2560.

Lisoprawski, A., Herve, D., Blanc, G., Glowinski, J. and Tassin, J. P., 1980. Selective activation of the mesocortico-frontal dopaminergic neurons induced by lesion of the habenula in the rat. Brain Res. 183, 229-234.

Ludwig, A., Zong, X., Jeglitsch, M., Hofmann, F. and Biel, M., 1998. A family of hyperpolarization-activated mammalian cation channels. Nature. 393, 587-591.

Ludwig, A., Zong, X., Stieber, J., Hullin, R., Hofmann, F. and Biel, M., 1999. Two pacemaker channels from human heart with profoundly different activation kinetics. Embo J. 18, 2323-2329.

Luthi, A. and McCormick, D. A., 1998. H-current: properties of a neuronal and network pacemaker. Neuron. 21, 9-12.

Magee, J. C., 2000. Dendritic integration of excitatory synaptic input. Nat Rev Neurosci. 1, 181-190.

Matsumoto, M., 2009. [Role of the lateral habenula and dopamine neurons in reward processing]. Brain Nerve. 61, 389-396.

Matsumoto, M. and Hikosaka, O., 2007. Lateral habenula as a source of negative reward signals in dopamine neurons. Nature. 447, 1111-1115.

Matsumoto, M. and Hikosaka, O., 2008. Negative motivational control of saccadic eye movement by the lateral habenula. Prog Brain Res. 171, 399-402.

Matsumoto, M. and Hikosaka, O., 2009a. Representation of negative motivational value in the primate lateral habenula. Nat Neurosci. 12, 77-84.

Matsumoto, M. and Hikosaka, O., 2009b. Two types of dopamine neuron distinctly convey positive and negative motivational signals. Nature. 459, 837-841.

McBride, W. J., Murphy, J. M. and Ikemoto, S., 1999. Localization of brain reinforcement mechanisms: intracranial self-administration and intracranial place-conditioning studies. Behav Brain Res. 101, 129-152.

McCormick, D. A. and Bal, T., 1997. Sleep and arousal: thalamocortical mechanisms. Annu Rev Neurosci. 20, 185-215.

Melander, T., Hokfelt, T. and Rokaeus, A., 1986. Distribution of galaninlike immunoreactivity in the rat central nervous system. J Comp Neurol. 248, 475-517.

Meneses, A. and Hong, E., 1999. 5-HT1A receptors modulate the consolidation of learning in normal and cognitively impaired rats. Neurobiol Learn Mem. 71, 207-218.

Mikkelsen, J. D., 1990. A neuronal projection from the lateral geniculate nucleus to the lateral hypothalamus of the rat demonstrated with Phaseolus vulgaris leucoagglutinin tracing. Neurosci Lett. 116, 58-63.

Miller, M. A., Kolb, P. E. and Raskind, M. A., 1993. Extra-hypothalamic vasopressin neurons coexpress galanin messenger RNA as shown by double in situ hybridization histochemistry. J Comp Neurol. 329, 378-384.

Moosmang, S., Biel, M., Hofmann, F. and Ludwig, A., 1999. Differential distribution of four hyperpolarization-activated cation channels in mouse brain. Biol Chem. 380, 975-980.

Moosmang, S., Stieber, J., Zong, X., Biel, M., Hofmann, F. and Ludwig, A., 2001. Cellular expression and functional characterization of four hyperpolarization-activated pacemaker channels in cardiac and neuronal tissues. Eur J Biochem. 268, 1646-1652.

Morris, G., Arkadir, D., Nevet, A., Vaadia, E. and Bergman, H., 2004. Coincident but distinct messages of midbrain dopamine and striatal tonically active neurons. Neuron. 43, 133-143.

Much, B., Wahl-Schott, C., Zong, X., Schneider, A., Baumann, L., Moosmang, S., Ludwig, A. and Biel, M., 2003. Role of subunit heteromerization and N-linked glycosylation in the formation of functional hyperpolarization-activated cyclic nucleotide-gated channels. J Biol Chem. 278, 43781-43786.

Murase, S., Grenhoff, J., Chouvet, G., Gonon, F. G. and Svensson, T. H., 1993. Prefrontal cortex regulates burst firing and transmitter release in rat mesolimbic dopamine neurons studied in vivo. Neurosci Lett. 157, 53-56.

Murray, R. M., Lappin, J. and Di Forti, M., 2008. Schizophrenia: from developmental deviance to dopamine dysregulation. Eur Neuropsychopharmacol. 18 Suppl 3, S129-134.

Nakamura, K., Matsumoto, M. and Hikosaka, O., 2008. Reward-dependent modulation of neuronal activity in the primate dorsal raphe nucleus. J Neurosci. 28, 5331-5343.

Nambu, T., Sakurai, T., Mizukami, K., Hosoya, Y., Yanagisawa, M. and Goto, K., 1999. Distribution of orexin neurons in the adult rat brain. Brain Res. 827, 243-260.

Nauta, W. J., 1958. Hippocampal projections and related neural pathways to the midbrain in the cat. Brain. 81, 319-340.

Nauta, W. J., 1960. Limbic system and hypothalamus: anatomical aspects. Physiol Rev Suppl. 4, 102-104.

Nieuwenhuys, R., Geeraedts, L. M. and Veening, J. G., 1982. The medial forebrain bundle of the rat. I. General introduction. J Comp Neurol. 206, 49-81.

Nishikawa, T., Fage, D. and Scatton, B., 1986. Evidence for, and nature of, the tonic inhibitory influence of habenulointerpeduncular pathways upon cerebral dopaminergic transmission in the rat. Brain Res. 373, 324-336.

Nissl, 1913. Die Großhirnanteile des Kanninchens.

Nolan, M. F., Dudman, J. T., Dodson, P. D. and Santoro, B., 2007. HCN1 channels control resting and active integrative properties of stellate cells from layer II of the entorhinal cortex. J Neurosci. 27, 12440-12451.

Notomi, T. and Shigemoto, R., 2004. Immunohistochemical localization of Ih channel subunits, HCN1-4, in the rat brain. J Comp Neurol. 471, 241-276.

Oades, R. D. and Halliday, G. M., 1987. Ventral tegmental (A10) system: neurobiology. 1. Anatomy and connectivity. Brain Res. 434, 117-165.

Olson, V. G. and Nestler, E. J., 2007. Topographical organization of GABAergic neurons within the ventral tegmental area of the rat. Synapse. 61, 87-95.

Omelchenko, N. and Sesack, S. R., 2009. Ultrastructural analysis of local collaterals of rat ventral tegmental area neurons: GABA phenotype and synapses onto dopamine and GABA cells. Synapse. 63, 895-906.

Palkovits, M., 1999. Interconnections between the neuroendocrine hypothalamus and the central autonomic system. Geoffrey Harris Memorial Lecture, Kitakyushu, Japan, October 1998. Front Neuroendocrinol. 20, 270-295.

Pape, H. C., 1996. Queer current and pacemaker: the hyperpolarization-activated cation current in neurons. Annu Rev Physiol. 58, 299-327.

Papez, J. W., 1932 The nucleus of the mamillary peduncle. Anat Rec. 52.

Peyron, C., Petit, J. M., Rampon, C., Jouvet, M. and Luppi, P. H., 1998. Forebrain afferents to the rat dorsal raphe nucleus demonstrated by retrograde and anterograde tracing methods. Neuroscience. 82, 443-468.

Phillipson, O. T., 1979. Afferent projections to the ventral tegmental area of Tsai and interfascicular nucleus: a horseradish peroxidase study in the rat. J Comp Neurol. 187, 117-143.

Qi, Y., Iqbal, J., Oldfield, B. J. and Clarke, I. J., 2008. Neural connectivity in the mediobasal hypothalamus of the sheep brain. Neuroendocrinology. 87, 91-112.

Rajakumar, N., Elisevich, K. and Flumerfelt, B. A., 1993. Compartmental origin of the striato-entopeduncular projection in the rat. J Comp Neurol. 331, 286-296.

Raman, I. M. and Bean, B. P., 1999. Properties of sodium currents and action potential firing in isolated cerebellar Purkinje neurons. Ann N Y Acad Sci. 868, 93-96.

Robinson, R. B. and Siegelbaum, S. A., 2003. Hyperpolarization-activated cation currents: from molecules to physiological function. Annu Rev Physiol. 65, 453-480.

Rodd-Henricks, Z. A., Melendez, R. I., Zaffaroni, A., Goldstein, A., McBride, W. J. and Li, T. K., 2002. The reinforcing effects of acetaldehyde in the posterior ventral tegmental area of alcohol-preferring rats. Pharmacol Biochem Behav. 72, 55-64.

Sagvolden, T., Johansen, E. B., Aase, H. and Russell, V. A., 2005. A dynamic developmental theory of attention-deficit/hyperactivity disorder (ADHD) predominantly hyperactive/impulsive and combined subtypes. Behav Brain Sci. 28, 397-419; discussion 419-368.

Sandyk, R., 1992. Pineal and habenula calcification in schizophrenia. Int J Neurosci. 67, 19-30.

Santoro, B., Chen, S., Luthi, A., Pavlidis, P., Shumyatsky, G. P., Tibbs, G. R. and Siegelbaum, S. A., 2000. Molecular and functional heterogeneity of hyperpolarization-activated pacemaker channels in the mouse CNS. J Neurosci. 20, 5264-5275.

Santoro, B., Liu, D. T., Yao, H., Bartsch, D., Kandel, E. R., Siegelbaum, S. A. and Tibbs, G. R., 1998. Identification of a gene encoding a hyperpolarization-activated pacemaker channel of brain. Cell. 93, 717-729.

Santoro, B. and Tibbs, G. R., 1999. The HCN gene family: molecular basis of the hyperpolarization-activated pacemaker channels. Ann N Y Acad Sci. 868, 741-764.

Schultz, W., 1998. The phasic reward signal of primate dopamine neurons. Adv Pharmacol. 42, 686-690.

Schweighofer, N., Tanaka, S. C. and Doya, K., 2007. Serotonin and the evaluation of future rewards: theory, experiments, and possible neural mechanisms. Ann N Y Acad Sci. 1104, 289-300.

Seeman, P., Chau-Wong, M., Tedesco, J. and Wong, K., 1976. Dopamine receptors in human and calf brains, using [3H]apomorphine and an antipsychotic drug. Proc Natl Acad Sci U S A. 73, 4354-4358.

Seeman, P., Weinshenker, D., Quirion, R., Srivastava, L. K., Bhardwaj, S. K., Grandy, D. K., Premont, R. T., Sotnikova, T. D., Boksa, P., El-Ghundi, M., O'Dowd B, F., George, S. R., Perreault, M. L., Mannisto, P. T., Robinson, S., Palmiter, R. D. and Tallerico, T., 2005. Dopamine supersensitivity correlates with D2High states, implying many paths to psychosis. Proc Natl Acad Sci U S A. 102, 3513-3518.

Shepard, P. D., Holcomb, H. H. and Gold, J. M., 2006. Schizophrenia in translation: the presence of absence: habenular regulation of dopamine neurons and the encoding of negative outcomes. Schizophr Bull. 32, 417-421.

Silver, R., Silverman, A. J., Vitkovic, L. and Lederhendler, II, 1996. Mast cells in the brain: evidence and functional significance. Trends Neurosci. 19, 25-31.

Skagerberg, G., Lindvall, O. and Bjorklund, A., 1984. Origin, course and termination of the mesohabenular dopamine pathway in the rat. Brain Res. 307, 99-108.

Stern, W. C., Johnson, A., Bronzino, J. D. and Morgane, P. J., 1979. Effects of electrical stimulation of the lateral habenula on single-unit activity of raphe neurons. Exp Neurol. 65, 326-342.

Sugama, S., Cho, B. P., Baker, H., Joh, T. H., Lucero, J. and Conti, B., 2002. Neurons of the superior nucleus of the medial habenula and ependymal cells express IL-18 in rat CNS. Brain Res. 958, 1-9.

Sutherland, R. J., 1982. The dorsal diencephalic conduction system: a review of the anatomy and functions of the habenular complex. Neurosci Biobehav Rev. 6, 1-13.

Swanson, L. W., 1976. An autoradiographic study of the efferent connections of the preoptic region in the rat. J Comp Neurol. 167, 227-256.

Swanson, L. W., 1982. The projections of the ventral tegmental area and adjacent regions: a combined fluorescent retrograde tracer and immunofluorescence study in the rat. Brain Res Bull. 9, 321-353.

Tsai, C., 1925. The optic tract and centers of the opossum, Didelphis virginiana. J Comp Neurol. 39, 173-216.

Ullsperger, M. and von Cramon, D. Y., 2003. Error monitoring using external feedback: specific roles of the habenular complex, the reward system, and the cingulate motor area revealed by functional magnetic resonance imaging. J Neurosci. 23, 4308-4314.

Ungerstedt, U., 1971. Stereotaxic mapping of the monoamine pathways in the rat brain. Acta Physiol Scand Suppl. 367, 1-48.

Vandael, D. H., Marcantoni, A., Mahapatra, S., Caro, A., Ruth, P., Zuccotti, A., Knipper, M. and Carbone, E., Ca(v)1.3 and BK channels for timing and regulating cell firing. Mol Neurobiol. 42, 185-198.

Varga, V., Kocsis, B. and Sharp, T., 2003. Electrophysiological evidence for convergence of inputs from the medial prefrontal cortex and lateral habenula on single neurons in the dorsal raphe nucleus. Eur J Neurosci. 17, 280-286.

Vazquez-Borsetti, P., Cortes, R. and Artigas, F., 2009. Pyramidal neurons in rat prefrontal cortex projecting to ventral tegmental area and dorsal raphe nucleus express 5-HT2A receptors. Cereb Cortex. 19, 1678-1686.

Vertes, R. P., 1991. A PHA-L analysis of ascending projections of the dorsal raphe nucleus in the rat. J Comp Neurol. 313, 643-668.

Vertes, R. P., Fortin, W. J. and Crane, A. M., 1999. Projections of the median raphe nucleus in the rat. J Comp Neurol. 407, 555-582.

Wang, R. Y. and Aghajanian, G. K., 1977. Physiological evidence for habenula as major link between forebrain and midbrain raphe. Science. 197, 89-91.

Weiss, T. and Veh, R. W., 2010. Morphological and electrophysiological characteristics of neurons within identified subnuclei of the lateral habenula in rat brain slices. Neuroscience.

Wise, R. A., 1989. Opiate reward: sites and substrates. Neurosci Biobehav Rev. 13, 129-133.

Wu, J., Chen, P. X. and Jin, G. Z., 1996. Dopamine-induced ionic currents in acutely dissociated rat neurons of CNS. Zhongguo Yao Li Xue Bao. 17, 23-27.

Yamaguchi, T., Sheen, W. and Morales, M., 2007. Glutamatergic neurons are present in the rat ventral tegmental area. Eur J Neurosci. 25, 106-118.

Yanez, J. and Anadon, R., 1994. Afferent and efferent connections of the habenula in the larval sea lamprey (Petromyzon marinus L.): an experimental study. J Comp Neurol. 345, 148-160.

Yanez, J. and Anadon, R., 1996. Afferent and efferent connections of the habenula in the rainbow trout (Oncorhynchus mykiss): an indocarbocyanine dye (DiI) study. J Comp Neurol. 372, 529-543.

Yang, L. M., Hu, B., Xia, Y. H., Zhang, B. L. and Zhao, H., 2008. Lateral habenula lesions improve the behavioral response in depressed rats via increasing the serotonin level in dorsal raphe nucleus. Behav Brain Res. 188, 84-90.

9. Publications

Full papers

Wolfram C. Poller, René Bernard, Christian Derst, Torsten Weiss, Vince I. Madai, Rüdiger W. Veh (2011) Lateral habenular neurons projecting to reward-processing monoaminergic nuclei express hyperpolarization-activated cyclic nucleotid-gated cation (HCN) channels. Neuroscience, July 2011

Poster presentations

Wolfram C. Poller, C. Derst, R. Bernard, V. I. Madai, R. W. Veh (2009)
Subnuclear and cellular distribution of HCN channel subunits in the rat habenular complex.
Annual meeting of the Society for Neuroscience (2009), Chicago, USA

Wolfram C. Poller, R. Bernard, V. I. Madai, T. Kahl, G. Laube, R. W. Veh (2010) Identification of lateral habenular neurons relaying hypothalamic input to monoaminergic hindbrain circuits.
Annual meeting of the Society for Neuroscience (2010), San Diego, USA

Wolfram C. Poller, R. Bernard, V. I. Madai, T. Kahl, G. Laube, R. W. Veh (2011) Identification of lateral habenular neurons relaying hypothalamic input to monoaminergic hindbrain circuits.
Annual Meeting of the German Neuroscience Society (2011), Göttingen, Germany

10. Danksagung

Ich danke herzlichst Herrn Prof. Dr. Rüdiger W. Veh, der mir stets ein Doktorvater im besten Sinne des Wortes war. Ich erhielt von Ihm nicht nur das sehr interessante Thema meiner Doktorarbeit, sondern vor allem die Möglichkeit, selbstständig meine Gedanken und Pläne zu verwirklichen. So konnte ich stets unter fachlicher Anleitung eine Vielzahl von Techniken erlernen und damit spannende Ergebnisse erzielen. Außerdem ermöglichte mir Prof. Veh die Reise zu zwei internationalen Kongressen, wo ich meine Ergebnisse präsentieren durfte. Prof. Veh war mir über die ganzen Jahre ein außergewöhnlicher Lehrer und ein Vorbild, sowohl in der Medizin als auch in der Wissenschaft.

Desweiteren gilt mein besonderer Dank den wissenschaftlichen Mitarbeitern des Instituts, insbesondere Dr. René Bernard und Dr. Christian Derst, die mir über die ganze Zeit beratend und hilfreich zur Seite standen. Vieles hätte ich ohne ihre Hilfe nicht verwirklichen können. Auch allen anderen Mitarbeitern des Instituts gilt mein Dank für ihre geduldige Unterstützung und stete Hilfsbereitschaft.

Nicht zuletzt gilt mein Dank aber auch meiner Familie und meinen Freunden, die mich in allen Bereichen bei der Anfertigung der Arbeit unterstützt haben.

Liebe Zeynep, ich danke dir für Deine tolle Unterstützung und Deine Geduld, die Du mir auch in schwierigen Zeiten stets entgegen gebracht hast.

11. Eidesstattliche Erklärung

„Ich, Wolfram Poller, erkläre, dass ich die vorgelegte Dissertation mit dem Thema: „The Lateral Habenula – Crossroad between Homeostatic Systems and Reward Circuitries“ selbst verfasst und keine anderen als die angegebenen Quellen und Hilfsmittel benutzt, ohne die (unzulässige) Hilfe Dritter verfasst und auch in Teilen keine Kopien anderer Arbeiten dargestellt habe.“

05.08.2011

Datum Unterschrift

12. Curriculum vitae

Mein Lebenslauf wird aus datenschutzrechtlichen Gründen in der elektronischen Version meiner Arbeit nicht veröffentlicht.